Dtsch. Entomol. Z. 65 (1) 2018, 1–63 | DOI 10.3897/dez.65.21000

PENSOFT museum für naturkunde

Cladistic classification of *Mecyclothorax* Sharp (Coleoptera, Carabidae, Moriomorphini) and taxonomic revision of the New Caledonian subgenus *Phacothorax* Jeannel

James K. Liebherr[1]

1 *Cornell University Insect Collection, John H. and Anna B. Comstock Hall, Cornell University, Ithaca, NY 14853-2601, USA*

http://zoobank.org/73DEE0F3-2BB0-4A21-B445-5E168FE50F54

Corresponding author: *James K. Liebherr* (JKL5@cornell.edu)

Received 14 September 2017
Accepted 15 December 2017
Published 18 January 2018

Academic editor:
Dominique Zimmermann

Key Words

aptery
conservation prioritization
endemism
genitalic variation
revisionary systematics

Abstract

The 15 species of *Mecyclothorax* Sharp precinctive to New Caledonia are revised and shown by cladistic analysis to comprise a monophyletic lineage, here treated as subgenus *Phacothorax* Jeannel. The New Caledonian species of subgenus *Phacothorax* include *Mecyclothorax fleutiauxi* (Jeannel), *M. najtae* Deuve, and 13 newly described species: *M. jeanneli* **sp. n.**, *M. laterobustus* **sp. n.**, *M. laterorectus* **sp. n.**, *M. laterosinuatus* **sp. n.**, *M. laterovatulus* **sp. n.**, *M. manautei* **sp. n.**, *M. megalovatulus* **sp. n.**, *M. octavius* **sp. n.**, *M. paniensis* **sp. n.**, *M. picdupinsensis* **sp. n.**, *M. plurisetosus* **sp. n.**, and two jointly authored species; *M. kanak* Moore & Liebherr **sp. n.,** and *M. mouensis* Moore & Liebherr **sp. n.**. Subgenus *Phacothorax* is one of five subgenera recognized within genus *Mecyclothorax* based on cladistic analysis of 65 exemplar taxa utilizing information from 137 morphological characters. The four other monophyletic subgenera include the precinctive Australian *Eucyclothorax* **subgen. n.** (type species *Mecyclothorax blackburni* [Sloane]), the precinctive Queensland *Qecyclothorax* **subgen. n.** (type species *Mecyclothorax storeyi* Moore), the precinctive New Zealand *Meonochilus* Liebherr & Marris **status n.**, and the geographically widespread and very diverse nominate subgenus, distributed from St. Paul and Amsterdam Islands, eastward across Australia and New Guinea, and in the Sundas, Timor Leste, Lord Howe and Norfolk Islands, New Zealand, and the Society and Hawaiian Islands. The biogeographic history of *Mecyclothorax* can be derived from the parsimony cladogram time-calibrated by times of origin of particular geographic areas inhabited by resident representative species. Based on sister-group status of subgenus *Phacothorax* and subgenus *Mecyclothorax*, and occupation of Lord Howe Island–an island originating no earlier than 6 Ma–by the earliest divergent lineage within subgenus *Mecyclothorax,* the ancestor of present-day *Phacothorax* spp. is hypothesized to have colonized New Caledonia 6 Ma, subsequent both to Cretaceous Gondwanan vicariance as well as any Oligocene submergence. Area relationships among the New Caledonian *Phacothorax* point to earliest diversification incorporating the northern massifs, and most recent diversification on the ultramafic volcanic substrates in the south of Grand Terre. Flight wing loss has played an important role in shaping the various island faunas, both in their morphology as well as their diversity. The retention of flight capability in only a few of the many hundred *Mecyclothorax* spp. is presented in light of how populations evolve from macropterous colonizing propagules to vestigially winged specialists. Interspecific differences in genitalic structures for the sister-species pair *M. fleutiauxi* + *M. jeanneli* are shown to involve functional complementarity of male and female structures. Extensive geographic variation of male genitalia is demonstrated for several New Caledonian *Mecyclothorax* spp. This variation deviates from the geographically uniform male genitalia exhibited by species in the hyperdiverse *Mecyclothorax* radiation of Haleakalā volcano,

Maui, suggesting that extensive sympatry occurring among species in that diverse species swarm selects for stability within this mate recognition system. Conversely, lower levels of sympatry characterizing the depauperate New Caledonian radiation permit the presence of more extensive male genitalic variation, this variation not selected against due to the lower likelihood of interspecific mating mistakes.

Introduction

The carabid beetle fauna of New Caledonia comprises elements ranging from the mundane to the bizarre. Typical of the more mundane representatives of the fauna would be the geographically widespread species *Platycoelus melliei* (Montrouzier), native to Australia and present in New Caledonia likely due to human transport (Will 2011). Somewhat less mundane would be a generalized native such as *Notagonum kanak* (Fauvel), the single New Caledonian representative species of a geographically widespread, southwest Pacific grade of platynine carabid beetles (Darlington 1952), most species of which include flight capable individuals (Liebherr 2017a). Though the New Caledonian *N. kanak* is precinctive to the island, and is the product of speciation within New Caledonia, its presence on the island can tell us little about the history of New Caledonia. Of much more interest both morphologically and potentially biogeographically are those lineages that have radiated in New Caledonia resulting in numerous native, precinctive species. Such biological diversity may belie longer periods of residency by these lineages offering the possibility that earlier geological events influenced their phylogenetic history. *Abacophrastus* Will, an endemic New Caledonian genus of pterostichine Carabidae with seven precinctive New Caledonian species (Will 2011), is a candidate for implicating events of earth history based on the phylogenetic relationships both within and external to the genus. *Cyphocoleus* Chaudoir, a New Caledonian endemic genus described in tribe Platynini, and placed in terminal position with that tribe in catalogues (Csiki 1931, Lorenz 2005) due to its bizarre "platynine" anatomy, is actually an aberrant member of the Odacanthini with relatives in both Australia and South America, suggesting a Cretaceous-aged biogeographic link via an Antarctic pathway (Liebherr 2016). Only phylogenetic analysis of *Cyphocoleus* plus a broad array of potential outgroups allowed such a hypothesis to be proposed. Conversely, immense disparity across an island radiation may evolve adaptively in isolated and restricted island situations over a very short time, such as with *Mecyclothorax* carabid beetles of the Society and Hawaiian Islands (Liebherr 2013, 2015). Characterizing such biological diversity is the first step toward hypothesizing the context within which a particular lineage has evolved. Cladistic analysis of the recognized species-level taxa, in light of appropriate outgroups (Hennig 1966), comprises the second step. Only then can biogeographic hypotheses be proposed and tested using area-based methods such as vicariance biogeography (Nelson and Platnick 1981, Ladiges and Cantrill 2007), or temporal-calibration methods such as lineage divergence dating based on molecular sequence data (Grandcolas et al. 2008, Nattier et al. 2017).

This contribution sets out to establish the phylogenetic context of a taxon of New Caledonian carabid beetles initially proposed as the distinct genus *Phacothorax* Jeannel (1944). Jeannel proposed recognition of this group at the generic level due to its distinct external anatomy, though he noted that *Phacothorax* shared male genitalic characters with the Australian and Hawaiian, geographically widespread genus *Mecyclothorax* Sharp. Once phylogenetic relationships of the *Phacothorax* radiation and its outgroups are established, the sister group relationships of the constituent clades allow a concise hypothesis for time of origin of the New Caledonian radiation. This allows addition of *Phacothorax* spp. to the panoply of New Caledonian taxa for which hypothesized ages of origin range from the Pleistocene to much earlier in the Eocene to Cretaceous (Nattier 2017). In addition to proposing phylogenetic relationships for the *Phacothorax* radiation, all presently known species are validated through species description, with a dichotomous key provided for taxonomic study of this radiation. These species-level treatments establish distributional hypotheses that define areas of endemism appropriate for conservation prioritization, and expose biogeographic factors associated with species diversification. The role of flight wing loss during the evolution of *Mecyclothorax* is investigated. Differences in genitalic morphology both within and between species are presented, these pointing to functional interactions of the male intromittent organ and the female reproductive tract, as well as providing information on the level of cohesion among populations comprising geographically widespread species. This variation is compared to that observed in more diverse Polynesian *Mecyclothorax* radiations, with the differences related to requirements of an evolutionarily stable mate recognition system.

Material and methods

Taxonomic material. Revision of New Caledonian *Mecyclothorax* is based on 676 specimens deposited in 12 institutional or personal collections. The bulk of the material–518 specimens–was collected during various expeditions by Dr. Geoff Monteith and colleagues, Queensland Museum, Brisbane (QMB). Material from the Museum of Natural History, Wrocław University (MNHW) complements the QMB material in the careful annotation of geographic coordinates, elevation, and collecting method

or situation. Use of label data from these two institutional collections provided the principal core of information for characterizing microhabitat occupation for the species. Additional material deposited in the following institutional collections was also studied: B. P. Bishop Museum, Honolulu (BPBM); Canadian National Collection, Agriculture Canada, Ottawa (CNC); Cornell University Insect Collection (CUIC); Essig Museum of Entomology, University of California, Berkeley (EMEC); Hungarian Natural History Museum, Budapest (HNHM); Muséum d'Histoire naturelle, Genève (MHNG); Muséum national d'Histoire naturelle, Paris (MNHN); Naturhistorisches Museum, Wien (NHMW); Queensland Museum, Brisbane (QMB); Martin Baehr personal collection (MBC); Pier M. Giachino personal collection (PMGC).

Material collected by Herbert Franz in 1970 (NHMW) were labeled only with a key code, with the codes deciphered in his field notebook (Jäch, pers. comm.).

All type specimens are labeled as such, with data for holotypes presented verbatim, including typographic spacing and capitalization. Individual lines on a label are separated by a slash "/" and different labels are indicated by a double slash "//". The complete list of scientific names for species included in the cladistic analysis, with authorship, is provided in Table 1, obviating the need to clutter the text with author names.

Laboratory techniques. Dissection and staining techniques are fully described in Liebherr (2015: 18–20). All male and female dissections were photographed using a Microptics (now Visionary Digital®) macrophotographic apparatus, using a Nikon D1X camera, fibre-optic strobe light source, and K-series Microptics lenses. Specimens were slide-mounted and photographed with backlighting provided by a transmitted light stage, or backlighting plus direct lighting provided by multiple fibre-optic cables. All specimens photographed with direct lighting were surrounded with two nested Lucite® tubes lined with translucent plastic drafting film.

Table 1. Species-level taxa included in cladistic analysis. *Mecyclothorax* subgeneric classification based upon results of cladistic analysis. Type species indicated for *Mecyclothorax* generic-level taxa. *Mecyclothorax andersoni* represented by infraspecific aedeagal forms with either a short or long median lobe apex (Liebherr 2017b). *Mecyclothorax* sp. n. D treated as non-valid terminal; species to be described subsequently.

Moriomorphina [secondary outgroup]
Neonomius laevicollis (Sloane)
Amblytelina [primary outgroups]
Amblytelus brevis Blackburn
Amblytelus curtus (F.)
Amblytelus matthewsi Baehr
Dystrichothorax amplipennis (MacLeay)
Epleyx lindensis Blackburn
Paratrichothorax brevistylus Baehr
***Mecyclothorax* Sharp [ingroup]**
subgenus *Eucyclothorax* Liebherr subgen. n
Mecyclothorax (*Eucyclothorax*) *blackburni* (Sloane) [type species]
Mecyclothorax (*Eucyclothorax*) *curtus* (Sloane)
Mecyclothorax (*Eucyclothorax*) *eyrensis* (Blackburn)
Mecyclothorax (*Eucyclothorax*) *lophoides* (Chaudoir)
Mecyclothorax (*Eucyclothorax*) *moorei* Baehr
Mecyclothorax (*Eucyclothorax*) *peryphoides* (Blackburn)
Mecyclothorax (*Eucyclothorax*) *punctatus* (Sloane)
Mecyclothorax (*Eucyclothorax*) sp. n. D
subgenus *Qecyclothorax* Liebherr subgen. n.
Mecyclothorax (*Qecyclothorax*) *impressipennis* Baehr
Mecyclothorax (*Qecyclothorax*) *inflatus* Baehr
Mecyclothorax (*Qecyclothorax*) *lewisensis* Moore
Mecyclothorax (*Qecyclothorax*) *storeyi* Moore [type species]
subgenus *Meonochilus* Liebherr & Marris status n.
Mecyclothorax (*Meonochilus*) *amplipennis* (Broun) [type species]
Mecyclothorax (*Meonochilus*) *bellorum* (Liebherr & Marris)
Mecyclothorax (*Meonochilus*) *eplicatus* (Broun)
Mecyclothorax (*Meonochilus*) *rectus* (Liebherr & Marris)
Mecyclothorax (*Meonochilus*) *spiculatus* (Liebherr & Marris)
subgenus *Phacothorax* Jeannel
Mecyclothorax (*Phacothorax*) *fleutiauxi* (Jeannel) [type species]
Mecyclothorax (*Phacothorax*) *jeanneli* Liebherr sp. n.
Mecyclothorax (*Phacothorax*) *kanak* Moore & Liebherr sp. n.
Mecyclothorax (*Phacothorax*) *laterobustus* Liebherr sp. n.
Mecyclothorax (*Phacothorax*) *laterorectus* Liebherr sp. n.
Mecyclothorax (*Phacothorax*) *laterosinuatus* Liebherr sp. n.
Mecyclothorax (*Phacothorax*) *laterovatulus* Liebherr sp. n.
Mecyclothorax (*Phacothorax*) *manautei* Liebherr sp. n.
Mecyclothorax (*Phacothorax*) *megalovatulus* Liebherr sp. n.
Mecyclothorax (*Phacothorax*) *mouensis* Moore & Liebherr sp. n.
Mecyclothorax (*Phacothorax*) *najtae* Deuve
Mecyclothorax (*Phacothorax*) *octavius* Liebherr sp. n.
Mecyclothorax (*Phacothorax*) *paniensis* Liebherr sp. n.
Mecyclothorax (*Phacothorax*) *picdupinsensis* Liebherr sp. n.
Mecyclothorax (*Phacothorax*) *plurisetosus* Liebherr sp. n.
subgenus *Mecyclothorax* Sharp
Mecyclothorax (*Mecyclothorax*) *amingwiwae* Liebherr
Mecyclothorax (*Mecyclothorax*) *andersoni* Liebherr
Mecyclothorax (*Mecyclothorax*) *andersoni* Liebherr (long aedeagus)
Mecyclothorax (*Mecyclothorax*) *baehri* Guéorguiev
Mecyclothorax (*Mecyclothorax*) *brispex* Liebherr
Mecyclothorax (*Mecyclothorax*) *goweri* Moore
Mecyclothorax (*Mecyclothorax*) *gressitti* Liebherr
Mecyclothorax (*Mecyclothorax*) *howei* Moore
Mecyclothorax (*Mecyclothorax*) *kavanaughi* Liebherr
Mecyclothorax (*Mecyclothorax*) *medioconstrictus* Liebherr
Mecyclothorax (*Mecyclothorax*) *sedlaceki* Darlington
Mecyclothorax (*Mecyclothorax*) *ambiguus* (Erichson)
Mecyclothorax (*Mecyclothorax*) *basipunctus* Louwerens
Mecyclothorax (*Mecyclothorax*) *globicollis* (Mandl)
Mecyclothorax (Mecyclothorax) lateralis (Laporte de Castelnau)
Mecyclothorax (Mecyclothorax) lissus (Andrewes)
Mecyclothorax (*Mecyclothorax*) *marau* Perrault
Mecyclothorax (*Mecyclothorax*) *minutus* (Laporte de Castelnau)
Mecyclothorax (*Mecyclothorax*) *monteithi* Moore
Mecyclothorax (*Mecyclothorax*) *montivagus* (Blackburn) [type species]
Mecyclothorax (*Mecyclothorax*) *oopteroides* Liebherr
Mecyclothorax (*Mecyclothorax*) *otagoensis* Liebherr
Mecyclothorax (*Mecyclothorax*) *punctipennis* (MacLeay)
Mecyclothorax (Mecyclothorax) rectangulus Louwerens
Mecyclothorax (*Mecyclothorax*) *rotundicollis* (White)
Mecyclothorax (*Mecyclothorax*) *sculptopunctatus* (Enderlein)

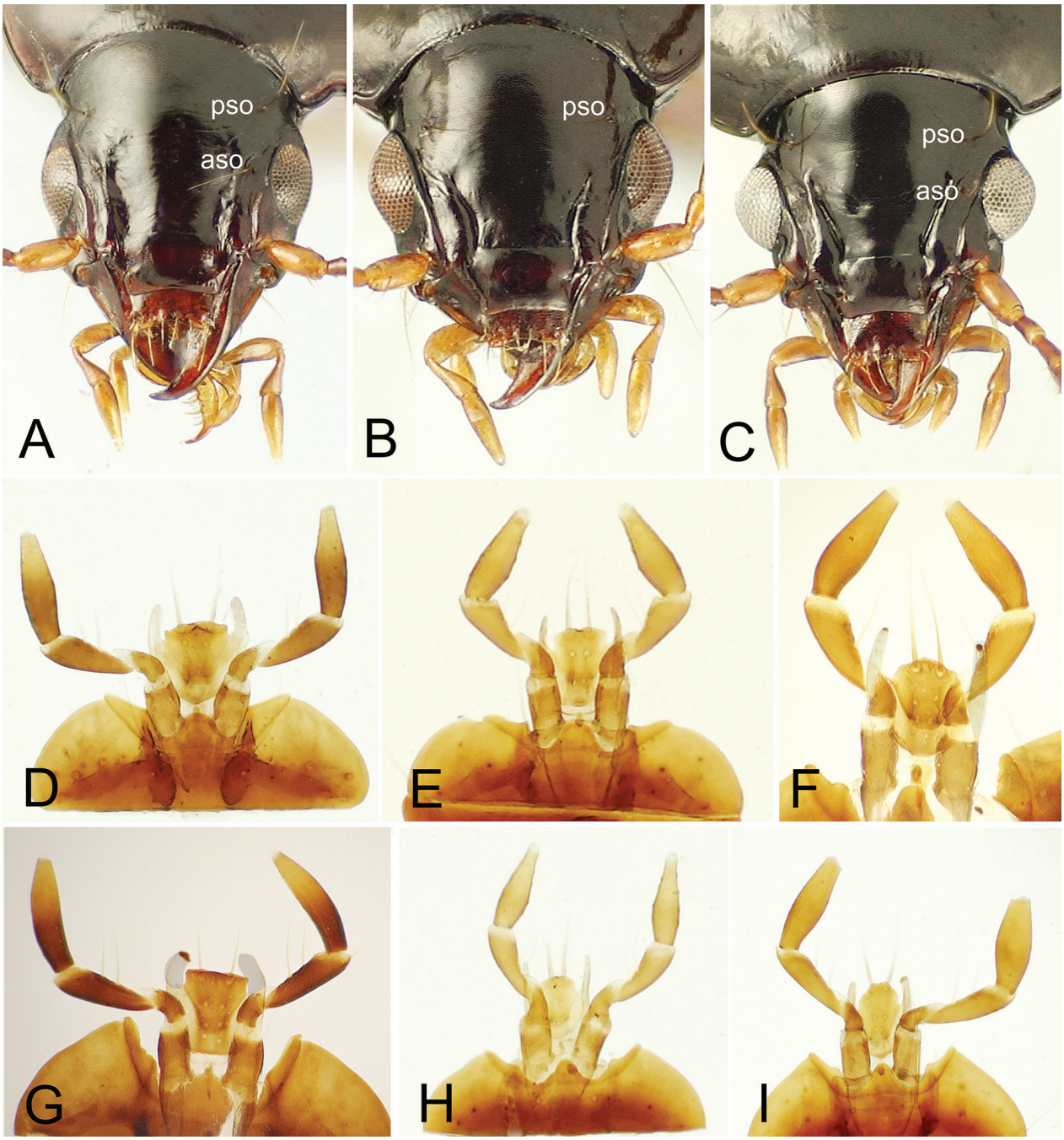

Figure 1. Head and mouthpart structures of *Mecyclothorax* spp. **A–C**. Head capsule, dorsal view: **A**, *M. goweri*; **B**, *M. fleutiauxi*; **C**, *M. laterorectus*. **D–I**, Mentum, labial palps and ligula: **D**, *M. peryphoides*, ventral view; **E**, *M. storeyi*, ventral view; **F**, *M. amplipennis*, dorsal view; **G**, *M. montivagus*, dorsal view; **H**, *M. kanak*, ventral view; **I**, *M. fleutiauxi*, ventral view. Abbreviations include: **aso**, anterior supraorbital seta; **pso**, posterior supraorbital seta.

Descriptive conventions. Several measurements proved useful for diagnosing species. Eye development was quantified by the ocular ratio: MHW/mFW, or maximum head width across eyes divided by the minimum frons width between eyes. The breadth of the eye socket on the head capsule varies from smaller, with the eye covering less of the extended ocular lobe (Fig. 1A), to larger, with the eye covering much of the lateral surface of the ocular lobe (Fig. 1B). This amount of coverage was quantified by the ocular lobe ratio, EyL/OLL, or the diameter of the eye measured in dorsal view divided by the distance from the anterior margin of the eye to the constriction of the head capsule posterad the ocular lobe. Thirdly, the convexity of the outer eye surface was quantified by the eye length measured in dorsal aspect divided by the eye depth, EyL/EyD, measured so that the entire dorsal margin of the eye lay perpendicular in the field of view. This ratio was influenced by the position of the eyes on the head capsule, for some species have eyes placed more dorsally on the head capsule, necessitating determination

of eye depth such that the head was not horizontal when the latter measurement was made.

Elongation of the mandibles was quantified relative to the anterior margin of the labrum by the ratio of the distance from the base of the dorsal (anatomically anterior) condyle of the mandible to the mandibular apex divided by the distance from condylar base to the anterolateral margin of the labrum. Specimens with a non-retracted or angularly retracted labrum were used for this ratio when possible; otherwise the position of a non-retracted labrum was estimated.

Dimensions of the pronotum were routinely used to diagnose several of the species, with four measurements made: **1**, MPW, maximum pronotal (or prothoracic) width, measured either across the pronotum, or across the externally bulging proepisternum if visible in dorsal view; **2**, APW, apical pronotal width, measured between the two most anterior points along the anterior pronotal margin; **3**, BPW, basal pronotal width, measured across the base of the pronotum along the lateral marginal bead; and **4**, PL, pronotal length, or the distance from the apex of the pronotum to the basal margin measured along the midline. These measurements were variously combined into the ratios APW/BPW, MPW/BPW, and MPW/PL, in order to describe prothoracic configuration. Two measurements of the elytra were also used to describe body shape: **1**, MEW, maximal elytral width; and **2**, EL, elytral length, or the distance from the base of the scutellum to the elytral apex, measured parallel to the suture, and to the farther of the two apices if they are separated by a median invagination at the suture. These measurements were combined into the ratio MEW/EL. The ranges of all ratios are used for descriptive purposes only without any statistical connotations. When sufficiently available, at least five specimens were chosen for calculation of ratios, encompassing the largest and smallest specimen available, plus male and female representatives. For widespread species, five specimens from various localities were measured in order to give a view to any infraspecific trends in size or shape. The number of specimens used is presented at the start of each description. The number of male and female dissections used to elucidate male genitalic and female genitalic and reproductive tract characters is provided at the start of those sections of the species treatment.

Standardized body length used to describe body size is the sum of three measurements: **1**, head length measured from the labral medioapical margin to the cervical ridge at the head-pronotal juncture; **2**, pronotal length as measured above; **3**, elytral length as measured above. As this sum of measurements ignores the apical portion of the elongate mandibles (always in variable positions specimen to specimen) and any distended portions of the abdomen (also variable dependent on specimen condition when prepared), the standardized body length measure will be smaller than the size perceived by eye.

Dorsal body setation exhibited by each species is summarized in the diagnosis using a chaetotaxic formula expanded from that first proposed for *Mecyclothorax* by Perrault (1984). The formula designates presence (+) or absence (–) of the anterior supraorbital seta, posterior supraorbital seta, lateral pronotal seta, basal pronotal seta, parascutellar seta, and the subapical and apical elytral seta. The number of dorsal elytral setae associated with the third elytral interval is indicated using Arabic numbers. The positions of these setae are illustrated in Liebherr (2013: fig. 2) and Liebherr (2015: fig. 7). For this contribution, the formula +/+//+/–//+/2/+/+ designates presence of both supraorbitals, presence of the lateral pronotal seta but absence of the basal seta, presence of the parascutellar seta, presence of two dorsal elytral setae, and presence of both subapical and apical elytral setae. The various body regions–head, pronotum, elytra–are separated by double slashes (//). For variable numbers of dorsal elytral setae among individuals, the range of setae present is given. If a seta is variably present or absent, this variation is indicated using "+–."

Comprehensive descriptions to complement the diagnoses are provided for all newly described species. The various ratios that quantify proportions of body somites or their constituent structures–e.g., antennae, mandibles, eyes, pronota, elytra–are presented for all species. All character data were recorded in an Excel® spreadsheet, the characters grouped onto sheets according to body region. This spreadsheet is available from the author upon request. Also, many of the character states used as the basis for taxonomic description are also presented in the cladistic analysis (Fig. 7, Suppl. material 1).

Cladistic analysis

Ingroup circumscription. Based on a tribal analysis of Moriomorphini (Liebherr 2011), it was determined that the genera *Amblytelus* and *Mecyclothorax* constituted components of a monophyletic moriomorphine subtribe Amblytelina. The New Caledonian species were first considered to represent the distinct genus *Phacothorax* Jeannel (Jeannel 1944), though the second-known species was described as *Mecyclothorax najtae* (Deuve 1987). Based on preliminary dissections of the material revised herein, Liebherr and Marris (2009) synonymized *Phacothorax* with *Mecyclothorax*. In order to elucidate the phylogenetic relationships of the revised New Caledonian taxa, and thereby to determine their generic-level classification within Amblytelina, they were analyzed along with a broad array of other *Mecyclothorax* taxa (Table 1). This constituted a broad representation of described Australian taxa, plus representative species from Papua New Guinea, Java, Borneo, New Zealand, St. Paul and Amsterdam Islands, Lord Howe Island, Norfolk Island, and the Society and Hawaiian Islands. Outgroup taxa representing other amblyteline lineages were chosen based on the classification of Baehr (2004), including three species of *Amblytelus* Erichson, *Dystrichothorax amplipennis*, *Epelyx lindenensis*, and *Paratrichothorax brevistylus*. The entire analysis was rooted between the *Amblytelus-Mecyclothorax* ingroup and the outgroup *Neonomius laevicollis,* a

species similar in external appearance to *Mecyclothorax* species, but differing in male and female genitalic characters such that it is properly considered a member of the subtribe Moriomorphina instead of subtribe Amblytelina (Liebherr 2011).

Characters. Information from 137 binary or multistate characters was recorded for 65 moriomorphine taxa; 7 outgroup taxa and 58 terminals assignable to the genus *Mecyclothorax*. In the listing of characters below, multistate characters are presented as either ordered (+) or unordered (–). The initial state descriptions are nearly verbatim relative to the Winclada dataset (Suppl. material 1), although in some instances a more expanded description of the character states supported by illustrations is required. Characters are numbered as per the Winclada default: starting at 0.

0. 3rd antennomere (–): glabrous except for apical ring of setae (0); a few short setae basad distal ring (1); with 3–4 series of elongate setae along shaft (2); setose in apical half (3). This character is treated as unordered so as not to require that the state of a setose apical half of the antennomere be derived only from the state wherein a few setae accompany the apical ring of setae.

1. Antennomere 9 length/width ratio (+): $1.46 < x \leq 1.92$ (0); $2.0 < x < 2.8$ (1); $x \geq 2.89$–3.43 (2). The ratio values for the three states span the limits presented.
2. Labrum front margin (+): straight (0; Fig. 9A); slightly emarginate (1; Fig. 1B–C)); moderately to deeply emarginate (2; Fig. 1A).
3. Mandibular length ratio (+): very short, ratio 1.18–1.55 (0); moderately elongate, ratio of 1.57–1.92 (1; Fig. 1B–C); elongate, ratio of 1.95–2.33 (2; Fig. 1A). The distributional limits of the ratios representing the three states are reflected in the values presented.
4. Apical 2 maxillary palpomeres (+): apparently glabrous (0; Figs 1A–C); with sparse pelage of short setae (1); with pelage of elongate setae (2).
5. Anterior supraorbital seta: present (0; Fig. 1A, C)); absent (1; Fig. 1B).
6. Frontal grooves: very shallow, not evident between eyes (0); shallow to deep, evident between eyes (1).
7. Frontal grooves (–): subparallel (0; Figs 1A, 8D–E); arcuately convergent, then divergent anterad (1; Figs 1B, 8A–B); very deep from front of eye, large lateral callous, pit at frontoclypeal suture (2; Figs 1C, 8C); shallow, convergent from front of eye, no pit at frontoclypeal suture (3).
8. Frontal grooves: not extended onto, or much shallower on clypeus (0; Fig. 8C–E); extended onto clypeus (1; Figs 1, 8A–B).
9. Neck impression (+) absent, dorsum of head convex (0; Figs 1B-C, 8A–B); flat area between hind margins of eye (1); transverse depression behind hind margins of eyes (2; Figs 1A, 8C–E).
10. Ocular lobe assessed behind eye (dorsal view): protruded, meeting gena at obtuse angle (0; Fig. 8A, D–E); little protruded, meeting gena at very obtuse angle (1; Figs 1, 8B–C).
11. Ocular lobe groove behind eye (+): distinct groove present (0; Fig. 8D–E); shallow groove present (1; Figs 1A, 8A–C); no groove present, juncture simple change in angle of surfaces (2; Fig. 1B–C).
12. Mentum tooth: sides acute to subparallel, apex tightly rounded (0; Fig. 1F–I); sides more obtuse, apex broadly rounded (1; Fig. 1D–E).
13. Mentum width/length ratio (+): $2.3 < x < 3.11$ (0); $3.14 < x < 3.5$ (1); $3.70 < x < 4.0$ (2). This ratio is defined as the maximum breadth of the mentum measured across its convex lateral margins divided by the distance from the mentum-submentum suture to the apex of a lateral lobe. The distributional limits of the states are reflected in the values presented.
14. Apex of ligula (+): apically rounded or with narrow concave apex between setae (0; Fig. 1E–F, H–I); broad, longer medially with shorter lateral wings (1; Fig. 1D); broadly truncate, margin straight and heavily sclerotized (2; Fig. 1G).
15. Apical two ligular setae: proximate, separated by 1–2 setal diameters (0; Fig. 1E, F, H–I); distant, separated by 3–4 or more setal diameters (1; Fig. 1D, G).
16. Paraglossae (+): extended only slightly beyond apex of ligula (0); extended 1/2 distance from base to ligular apex beyond apex (1; Fig. 1G, I); extended as far beyond apex as basal length to apex (2; Fig. 1F); extended 2× as far beyond apex as basal length of apex (3; Fig. 1D–E, H).
17. Ocular ratio (+): $1.31 < x \leq 1.42$ (0; Fig. 1A); $1.43 \leq x \leq 1.54$ (1; Fig. 1B–C): $1.55 \leq x < 1.75$ (2). Although the limits of the ratios for the three states were chosen to maximize fidelity to each state, there were seven species that exhibit infraspecific eye development requiring they be coded polymorphic for states 0 and 1: *Mecyclothorax bellorum*, *M. eyrensis*, *M. inflatus*, *M. kanak*, *M. laterostinuatus*, *M. megalovatulus*, and *M. mouensis* (Suppl. material 1)
18. Ocular lobe ratio (+): $0.59 < x < 0.72$ (0; Fig. 1A); $0.73 < x < 0.87$ (1; Fig. 1C); $0.88 < x < 0.97$ (2; Fig. 1B). As for character 17, numerous species exhibit polymorphism in this character: one for states 0 and 1 (*M. spiculatus*); and seven for states 1 and 2 (*M. blackburni*, *M. curtus*, *M.* n sp. D, *M. eyrensis*, *M. laterosinuatus*, *M. montivagus*, and *M. rectus*) (Suppl. material 1).
19. Eye convexity (EyL/EyD) (+): convex or popeyed, $2.0 < x < 2.53$ (0); moderately convex, $2.55 < x < 2.89$ (1; Fig. 1C); little convex, $2.90 < x < 4.18$ (2; Fig. 1A–B). As for the other two eye ratios, six species were coded as polymorphic under this character coding scheme: *M. curtus* for states 0 and 1, and five species–*M. bellorum*, *M. blackburni*, *M. eplicatus*, *M. lophoides*, and *M. peryphoides*–for states 1 and 2 (Suppl. material 1).
20. Number of ommatidia across horizontal diameter of eye (+); 11–15 (0; Fig. 1A, C); 16–20 (1; Fig. 1B); 21–30 (2); 31–40 (3).
21. Pronotum: broad basally, MPW/BPW = 1.23–1.80 (0; Fig. 2A); narrow basally, MPW/BPW = 1.82–3.91 (1;

Fig. 1B). Only *M. eyrensis* failed to adhere to the ratio limits used to define the two states of this character, as individuals exhibited ratios = 1.77–1.82.

22. Pronotal lateral seta: present (0; Fig. 2A–B); absent (1; Fig. 9D–E).
23. Pronotal basal seta: present (0; Fig. 8D–E); absent (1; Fig. 2A–B).
24. Lateral pronotal setal position (if present) (+) with: articulatory socket in or adjoining lateral marginal depression (0); articulatory socket 1/2–2 setal diameters medially from marginal depression (1); articulatory socket 2–4 setal diameters medially from marginal depression (2).
25. Pronotal hind seta (if present): situated at hind angle (0); visibly anterad hind angle (1).
26. Pronotal hind angles (+): nearly right to obtuse, with sides subparallel anterad hind angle (0; Fig. 2A); obtuse, sides divergent anterad hind angle (1); projected denticle on rounded lateral margin (2); obsolete, lateral and basal margins convex (3, Fig. 9D–E).
27. Pronotal hind angle: rounded to right-angled (0; Fig. 2A–B); acute, with acuminate lateral projection at angle (1; Fig. 8C).
28. Pronotal basal margin: straight or convex mesad hind angles (0; Fig. 8C); distinctly sinuate inside hind angles (1; Fig. 8A).
29. Pronotal median base (+): coplanar with disc medially (0; Fig. 2A); depressed relative to disc medially (1; Figs 2B, 8A–B, D); greatly depressed relative to disc medially (2; Fig. 8C, E).
30. Pronotum median base (+): smooth laterally mesad laterobasal depressions (0; Fig. 2A–B); with 3–10 punctures each side mesad laterobasal depressions (1; Fig. 8B); with >12 punctures each side mesad laterobasal depressions (2; Fig. 8A, C–E).
31. Pronotal basal margin: beaded medially (0; Fig. 8A); convex medially, marginal bead only behind laterobasal depression (1; Figs 2A–B, 8B–E).
32. Pronotal basal marginal bead (if present; i.e. state 0, #31): narrow, continuous with lateral bead (0); broader, discontinuous with lateral bead (1).
33. Pronotal median longitudinal impression (+): well defined, continuous on pronotal disc (0; Figs 2B, 8B–C); fine and shallow on disc (1; Figs 2A, 8A, D–E); reduced to small punctures, obsolete, or obscured by punctures (2).
34. Anterior transverse impression (+): obsolete to absent medially, anterior callosity not defined (0; Fig. 16B–C); broad and shallow medially, anterior callosity broadly convex (1; Figs 2A–B, 8A, C); broad and deep medially, anterior callosity well defined posteriorly (2; Fig. 8B, D–E).
35. Anterior transverse impression (+): absent to obsolete laterally (0; Fig. 2A–B); visible only in outer 1/4–1/3 of breadth each side (1); visible in outer 1/2 of breadth each side (2); visible across entire breadth of notum (3; Fig. 8B–E).
36. Pronotal anterior margin: unmargined (0); with marginal bead medially (1).
37. Pronotal front angles (+): not protruded, rounded behind (0; Fig. 8A); slightly protruded, broadly rounded (1; Fig. 8B, D–E); slightly protruded, narrowly to tightly rounded (2; Figs 2A–B, 8C); protruded, obtusely rounded to angulate (3; Fig. 9D–E); protruded, broadly rounded (4).
38. Pronotal lateral marginal depression (at midlength) (+): very narrow, margin beaded (0; Fig. 8A–C); moderately narrow, microsculpture visible at depth (1; Fig. 2A–B); broad to very broad, lateral margin variously explanate, microsculpture evident (2; Fig. 8D–E).
39. Pronotal laterobasal depression (–): broad, smoothly extended to lateral margin (0; Fig. 9D–E); continuous linear broadening of lateral marginal depression (1; Fig. 2B); with median longitudinal/punctate depression and lateral tubercle (2; Fig. 2A); not depressed, surface rugose or punctate (3).
40. Prosternal process: smooth ventrally, rounded behind (0; Fig. 2D–F); margined ventrally, a bead defining ventroposterior margin (1).
41. Proepisternum (+): smooth (0; Fig. 2C, E); with large punctures ventrally along sternum (1; Fig. 2D); covered with large punctures (2; Fig. 2F).
42. Prosternum (+): medially convex anterad and between coxal cavities (0); medially depressed only between coxal cavities (1; Fig. 2D); medially depressed between and anterad coxal cavities (2; Fig. 2C, D–F).
43. Prosternum (+): smooth medially (0; Fig. 2C); with 2 punctures medially (1); with 5–7 punctures medially (2; Fig. 2D–F).
44. Lateral portion of prosternum: impunctate except for anteapical furrow (0; Fig. 2C); irregularly punctate (1; Fig. 2D–F).
45. Prosternal anterior margin (+): without or with very shallow indistinct groove (0); with smooth depression or groove (1; Fig. 2C); with indistinctly punctate groove (2); with distinctly punctate groove (3; Fig. 2D–E); with groove reduced to large, serially isolated punctures (4; Fig. 2F).
46. Prosternal anteapical groove (if present at all in some form; i.e. states 1–4, #45) (+): very short, restricted to dorsodistal surface of prosternum (0); longer, extended from dorsodistal margin ventrad onto lateral surface of prosternum (1); continuous ventrally but shallower or irregular between the lateral reaches of prosternum (2; Fig. 2C–D, F); continuously deep ventrally between sides of prosternum (3; Fig. 2E).
47. Proepimeron (+): with anterior and posterior grooves smooth (0); with anterior groove minutely punctate, posterior smooth (1); with both anterior and posterior grooves irregular or punctate (2).
48. Parascutellar seta: present (0); absent (1).
49. Scutellum: narrower, W/L = 0.83–1.86 (0; Fig. 8A–E); broader, W/L = 2.0–2.5 (1; Fig. 9A). For this ratio, scutellar length is determined along the scutellar midline from the basal transverse depression to the apex, whereas width is determined along a line just apicad that depression.

50. Parascutellar striole: longer, terminated between sutural stria and suture where parallel (0; Fig. 8A, D–E); short, terminated between sutural stria and suture where convergent (1; Fig. 8C).
51. Parascutellar striole (+): present, continuous, smooth or punctate (0; Fig. 8A, C); present, consisting of 3–8 punctures, not connected by stria (1; Fig. 8D–E); present, consisting of 1–2 isolated punctures (2); absent (3; Figs 8B, 9D–E).
52. Dorsal elytral setal count (+): 0 (0); 1 (1; Fig. 8B–C); 2 (2; Fig. 8A, E); 3–5 (3; Fig. 8D).
53. Accessory dorsal setae (+); absent (0); in fifth elytral interval (1); in fifth and seventh elytral intervals (2). The presence of accessory setae in the fifth elytral interval is documented for *M. kavanaughi* (Liebherr 2008a), whereas the presence of accessory setae in both the fifth and seventh interval occurs in *Amblytelus brevis* and *A. curtus* (Fig. 2J).
54. Position of anterior (or single) dorsal elytral seta (–): at anterior 1/5–1/3 of length (0); at midlength (1); in posterior third (2). A single dorsal elytral seta at elytral midlength occurs in *M. storeyi* and *M. lewisensis* (Moore 1984) and other members of subgenus *Qecyclothorax*.
55. Supracarinal elytral seta (basad subapical seta) (+): absent (0; Fig. 2L); present (1); present and doubled (2; Fig. 2J). Additional setae in the seventh elytral interval basad the subapical seta, and mesad the carina associated with the seventh stria is a feature of *Amblytelus brevis* and *A. curtus* (Fig. 2J)
56. Elytral subapical seta: present (0); absent (1). This seta is plesiomorphically present in *Mecyclothorax* and its sister group comprising *Amblytelus* and allied genera, and is situated within the seventh stria (Fig. 2H), or in a position homologous with that stria if the stria is reduced (Fig. 2K)
57. Elytral apical seta: present (0); absent (1). This seta occurs just laterad the mesally curved apex of stria 2 near the elytral sutural apex (Fig. 2G–H).
58. Apex of elytral interval 8 (+): with same curvature as elytral apex (0; Fig. 2G); more convex than rest of elytra (1; Fig. 2H–I); with distinct ridge on inner margin near stria 7 (2; Fig. 2K); distinctly carinate on inner margin near stria 7 (3; Fig. 2J, L).
59. Elytral shape (+): broadly subquadrate, sides subparallel, humeri broad (0; Fig. 8A, D); subquadrate, humeri narrowed (1; Fig. 8E); ellipsoid to ovoid (2; Figs 8B–C, 9D–E).
60. Elytral shape (humeri moderately broad; i.e. state 2 of #59) (+): foreshortened, hemiovoid (0); elongate, ellipsoid (1; Fig. 9D–E); elongate, ovoid (2; Fig. 16A).
61. Elytral dorsal curvature (+): moderately convex, sides sloping to margins, disc flat (0; Fig. 8A, D–E); convex, sides nearly vertical, disc domed (1; Fig. 9D–E); very convex, sides nearly vertical to margins, apex depressed (2; Fig. 8B–C).
62. Elytral basal groove (+): hardly recurved (0; Fig. 8C); recurved (1; Fig. 8B, D); distinctly recurved, an angular hitch at humerus (2; Figs 8A, E).
63. Elytral humeral angle (+): rounded (0: Fig. 8C); tightly rounded to obtuse-angulate (1; Fig. 8D–E); angulate (2; Fig. 8A–B).
64. Elytral humeral angle: with evenly convex margin on base and lateral edge (0); with elevated humeral tooth at angle (1).
65. Elytral striae on disc (+): 1–8 present, complete (0; Fig. 8C); 1–6 present, 7 obsolete to absent (1; Fig. 8D); 1–5 present, 6–7 reduced to obsolete, to absent (2; Fig. 8A); 1–3 to 1–4 shallow, 5–7 progressively obsolete (3; Fig. 8B, E); only sutural stria 1 present, punctate, 2–7 obsolete (4; Fig. 20B); all reduced, obsolete to absent except stria 8 (5; Fig. 9D–E).
66. Elytral striae on apex (+): all present, deep (0; Fig. 2J); 1–7 present, traceable, though they may be shallow apically (1); 1–3 to 1–5 traceable on apex, 7 evident mesad subapical sinuation (2; Figs 2K, 8C–D); only striae 1–2 and 7 visible near apex, 3–6 obsolete (3; Fig. 8E); only sutural stria and 7th traceable near apex, others obsolete (4); only sutural stria traceable near apex (5; Fig. 8B); no striae visible at apex except 8th at subapical sinuation (6; Fig. 16A).
67. Elytral apex along suture: not upraised in a conjoined juncture (0; Fig. 8A, D–E); upraised in a conjoined juncture (1; Fig. 8B–C).
68. Elytral strial punctation (+): absent (0; Fig. 9D–E); small, not expanding strial diameter (1; Fig. 8B–C); larger, elongate or round but little expanding strial diameter (2; Fig. 8D–E); large, deep, expanding strial diameter (3; Fig. 8A).
69. Setal depressions of dorsal elytral setae (+): shallow, extended over 1/4 breadth of interval 3 or less (0; Fig.9D–E); evident, extended over 1/3–1/2 breadth of interval 3 (1; Fig. 8D–E); broad, deep, extended over 3/4 breadth of interval 3 (2).
70. Elytral stria 8 (+): smoothly impressed along midlength (0; Fig. 2K); serially punctate, irregular along midlength (1; Fig. 2L).
71. Elytral lateral marginal depression (+): very narrow throughout length (0; Fig. 8C); narrow to moderately broad, microsculpture visible in deepest part (1; Fig.8A, D–E); broad anteriorly, moderately broad behind (2; Figs 2J, 8B).
72. Subapical sinuation: deep, distinct, more abruptly curved anteriorly (0; Figs 2J, 8D); broad, shallow (1; Figs 2G–I, 8E).
73. Mesepisternal punctures (+): none, surface smooth (0; Fig. 3B); 5–6 small punctures in single curved line (1); 5–9 large punctures in 2–3 rows (2; Fig. 3A); 10 or more large punctures in 3 rows (3).
74. Mesosternal/mesepisternal suture: present (0; Fig. 3A); absent anteriorly, sclerites fused near prothorax (1; Fig. 3B).
75. Metathoracic flight wings (–): fully developed, venated, with reflexed apex (0; Fig. 3C); brachypterous, with reduced apex, venation reduced (1); stenopterous, reduced to a narrow strap longer than metanotum (2; Fig. 3D); vestigial, wing rudiment not extended to apex of metanotum (3).

76. Metepisternal width/length ratio (–): 0.30 < x < 0.60 (0); 0.60 < x < 0.87 (1); 0.87 < x < 1.46 (2; Fig. 3A–B). For this ratio, the metepisternal length is measured along the lateral margin from the juncture with the mesepimeron to the metepimeron. Metepisternal width is the maximal perpendicular distance from this line to the metepisterna-mespimeral-mesosternal 3-point junction, measured with the metepisternum level in the field of view.
77. Metepisternum-metepimeron suture: distinct, a distinct line (0; Fig. 3B); incomplete, reduced laterally (1; Fig. 3A).
78. Tarsomeres: dorsally glabrous (0); dorsally setose (1).
79. Metatarsomeres 4 (+): narrow, with short apical lobes (0); broadly triangular, broader apex with very short lobes (1); broad overall, bilobed, apical lobes broad, elongate (2).
80. Suture between abdominal ventrites 1 and 2: straight to sinuous with ventrite 2 not or only slightly depressed (0); sinuous with ventrite 2 distinctly depressed inside curve (1).
81. Suture between abdominal ventrites 2 and 3: shallow, complete, traceable to margin (0); reduced, incomplete, absent laterally (1).
82. Abdominal ventrites 3–5 (–): with irregular linear plaques in lateral reaches (0); with round, smooth depressed plaques in lateral reaches (1); with surface punctate obscuring any other features (2).
83. Apical abdominal ventrite 6 (male) (–): with 1 seta each side (total of 2) (0); with 2 setae each side (total of 4) (1); with 3 setae each side (total of 6) (2); with 4 setae each side (total of 8) (3).
84. Apical abdominal ventrite (female) (–): with 2 setae each side (total of 4) (0); with 3 setae each side (total of 6) (1); with 4 setae each side (total of 8) (2).
85. Apical abdominal ventrite 6 (female) (–): glabrous medially between apical setae (0); with setose patch of 4–5 setae medially (1); with pair of subapical setae medially (2).
86. Microsculpture on frons (–): granulate isodiametric sculpticells (0); evident to shallow isodiametric mesh (1); isodiametric to transverse mesh in transverse rows (2); indistinct transverse mesh or lines (3); absent, surface glossy (4). All terms for microsculptural configurations are derived from Lindroth (1974), though the term sculpticell was coined by Allen and Ball (1980).
87. Microsculpture of pronotal disc (–): isodiametric in transverse rows mixed with transverse mesh, 2–3× broad as long (0); transverse mesh, sculpticells 3–4× broad as long (1); mix of transverse mesh and transverse lines (2); reduced, surface glossy, with indistinct transverse mesh or lines (3).
88. Microsculpture of pronotal base (–): isodiametric between basal punctures (0); transversely stretched isodiametric between punctures (1); evident transverse mesh, sculpticells 2–3× broad as long (2); indistinct, elongate transverse mesh or unconnected lines (3).
89. Microsculpture of elytral disc (–): a mix of distinct isodiametric and transverse sculpticells (0); a regular transverse mesh, sculpticell breadth 2–3× length (1); a mix of transverse mesh 3–4× broad as long and transverse lines (2); reduced, surface glossy, indistinct mesh plus lines over part (3).
90. Microsculpture on abdominal lateral base: swirling isodiametric and transverse sculpticells (0); reduced, surface glossy with indistinct sculpticells (1).
91. Body coloration (–): dark, elytral margins concolorous or indistinctly, narrowly paler (0); ferruginous, elytra bicolored with outer 4–5 intervals much paler (1); ferruginous, elytra bicolored, outer 3–4 intervals and apex much paler (2).

See Table 2 for abbreviations used to label structures of the male genitalic and female reproductive tract illustrations.

92. Antecostal margin of male mediotergite IX (ring sclerite): angulate (0; Fig. 10C, E, H, J, O)); broadly rounded (1; Fig. 17F).
93. Distal terminus of male mediotergite IX antecostal margin: not extended (0; Fig. 10C, H, H, J, O); extended, the proximal angle with an elongate extension (1; Figs 10E, 17B).
94. Aedeagal ventral (right, except *M. storeyi*) paramere shape (+): elongate, paddle-like, apex broadly subparallel to rounded tip (0); quadrate-conchoid, dorsal and ventral margins subparallel to apex (1; Fig. 5C, lower paramere); elongate-conchoid, apex narrowed so shape is subtriangular (2; Fig. 5B, upper paramere); very elongate, moderately narrow, paramere > 0.85 lobe gape (3; Fig. 5A, lower paramere); very elongate, apical half narrowed to whiplike extension (4; Fig. 5D, lower paramere). State 0 of this character is diagnostic for taxa of the subtribe Moriomorphina, represented in this analysis by the ultimate adelphotaxon *Neonomius laevicollis* (Moore 1963). Note that males of *M. storeyi* are characterized by a bilaterally inverted aedeagal assembly, necessitating recognition of the ventral paramere in repose being the anatomically left paramere, and vice versa (Moore 1984).
95. Aedeagal ventral (right, except for *M. storeyi*) paramere (+): densely setose on apicoventral margin, apical setae not present (0); densely setose on apicoventral margin, apical setae not differentiated (1; Fig. 5C); with 8–21 setae on ventral margin, apical setae distinct (2; Fig. 5D); with 2–7 setae on ventral margin well separated from apical setae (3; Fig. 5A); glabrous (or a single seta) on ventral margin plus 2 apical setae (4; Fig. 5E).
96. Aedeagal ventral (right, except for *M. storeyi*) paramere: with dorsal surface glabrous or a single small seta subapically (0; Fig. 5A–B, E); with dorsal surface setose (4–18 setae present along apical half) (1; Fig. 5C, D).
97. Aedeagal dorsal (left, except *M. storeyi*) paramere shape (+): broad basally, apical half elongate, margins subparallel (0); broad basally, apex short, narrowly rounded, subangulate (1; Fig. 5C); broadly quadrate basally; apical extension narrowly attenuate (2; Fig. 11D);

Table 2. Key to abbreviations for structures of male genitalia, and female genitalia and reproductive tracts.

Abbreviation	Structure
aai	male aedeagal apical invagination
af	apical face of male aedeagal median lobe
afs	lateroapical fringe setae, female gc1
al	apical lobe of male aedeagal internal sac
ans	apical nematiform setae, female gc2
bc	female bursa copulatrix
bcd	female bursa copulatrix dorsal lobe
co	female common oviduct
des	dorsal ensiform seta, female gc2
dgd	defensive gland duct
dgr	defensive gland reservoir
dl	dorsal lobe of male aedeagal internal sac
dp	dorsal plate of male aedeagal internal sac
fl	flagellum of male aedeagal internal sac
fs	flagellar sheath of male aedeagal internal sac
fp	flagellar plate of male aedeagal internal sac
gc1	basal gonocoxite of female
gc2	apical gonocoxite of female
gp	gonopore of male aedeagal internal sac
hg	hindgut
hs	helminthoid sclerite of female
les	lateral ensiform setae, female gc2
la	ligular apophysis of female
lp	left paramere of male aedeagus
mac	dorsal macrospicules of male internal sac
mbs	mediobasal shagreening of female gc1
ms	medial setae, female gc 1
mtIX	antecostal margin of male mediotergite IX
ovo	ostial ventroapical operculum, male aedeagus
r	ramus of female gc1
rp	right paramere of male aedeagus
sd	female spermathecal duct
sg	female spermathecal gland
sp	female spermatheca
spi	spiracle
vss	ventral spicular sclerite of male internal sac

narrower basally, evenly narrowed to whip-shaped apex (3; Fig. 5A–B, D–E). State 0 of this character occurs in *Paratrichothorax brevistylus* (Baehr 2004, fig. 108d) and in *Neonomius laevicollis* (Moore 1963).

98. Aedeagal dorsal (left, except for *M. storeyi*) paramere (+): glabrous apically, though setae may be present on the ventral surface (0; Fig. 5C); 2–4 very short setae at apex (1); 2–4 (or 1) longer setae at apex (2; Fig. 5A–B, D–E); 2–4 apical setae plus 4 additional shorter subapical setae (3). State 3 has only been observed in males of *M. lissus*.
99. Aedeagal median lobe ostial opening: without ventroapical operculum (0; Fig.4A–E); with hinged ventroapical opercular flap (1; Fig. 4F–G).
100. Aedeagal internal sac: unilobed, short to long (0; Fig. 4F–G); bilobed, with distinct dorsal and apical lobes (1; Fig. 10L, Q)).
101. Aedeagal internal sac (–): with flagellum associated with gonopore (0; Fig. 4A–E); with circular flagellar plate associated with gonopore (1; Fig. 4F–G); without flagellum, only dorsal plate present (2; Fig. 21A, E–F, H, J, L).
102. Short to elongate flagellar condition (i.e. state 0 of #101) (+): thin, lightly sclerotized, may be short, sinuous, or long and whiplike (0; Fig. 4C–E); broad, porrect, spikelike (1); crescent-shaped remnant of flagellar sheath base (2; Fig. 10L, Q).
103. Apical flagellar plate (i.e. state 1 of #101): a donut-like roll, lightly sclerotized or spiculated, gonopore within convexity (0); a well-sclerotized and ridged plate, gonopore on convex side (1; Fig. 4F–G). A lightly sclerotized flagellar plate is observed in New Guinean males, such as in *M. andersoni*, *M. baehri*, and *M. gressitti* (Guéorguiev 2013, Liebherr 2017b).
104. Aedeagal sac dorsal plate: absent, flagellum and/or flagellar sheath only (0; Figs 4E, 10L, Q); present in addition to or instead of flagellum and flagellar sheath (1; Fig. 4C–D).
105. Aedeagal sac dorsal plate (i.e. state 1 #104): translucent, covered with microspicules (0; Fig. 10A, G); well sclerotized, smooth (1; Fig. 4C).
106. Aedeagal internal sac surface dorsad position of dorsal plate: unarmored (0); with patch of robust macrospicules (1; Fig. 17I, M).
107. Aedeagal internal sac ventral sclerite patch: absent, area basad flagellum and sheath unsclerotized (0); present as distinct sclerite basad flagellum and sheath (1). This ventral sclerotic patch is observed in species of the outgroups, *Dystrichothorax* and *Amblytelus*.
108. Aedeagal internal sac ventrobasal spicular sclerite: absent (0); present (1; Fig. 4F–G).
109. Aedeagal median lobe shaft: gracile, aedeagus relatively narrow dorsoventrally, parallel-sided (0; Fig. 4F–G); broad, aedeagus robust, broadest at midlength (1; Fig. 4A–E).
110. Aedeagal median lobe tip (–): extended narrowly beyond ostium (0; Figs 4F–G, 10I, L); narrow, not extended beyond ostium (1; Fig. 10N–R); broadly expanded dorsoventrally, extended beyond ostium (2; Fig. 10A, C–D); broadly expanded dorsoventrally, not extended beyond ostium (3; Fig. 4A–C).
111. Broad extension of aedeagal median lobe (i.e. states 2, 3 #110) (+): parallel-sided dorsoventrally to rounded tip (0; Fig. 10A, C–D); convexly spoon shaped, expanded both dorsally and ventrally (1; Figs 17A–B, E–F); downturned, tip at angle to shaft, apical face straight (2; Fig. 17I, M); apex expanded dorsally and ventrally, adze-shaped (3; Fig. 4A); broadly downturned in fishhook configuration, tip pointed (4). State 4 characterizes males of *M. lewisensis* and *M. inflatus* (Baehr 2003, figs 1D–F).
112. Aedeagal median lobe apical margin (+): smoothly convex to acuminate, no abrupt change in curvature along margin (0; Fig. 17I–N); with hitch to distinct invagination along apical margin (1; Fig. 21L); with distinct invagination along margin resulting in dentate margin (2, Figs 21A–K, 26).

113. Aedeagal median lobe apex: smoothly extended past ostial opening (0; Fig. 17A, E); with dorsoventral crease distad ostial opening resulting in an apical hook-like tip (1; Fig. 17C).
114. Female bursa copulatrix shape: elongate, columnar, length/width > 2.0–3.25 (0; Fig. 6A–C, F); short and columnar, length/width 1.0–2.0 (1; Fig. 6D–E).
115. Female bursa copulatrix surface (+): membranous, not wrinkled, transparent (0; Fig. 6D); thin, surface wrinkled and translucent (1; Fig. 6A–C, E); thick, surface wrinkled and not transparent (2; Fig. 6F).
116. Female bursal copulatrix apicoventral surface: membranous as remainder of bursa (0); sclerotized into plate-like structure (1). Bursal sclerites are observed in females of *M. kavanaughi* (Liebherr 2008a) and *M. oopteroides* (Liebherr and Marris 2009, fig. 18)
117. Female bursa copulatrix: of approximately equal diameter throughout length (0; Fig. 6A–D, F); with smaller apical portion, diameter there much less than basal part (1; Fig. 6E).
118. Spermathecal duct placement (+): on bursa near common oviduct/bursa juncture (0; Fig. 6A–E); apically on bursa copulatrix main lobe (1; Fig. 23D–E); dorsoapically on bursa copulatrix main lobe (2); basodorsally on bursa, dorsad common oviduct/bursa juncture (3; Fig. 6F). A dorsoapical position of the spermatheca (state 2) is observed in *M. amplipennis* (Liebherr and Marris 2009, fig. 6)
119. Spermathecal duct placement near common oviduct (i.e. state 0, #118): on right side of bursa laterad common oviduct (0; Fig. 6A–B); on ventral side of bursa distad common oviduct (1; Fig. 6E).
120. Female bursa copulatrix configuration (+): unipartite, without dorsal lobe (0; Fig. 6A–F); bipartite, spermathecal duct entering apex of dorsal lobe which is shorter than ventral lobe (1; Fig. 12D): bipartite, spermathecal duct entering dorsal lobe equal in length to ventral lobe (2; Fig. 12E).
121. Helminthoid sclerite at base of spermathecal duct (–): present as elongate sclerotized apodeme (0; Fig.6A–B); base of spermathecal duct sclerotized as rounded projection (1; Fig. 6C); base of spermathecal duct sclerotized as two parallel apodemes (2); absent (3; Fig. 6E). The helminthoid sclerite observed in females of *M. moorei* comprises state 2.
122. Ligular apophysis on common oviduct: absent (0; Fig. 6A–F); present (1; Fig. 12D–E). The ligular apophysis (Liebherr and Will 1998) is a sclerotic expansion with highly dissected surface on the common oviduct's ventral surface. This suggests a muscular attachment at this point along the oviduct.
123. Spermathecal duct: present, spermatheca stalked (0; Fig. 6A–F); absent, spermatheca appressed (1). A spermatheca appressed to the bursal surface is observed in females of *M. amplipennis* (Liebherr and Marris 2009, fig. 6)
124. Spermathecal duct (i.e. state 0 of #123): subequal to spermathecal length (0; Fig. 6C); 1.25–3.0× spermathecal length (1; Fig. 6E).
125. Spermathecal shape (+): fusiform or ovoid bulb on narrow duct (0; Fig. 6); filiform reservoir on equal-sized duct (1; Fig. 23D); appressed bulb (2).
126. Spermathecal gland duct: entering on spermathecal duct at spermathecal base (0; Fig. 6B–C, E); entering on spermathecal reservoir (1; Fig. 12E).
127. Ramus (gonocoxite VIII of Deuve [1993]): present as defined membranous fold (0; Figs 13, 24); present, heavily sclerotized (1). Heavily sclerotized rami occur sporadically throughout the *Mecyclothorax* lineage. Among the taxa studied here, they are observed in *M. peryphoides*, *M. eyrensis*, and *M. lissus*.
128. Lateroapical fringe of setae on gonocoxite 1 (+): composed of single seta (0); composed of 2 setae (1; Fig. 13A–B, D–F); composed of 2–5 setae (at least 3 setae unilaterally) (2; Fig. 13C, G).
129. Medial setae of gonocoxite 1 (–): absent along entire mesal margin (or only 1–2 small seta apically) (0; Fig. 13G); absent at apex but several subapically along margin (1; Figs 13A–F, 24); large seta at apical angle plus other setae along mesal margin (2). A large apical angle seta (state 3) is observed in females of many species in subgenus *Mecyclothorax*; e.g. *M. montivagus* (Liebherr 2015, fig. 129B).
130. Mediobasal surface of gonocoxite 1: smooth (0; Figs 13, 24A–B); extensively shagreened with overlapping cuticular scales (1; Fig. 24C–E).
131. Apical gonocoxite 2 (+): broadly subtriangular, apex rounded, mitten-shaped (0); narrowly subtriangular, basal width < 0.4× length (1); more broadly subtriangular, basal width about half length (2); with lateral apodeme basally, basal width 0.6–0.7× length (3; Fig. 13F); falciform with basolateral apodeme, basal width > 0.75 length (4; Fig. 13D–E).
132. Lateral ensiform setal count for apical gonocoxite 2 (+): 1 (0); 2–3 (at least 2 unilaterally) (1; Figs 13, 24); 3–5 (3 or more both sides) (2).
133. Lateral ensiform setae of apical gonocoxite 2: shorter, basal seta 0.25–0.40× gonocoxite length (0; Figs 13A–C, G, 24); longer, basal seta 0.40–0.50× gonocoxite length (1; Fig. 13D–F).
134. Lateral ensiform setae of gonocoxite 2: on lateral margin of gonocoxite (0; Figs 13, 24); on ventral surface of gonocoxite (1). Ventrally oriented ensiform setae occur in *Amblytelus* and the allied genera *Dystrichothorax*, *Epelyx*, and *Paratrichothorax* (Baehr 2004, figs 124–146)
135. Apical nematiform setae of gonocoxite 2: in fossa 1/4–1/5× length from apex (0; Figs 13, 24); in fossa 1/2–1/4× length from apex (1). The more basal position of the apical nematiform setae is a character defining subgenus *Qecyclothorax*; i.e., *M. storeyi* and allies.
136. Mesal surface of laterotergite IX: setose (0); spiculose (1). Spiculose laterotergites diagnose the genera *Amblytelus*, *Epelyx*, and *Dystrichothorax* (Baehr 2004, figs 124–145).

Cladistic methods. The character-state matrix was developed using Winclada (Nixon 2002) and is presented along with the results of the analysis as Suppl. material 1. The matrix was submitted to Nona (Goloboff 1999), with tree searches conducted using the ratchet (Nixon 1999), using 200, 1000, and 10,000 ratchet iterations under default values. Results inherent in the various most-parsimonious trees were summarized using strict consensus. The strict consensus (Fig. 7) presented character-state changes under fast optimization.

Results

Under all three numbers of ratchet iterations, eight equally parsimonious trees of 1203 steps were found (CI = 0.21, RI = 0.66), with those trees and the character-state changes summarized for presentation using the 1216-step strict consensus cladogram under fast optimization (Fig. 7), that optimization allowing all characters to be represented on the cladogram. Use of unambiguous optimization results a consensus tree of identical topology. There is strong support for the mutual monophyly of *Amblytelus* and related genera versus *Mecyclothorax*, with 25 state changes supporting the exemplar array of the former, and 17 state changes supporting *Mecyclothorax* monophyly. Baehr (2004) comprehensively summarized the many characters defining the *Amblytelus* related genera, with salient characters such as the large, convex eyes (characters 17, state 2, and 19 state 0), anteriorly margined pronotum (character 36, state 1) with broadly explanate lateral margins (character 38, state 2), apically carinate elytral interval 8 (character 58, state 3), and broadly triangular fourth metatarsomeres (Character 79, state 1), among others, defining monophyly of this lineage.

The converse monophyly of *Mecyclothorax* is supported in the resulting cladogram by many characters that reverse among the dense sampling of *Mecyclothorax* spp., however the presence of 4–5 setae medially on the apical abdominal ventrite (character 85, state 1) is an unreversed synapomorphy among the species analyzed here. The groundplan elytral striation for *Mecyclothorax* is more derived than observed among the "*Amblytelus*" genera, as striae 6 and 7, or 5 to 7 are reduced on the disc (character 65, states 2 to 5), versus all striae present or only the seventh reduced in the former. This strial reduction also affects the expression of striae on the elytral apex, with most *Mecyclothorax* taxa exhibiting reduction in striae 4–6 or 3–6 apically. The lone exception includes species of subgenus *Meonochilus* from New Zealand, a clade previously described as a distinct genus (Liebherr and Marris 2009), but falling within the phylogenetic network of species currently placed in *Mecyclothorax*. These species have all striae traceable on the elytral apex. Finally, just as *Amblytelus* and related genera exhibit a distinct carina laterad the seventh elytral interval (Fig. 2J), nearly all *Mecyclothorax* lack a carina at this position. The lone exceptions are *M. blackburni* (Fig. 2L) and *M. curtus*, members of the first divergent lineage within *Mecyclothorax*: the subgenus *Eucyclothorax*.

Classification of *Mecyclothorax* Sharp, 1903

Taxonomic treatment

The classification of *Mecyclothorax* subgenera is based on the results of the cladistic analysis (Fig. 7, Table 1). The various recognized subgenera are diagnosed below with type species designated as per The Code (I.C.Z.N. 1999). Synapomorphic and symplesiomorphic diagnostic characters are sequentially presented for each proposed subgeneric taxon. The species of subgenus *Phacothorax* Jeannel are subsequently revised, following all conventions of The Code.

Genus *Mecyclothorax* Sharp

Mecyclothorax Sharp, 1903: 243 (type species *Cyclothorax montivagus* Blackburn by Andrewes 1939).

Cyclothorax MacLeay, 1871: 104 (not *Cyclothorax* Frauenfeld, 1868; type species *Cyclothorax punctipennis* MacLeay by monotypy; synonymy Sloane 1903).

Thriscothorax Sharp, 1903: 257 (type species *Cyclothorax unctus* Blackburn by original designation; synonymy Britton 1948).

Atelothorax Sharp, 1903: 269 (type species *Atelothorax optatus* Sharp by monotypy; synonymy Britton 1948).

Metrothorax Sharp, 1903: 269 (type species *Metrothorax molops* Sharp by Lorenz 1998; synonymy Britton 1948).

Antagonaspis Enderlein, 1909: 488 (type species *Antagonaspis sculptopunctata* Enderlein by original designation; synonymy Jeannel 1940).

Phacothorax Jeannel, 1944: 84 (type species *Phacothorax fleutiauxi* Jeannel by original designation; synonymy Liebherr and Marris 2009; designated as subgenus herein).

Loeffleria Mandl, 1969: 54 (synonymy Baehr and Lorenz 1999; type species *Loeffleria globicollis* Mandl by monotypy).

Meonochilus Liebherr & Marris, 2009: 10 stat. n. (type species *Tarastethus amplipennis* Broun designated by Liebherr and Marris 2009: 10; designated as subgenus herein).

Eucyclothorax subgen. n. (type species *Cyclothorax blackburni* Sloane hereby designated).

Qecyclothorax subgen. n. (type species *Mecyclothorax storeyi* Moore hereby designated).

Eucyclothorax subgen. n.

http://zoobank.org/03AF91A5-C31D-414B-852D-D6A40D71C718

Diagnosis. Species of this subgenus can be diagnosed by the synapomorphic presence of punctures on the prosternum (Fig. 2D–F), and the presence of a distinctly punctate prosternal anteapical groove, or the presence of punctures so deep and large that they obscure any groove (Fig. 2F). The pronotal front angles narrow and are not protruded (Fig. 8A) in all species except *M. curtus* and *M*. nsp. D, in which these angles are little protruded and more rounded (Fig. 2D). The paraglossae are generally

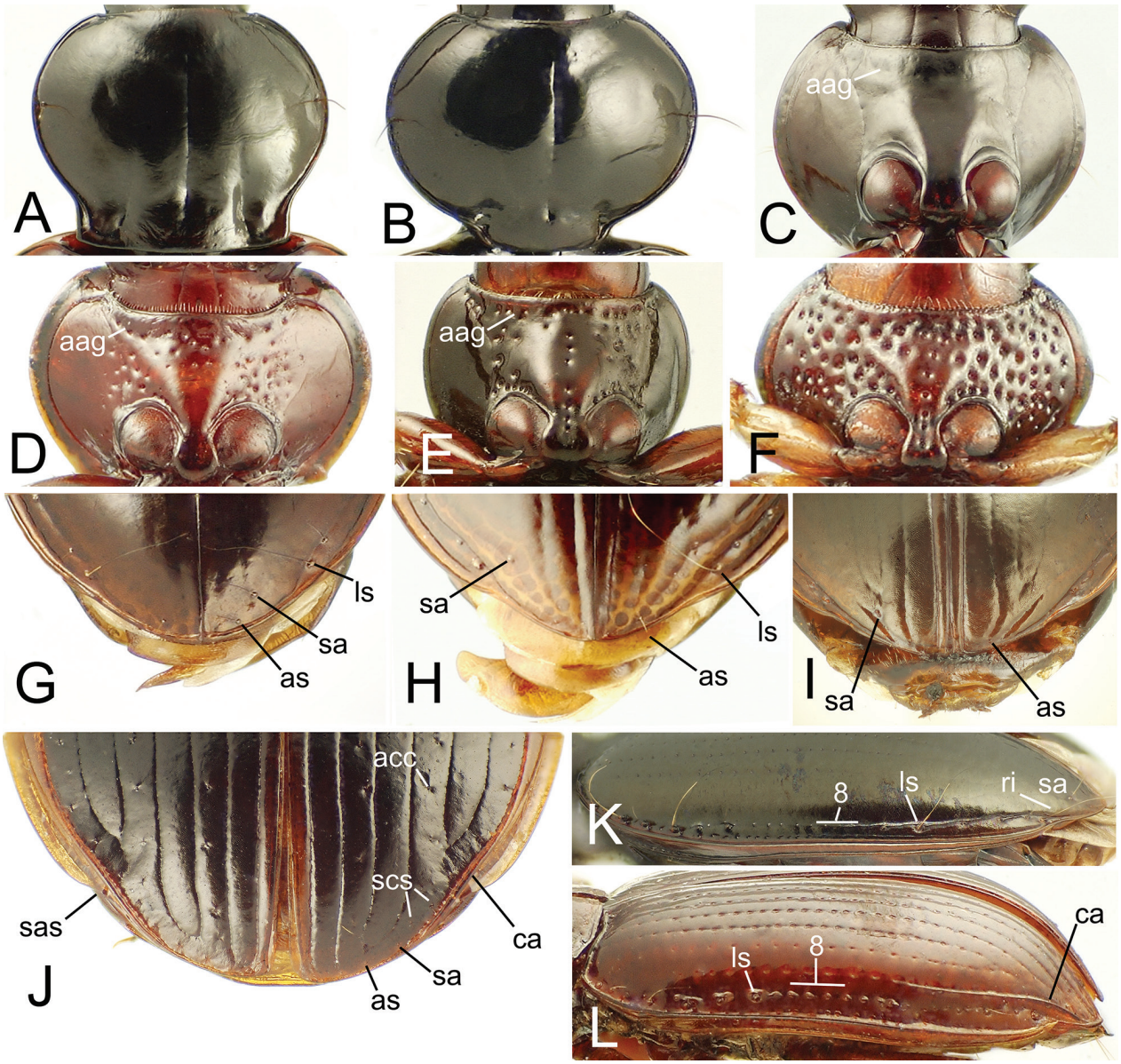

Figure 2. Thoracic structures of *Mecyclothorax* and *Amblytelus* spp. **A–B**. Pronotum, dorsal view: **A**, *M. laterorectus*; **B**, *M. mouensis*. **C–F**. Prosternum, ventral view: **C**, *M. fleutiauxi*; **D**, *M. curtus*; **E**, *M. blackburni*; **F**, *M. moorei*. **G–J**. Elytral apices, dorsal view: **G**, *M. fleutiauxi*; **H**, *M. laterorectus*; **I**, *M. lissus*; **J**, *A. curtus*. **K–L**. Elytral lateral margin showing eighth stria, lateral view: **K**, *M. ambiguus*; **L**, *M. blackburni*. Abbreviations include: **aag**, anteapical groove; **acc**, accessory elytral dorsal setae in interval 5; **as**, apical elytral seta; **ca**, carina laterad stria 7; **ls**, lateral elytral setae; **ri**, ridge mesad stria 8; **sa**, subapical elytral seta; **sas**, subapical sinuation of elytron; **scs**, supracarinal elytral setae; **8**, medial portion of stria 8.

elongate (Fig. 1D), extended twice as far from the anterior margin of the ligula than the distance from their base to the ligular margin; this is reversed in *M. punctatus* which has shorter paraglossae. The elytral striae are distinctly punctate (Fig. 8A), distinguishing *Eucyclothorax* spp. from species in *Qecyclothorax*, though not from other Australian members of subgenus *Mecyclothorax* such as *M. ambiguus* or *M. punctipennis*. Also, the eighth elytral stria is punctate at midlength in most species (Fig. 2L)–save *M. moorei* and *M. punctatus*–though this punctation is also seen in lesser development in some species of subgenus *Mecyclothorax* such as *M. punctipennis*. The surface of the basal abdominal ventrites is generally glossy without microsculpture, a synapomorphy, though this is reversed to a microsculptured surface in *M. lophoides* and *M*. sp. n. D. In the male genitalia the right paramere is elongate, with only 2–7 setae present on the ventral surface (Fig. 5A), and the internal sac bears a dorsal plate as well as a sinuous flagellum (Fig. 4C). Finally, the female reproductive tract has the spermathecal duct entering at the juncture of the common oviduct with the bursa (Fig. 6C), a symplesiomorphy shared with *Qecyclothorax* spp. (Fig. 6D), some *Amblytelus* spp. (Fig. 6A–B), *M. bellorum* of subgenus *Meonochilus* (Liebherr 2011, fig. 12). A

helminthoid sclerite is also symplesiomorphically present (Fig. 6C)

Member species. All Australian *Mecyclothorax* species have been examined, with the following species assignable to this subgenus represented in the analysis: *M. blackburni*, *M. curtus*, *M. eyrensis*, *M. lophoides*, *M. moorei*, *M. peryphoides*, and *M. punctatus* (Table 1; Moore et al. 1987, Baehr 2009). Baehr's (2016) southwestern Australian subspecies *M. punctatus peckorum* (Moore 1984, fig. 12) and *M. cordicollis* (Sloane) complement this list. An undescribed species from Queensland–sp. n. D–will be described in a subsequent publication.

Etymology. To indicate membership of species of this subgenus in *Mecyclothorax*, and to reflect the position of this taxon as the adelphotaxon to the remainder of *Mecyclothorax* sensu lato, the initial syllable "eu"–the Ancient Greek prefix *εύ*, meaning "proper" or "true"–is combined with the first name proposed for the genus, *Cyclothorax* (MacLeay 1871), resulting in the subgenus name *Eucyclothorax*. Based on the shared nominative masculine terminal syllable thorax, this epithet agrees in gender with the generic epithet.

Qecyclothorax subgen. n.

http://zoobank.org/4059AFC5-8924-40D4-B215-6B543F8E90BD

Diagnosis. These robust-bodied species (Fig. 8B) are geographically restricted to upland regions of Queensland, Australia, and have been recently revised by Baehr (2003). The pronotum of species in this subgenus is broad, with obtuse or obtusely rounded hind angles, and each elytron bears a single dorsal elytral seta just before midlength (Baehr 2003, fig. 3), a condition also observed in four species of subgenus *Meonochilus* (e.g. Fig. 8C). The mentum tooth is broadly rounded (Fig. 1E), though such a configuration is also observed in *M. blackburni* and *M. lophoides* of subgenus *Eucyclothorax*. The prothorax is depressed medially both between and anterad the procoxal cavities, a condition shared with most member species of *Eucyclothorax*, though prosternal punctures are never present here. The elytral striae are reduced, with striae 1–3 to 1–4 shallow, and striae 4– or 5–7 obsolete (Fig. 8B). Apically on the elytra the striae are reduced, with at most sutural and seventh stria present, and in several species only the sutural striae evident. The elytra are broadly convex, with the eighth interval not, or only slightly upraised (*M. lewisensis*) relative to the general curvature of the elytral surface. The suture between abdominal ventrites 1 and 2 is nearly straight, with the second ventrite hardly depressed relative to the first, whereas this suture is sinuous with the second ventrite depressed within the sinuosity in species of *Eucyclothorax* and *Meonochilus*. This condition varies among the New Caledonian *Phacothorax* spp. as well as across subgenus *Mecyclothorax*. The male aedeagal median lobe internal sac bears a flagellum (Fig. 4E), and the ventral paramere is elongate-conchoid in shape, broadly to narrowly subtriangular with ventral setae present (Fig. 5B; Baehr 2003, fig. 1). The female bursa copulatrix is relative short (Fig. 6D), with the spermathecal duct entering at the bursal-common oviduct juncture.

Member species. Baehr (2003) distinguishes the four species analyzed here (Fig. 7), recognizing seven subspecies.

Etymology. Given restriction of species in this subgenus to Queensland, the Queensland derived first syllable "qe" is combined with MacLeay's (1871) *Cyclothorax* to derive the subgeneric epithet. Just as in the original name of the Australian airline QANTAS–Queensland and Northern Territory Aerial Services Ltd.–*Qecyclothorax* obviates the unnecessary letter u while retaining the normal pronunciation of the letter Q. Based on the shared nominative masculine terminal syllable thorax, this epithet agrees in gender with the generic name.

subgenus *Meonochilus* Liebherr & Marris, 2009 [new status]

Diagnosis. Species of this subgenus share a robust, convex body shape with *Qecyclothorax* spp. (Fig. 8B–C), though in all *Meonochilus* spp. the elytral striae are well developed and punctate, with striae 1–7 deep at elytral midlength. The pronotal median base is depressed relative to the convex disc (Liebherr 2011, figs 9–10). The broad elytra are associated with a rounded humerus, a condition also observed among some New Caledonian *Phacothorax* and various species of subgenus *Mecyclothorax*. The head is transversely depressed behind the eyes, and the mentum is broad: over 3× broad as long. Opposed to New Zealand species of subgenus *Mecyclothorax* (as in Hawaii's *M. montivagus*, Fig. 1G), the ligula is rounded apically with the ligular setal sockets separated by only 2 diameters. The paraglossae extend beyond the ligular margin 1–2× the distance from their base to the ligula's margin (Fig. 1F). The male parameres also differ from those occurring among taxa of other *Mecyclothorax* subgenera, with the right paramere club-shaped and broadly setose apically (Fig. 5C), and the left paramere broadly conchoid.

Member species. The six species of this subgenus were revised by Liebherr (2011), and comprise the five species in this analysis (Fig. 7) plus *M. placens* (Broun). All species are restricted to North Island, New Zealand.

New taxonomic status. Liebherr and Marris (2009) proposed this clade as a distinct genus based on the great disparity between *Meonochilus* spp. and other New Zealand species currently assigned to subgenus *Mecyclothorax*. A subsequent cladistic analysis (Liebherr 2011) with taxon representation inadequate to display the phylogenetic structure within *Mecyclothorax* affirmed that generic status. The current analysis including a much more comprehensive sampling of *Mecyclothorax* spp. requires revision of that decision, with *Meonochilus* now treated as a subsidiary monophyletic subgenus of *Mecyclothorax* (Fig. 7). The member species include: 1, *Mecyclothorax* (*Meonochilus*) *amplipennis* (Broun) comb. n.; 2, *Mecy-*

clothorax (*Meonochilus*) *bellorum* (Liebherr) comb. n.; 3, *Mecyclothorax* (*Meonochilus*) *eplicatus* (Broun) comb. n. ; 4, *Mecyclothorax* (*Meonochilus*) *placens* (Broun) comb. n.; 5, *Mecyclothorax* (*Meonochilus*) *rectus* (Liebherr) comb. n.; 6, *Mecyclothorax* (*Meonochilus*) *spiculatus* (Liebherr) comb. n.

subgenus *Mecyclothorax* Sharp, 1903

Diagnosis. This subgenus holds most of the species-level diversity in the genus, and within those radiations character diversity is rampant, making setal configurations, body form, or mensural characters useless for diagnosis. The best means to diagnose this group is through male genitalic characters, as no species of this subgenus studied to date exhibit a flagellum on the internal sac. Instead, the gonopore is surrounded by either a donut-shaped, soft expansion, or this area of the sac bears a scoop-like flagellar plate, well sclerotized and even ridged, with the gonopore present in membrane lying on the convex surface of this plate (Fig. 4F, G). The male median lobe also exhibits an opercular flap: i.e. a sclerotized triangle articulated with membrane that lies at the distal end of the ostium (Fig. 4G). Male parameres are elongate, with the left paramere generally narrow basally with the apex extended as an attenuate whip (Fig. 5D). External characters differ greatly across the pectinate comb of taxa comprising the base of the radiation – *M. monteithi* to *M. globicollis* (Fig. 7) – though several external characters can assist in assignment of species to this subgenus. First, the labrum is emarginate apically, either distinctly as in *M. goweri* (Fig. 1A), or less so as in *M. montivagus* (Fig. 8D). The ligular margin is generally truncate with the ligular setae well separated (Fig. 1G), though as exceptions, the ligula is apically rounded in the Papuan taxa *M. brispex* and *M. andersoni* (Fig. 7, Liebherr 2017b). The prosternum exhibits a smooth to distinctly punctate anteapical groove, though never any other punctures. The parascutellar striole is present, and may be smooth or punctate, with up to 8 punctures along its length (Fig. 8D–E). The female reproductive tract is nearly exclusively characterized by the spermathecal duct entering the dorsal surface of the bursa directly dorsad the juncture of the common oviduct with the bursa copulatrix (Fig. 6F). However, based on the cladistic analysis (Fig. 7), entry of the spermathecal duct at the bursal-common oviduct juncture–as in subgenera *Eucyclothorax* and *Qecyclothorax*–atavistically and independently re-evolves in *M. brispex* and the Australian sister taxa *M. lateralis* and *M. minutus* (Fig. 6E).

Member species. The immense diversity of species comprising this subgenus is represented by 25 species in the cladistic analysis. The various species known from Norfolk Island (Moore 1985), Lord Howe Island (Moore 1992), Borneo (Baehr and Lorenz 1999), Java (Andrewes 1933, Louwerens 1949, 1953; 3 of 5 resident species analyzed); Papua New Guinea (8 species, Guéorguiev 2013, Liebherr 2008a, 2017b), St. Paul and Amsterdam Islands (Enderlein 1909, Jeannel 1940), and New Zealand (Liebherr and Marris 2009) all are members of this clade (Fig. 7). Examination of illustrations of male genitalia for other New Guinean species (Baehr 1992, 1995, 1998, 2002, 2008, 2014) indicates that the entire 22 species currently known from New Guinea belong to this subgenus. Phylogenetic placement of *M. montivagus* of Hawaii, and *M. marau* of Tahiti near *M. punctipennis* of Australia, the hypothesized colonist taxon for both the Hawaiian and Tahitian radiations (Liebherr 2013, 2015) indicates that these species appropriately act as surrogates for the entire 239 species of the Hawaiian *Mecyclothorax* radiation (Liebherr 2015) plus the 108 species comprising the Society Island radiation on Tahiti and Moorea (Liebherr 2012, 2013). The Australian *Mecyclothorax* fauna is shown to be biogeographically polyphyletic, with the Australian species *M. lateralis*, *M. minutus*, *M. ambiguus*, and *M. punctipennis* latecomers (Fig. 7) relative to member taxa of *Eucyclothorax* and *Qecyclothorax*, with the late-arriving branch of the Australian *Mecyclothorax* fauna having been derived from New Guinean roots. The two species recently described from Timor Leste (Baehr and Reid 2017) also appear to be members of this subgenus based on their gracile body form with cordate pronotum, largely impunctate ventral body surface, and lack of a flagellum in the male aedeagal median lobe.

subgenus *Phacothorax* Jeannel, 1944

Diagnosis. The species comprising this subgenus exhibit a remarkable diversity of body forms (Figs 9, 16, 20), but all species share a reduced or absent parascutellar striole (Jeannel 1944). The elytra either lack evident discal striae (Figs 9D–E, 16A, C), or the striae are shallow and smooth to only indistinctly punctate (Figs 9A–C, 16B–D, E, 20). The scutellum is narrow, less than twice as broad as long. As in the ground-plan for *Mecyclothorax*, the lateral elytral setae are arrayed in an anterior series of seven setae plus a posterior series of 6 setae. The vertex of the head is convex behind the eyes, and the ocular lobe meets the gena at a very obtuse angle without any groove marking the juncture. The prosternum, synapomorphously, either lacks an anteapical groove, or the groove is very broad, shallow and smooth (Fig. 2C). The abdomen bears a single seta each side of the apical ventrite in all males, and two setae each side in females complemented by a trapezoidal medial patch of 4–5 setae (for specimens of those genders observed among the various species). As Jeannel (1944, fig. 1) reported, the parameres are much like those of subgenus *Mecyclothorax* (Figs 5D–E, 11, 22). The male aedeagal median lobe internal sac may bear a well-developed flagellum, flagellar shield, and dorsal plate (e.g. Fig. 10D), or the flagellar apparatus may be secondarily reduced, as in *M. fleutiauxi* and *M. jeanneli*, where it is hypothesized that only the flagellar sheath remains (Fig. 10M, Q). As in males of the subgenera *Eucyclothorax* and *Qecyclothorax*, the male aedeagal

median lobe ostial opening is simple, without an ostial ventroapical operculum. The female reproductive tract exhibits extensive disparity in configuration, plesiomorphically exhibiting a helminthoid sclerite and spermathecal duct entering at the bursal-common oviduct juncture (Figs 12A–C, G, 23B), or in derived configurations at the apex of a single-lobed bursa copulatrix (Fig. 23A, D), or at the apex of a dorsal lobe in a bilobed bursal configuration (Fig. 12D–E). Finally, body coloration is uniformly somber, with head capsule piceous, pronotal disc piceous without contrasting margins, and slightly paler, rufopiceous elytra and concolorous sutural intervals. The legs are paler–brunneous, rufobrunneous, or flavobrunneous–generally without contrasting coloration on the femora (exceptions noted under appropriate species treatments).

Member species. There are 15 species assignable to subgenus *Phacothorax*, with all species restricted to New Caledonia.

Identification key to adults of *Mecyclothorax* subgenus *Phacothorax* of New Caledonia

1 Pronotal base broad, hind angles well defined, MPW/BPW = 1.30–1.40 (Figs 2A, 9A–C) 2
– Pronotal base narrow relative to maximal width, hind angles either broadly rounded, or if well-defined, MPW/BPW = 1.66–3.91 (Figs 2B, 9D–E, 16, 20)..... 4
2 Anterior and posterior supraorbital setae present; pronotal lateral seta present 3
– A single posterior supraorbital setae present; pronotal lateral seta absent..... 1. *M. laterobustus* Liebherr sp. n.
3 Sutural stria and striae 3–6 deep on disc, stria 2 shallower, nearly effaced between positions of dorsal elytral setae (Fig. 9B); male aedeagal median lobe broadly, smoothly rounded apically, flagellum broadly curved dorsally toward lobe apex (Fig. 10C–D)..... 2. *M. laterosinuatus* Liebherr sp. n.
– Sutural stria deep on disc, striae 2–6 nearly as deep, stria 2 smooth between positions of dorsal elytral setae (Fig. 9C); male aedeagal median lobe narrowly rounded to a downwardly oriented tip, flagellum curved ventral toward apex, a patch of large spicules apicad flagellum in uneverted condition (Fig. 10F–H) ..... 3. *M. laterorectus* Liebherr sp. n.
4 Head with only the posterior supraorbital seta present each side, the anterior supraorbital seta lacking (Fig. 1B) 5
– Head with two supraorbital setae each side (as in Fig. 1C) 6
5 Male aedeagal median lobe with apex prolonged beyond ostial opening to acuminate tip(Fig. 10I–M); female bursa copulatrix bilobed, but dorsal lobe much shorter than ventral lobe (Fig. 12D); distributed from Me Maoya to Ningua (Fig. 15) ..... 4. *M. fleutiauxi* (Jeannel)
– Male aedeagal median lobe briefly projected beyond ostial opening to a narrowly rounded tip (Fig. 10N–R); female bursa copulatrix bilobed with dorsal lobe as long as ventral lobe (Fig. 12E); distributed from Mt. Humboldt to Forêt Nord (Fig. 15)..... 5. *M. jeanneli* Liebherr sp. n.
6 Standardized body length larger, 4.7–5.9 mm..... 7
– Standardized body length smaller, 2.8–4.1 mm 9
7. Pronotum with only a single lateral seta each side at midlength; prosternum glabrous, metafemora with glabrous posterior margin..... 8
– Pronotum with single lateral seta on lateral reaches of disc at midlength, plus 13–14 accessory setae in the pronotal marginal bead, 4–5 setae anterad lateral seta, and 9 seta posterad; prosternum with sparse covering of elongate setae, metafemora with more than 10 fine, elongate setae along posterior margin ..... 6. *M. plurisetosus* Liebherr sp. n.
8 Elytral striae 1–8 fully developed, continuous and smooth from base to apex (Fig. 16B); pronotal disc glossy, microsculpture reduced; a deep fossa present at base of median longitudinal impression at median base, pronotal margin bead continuous across base ..... 7. *M. megalovatulus* Liebherr sp. n.
– Elytral surface smooth, striae at most suggested by obsolete longitudinal depressions on disc, any evidence of striae 1–7 absent apically (Fig. 16C); pronotal disc subiridescent due to well-developed transverse mesh microsculpture; pronotal median longitudinal impression broadened basally at pedunculate pronotal base, no marginal or basal bead present on base ..... 8. *M. octavius* Liebherr sp. n.
9 Pronotal hind angles very obtuse to obsolete, rounded, lateral margin immediately anterad angle at most slightly concave (Figs 16D–E, 20A)..... 10
– Pronotal hind angles obtuse to nearly right, lateral margin immediately anterad angle distinctly concave, the lateral margin sinuate (Fig. 20B–H)..... 12
10 Elytral striae 1–4 evident on disc, shallow to deep, contrasted with obsolete to absent striae 5–7 (Figs 16E, 20A)..... 11
– Elytral striae 1–7 all evident on disc, striae 3–4 shallower than striae 1–2, but striae 5–7 deep, smooth and continuous at elytral midlength (Fig. 16D)..... 9. *M. laterovatulus* Liebherr sp. n.
11. Elytra orbicular–MEW/EL = 0.96–and very convex (Fig. 16E), interval 8 outwardly bulging dorsad deeply impressed stria 8, the outer elytral intervals thus nearly vertical to orientation of lateral marginal depression, interval 9 not visible in dorsal view ..... 10. *M. najtae* Deuve
– Elytra more ellipsoid–MEW/EL = 0.79–0.84–and moderately convex (Fig. 20A), interval 8 convex dorsad narrowly impressed stria 8, but interval 9 visible in dorsal view, lateral intervals obtusely angled to orientation of lateral marginal depression ..... 11. *M. manautei* Liebherr sp. n.

12 Pronotal hind angles obtuse with rounded apex, not protruded (Fig. 20C–H); elytral striae 1–4 present on disc, smoothly impressed to slightly punctate, though outer striae are shallower than sutural stria 13
– Pronotal hind angles protruded, nearly right (Fig. 20B); elytra with sutural stria traceable though shallow on disc, outer striae 2–7 obsolete, their positions evidenced by discontinuous series of extremely shallow depressions over portions of the elytral length ..... 12. *M. paniensis* Liebherr sp. n.
13 Elytral lateral marginal depression narrow outside anterior series of lateral elytral setae, the depression piceous to its margin to match coloration of elytral disc (Fig. 20D–H); male aedeagal median lobe apex downturned at tip, a small hitch or deep invagination nearly always present along apical face (Fig. 21A–D, F–L) [except *M. kanak* form Q of couplet 15, Fig. 21E] 14
– Elytral lateral marginal depression broad outside anterior series of lateral elytral setae, translucent brunneous outer reaches of explanate margin contrasted with piceous inner portion and elytral disc (Fig. 20C); male aedeagal median lobe apex subparallel dorsoventrally, the apical face somewhat flattened but without small hitch or distinct invagination (Fig. 17M–N) ..... 13. *M. mouensis* Moore & Liebherr sp. n.
14 Male aedeagal median lobe rounded apically, with only a very small hitch in the apical margin or no hitch at all (Fig. 21E, L, N) 15
– Male aedeagal median lobe with distinct invagination along apical face (Fig. 21A–D, F–K), though curvature and dorsoventral breadth of median lobe apex may vary (Fig. 26); female basal gonocoxite with narrow spiculate band along mediobasal margin (Fig. 24D) ..... 14. *M. kanak* Moore & Liebherr sp. n.
15. Male aedeagal median lobe slightly narrowed apically, with tip rounded and smooth, ostial opening asymmetrical apically, its ventroapical margin extended more toward tip than dorsoapical margin (Fig. 21E) [see Male genitalia section of *M. kanak* species description] ..... 14. *M. kanak* Moore & Liebherr sp. n., form Q
– Male aedeagal median lobe apex broadly downturned, tip broadly rounded, apical margin with or without a minute hitch, ostial opening broadly rounded, symmetrical apically relative to tip (Fig. 21L, N); female basal gonocoxite with broad spiculate band along mediobasal margin, the spicules flattened, blunt apically (Fig. 24E).. 15. *M. picdupinsensis* Liebherr sp. n.

1. *Mecyclothorax laterobustus* Liebherr, sp. n.

http://zoobank.org/F59062DE-95C1-48B7-A947-CAFE2EA6F98C
Figures 5E, 9A, 10A–B, 12A, 13A, 14

Diagnosis. These beetles are very robust, with a broad pronotum and broadly convex elytra (Fig. 9A). The pronotal base is broad, with MPW/BPW = 1.30–1.32, and the hind angles are projected, with the pronotal lateral margin concave just before the angle. Only the posterior supraorbital seta is present, and the pronotum is glabrous. Elytral striae 1–5 are well developed basally, with striae 3–5 deeper than those of individuals of the similar appearing *M. laterosinuatus* and *M. laterorectus* (Fig. 9B–C). Standardized body length 4.1–4.4 mm. Chaetotaxy –/+//–/–//+/2/+/+.

Description (n = 5). Head capsule broad, eyes moderately convex, ocular lobe meeting gena at very obtuse angle; 16 ommatidia along horizontal diameter of eye; ocular ratio 1.33–1.42, EyL/EyD = 2.34–3.0; frontal grooves deep, arcuately convergent and deepest just posterad clypeus, briefly and shallowly extended onto clypeus; mandibles moderately elongate, mandibular ratio 1.67; ligular anterior margin rounded to ligular seta, concave between setae, the two setae separated by two setal diameters; paraglossae thin, extended as far beyond ligular margin as their basal length to margin; antennae moderately elongate, antennomere 9 length 2.0× maximal breadth; antennomere 3 glabrous except for apical ring of setae. Pronotum moderately constricted basally, with obtuse-rounded hind angles and lateral margins briefly sinuate anterad angles (Fig. 9A); MPW/BPW = 1.30–1.32, MPW/PL = 1.19–1.22; front angles protruded anteriorly, but anterior margin narrowly approaching head capsule, APW/BPW = 0.69–0.71; basal margin broadly convex, beaded from just mesad deep, longitudinal laterobasal depression to and around obtuse-rounded hind angle; median longitudinal impression deep and narrow on disc, broader and shallower approaching base, absent anterad very shallow anterior transverse impression; proepisternum separated from prosternum by a very shallow groove anteriorly, but with a deep, slightly punctate groove ventrally; prosternal process deeply and narrowly depressed between procoxae, that depression extended 1/3 distance toward anterior prothoracic margin. Elytra broadly ovoid, humeri broad, humeral angle obtusely rounded laterad pronotal hind angles; MEW/EL = 0.87–0.93; basal groove evenly arcuate from scutellum to humeral angles, with depression at bases of sutural and elytral striae 4–5; sutural stria deep throughout length, stria 2 obsolete though traceable, stria 3 somewhat deeper, striae 4–5 deep in basal half, striae 6–7 obsolete; only sutural stria and stria 8 evident apically, elytra appressed and conjoined apically, sutural intervals narrower and upraised at apex. Pterothoracic mesepisternal anterior furrow with 6–7 deep punctures; mesosternal-mesepisternal suture complete (as in Fig. 3A); metepisternum maximum width/lateral length = 1.0; metepisternal-metepimeral suture incomplete, shallower and incomplete laterally. Abdomen with deep crescent-shaped depression along suture between first and second ventrite, second ventrite depressed within crescent; suture between second and third ventrites reduced though traceable laterally; ventrites 2–6 with broad, shallow, linear plaques near lateral margin. Microsculpture of frons a shallow transverse mesh, sculpticells twice as

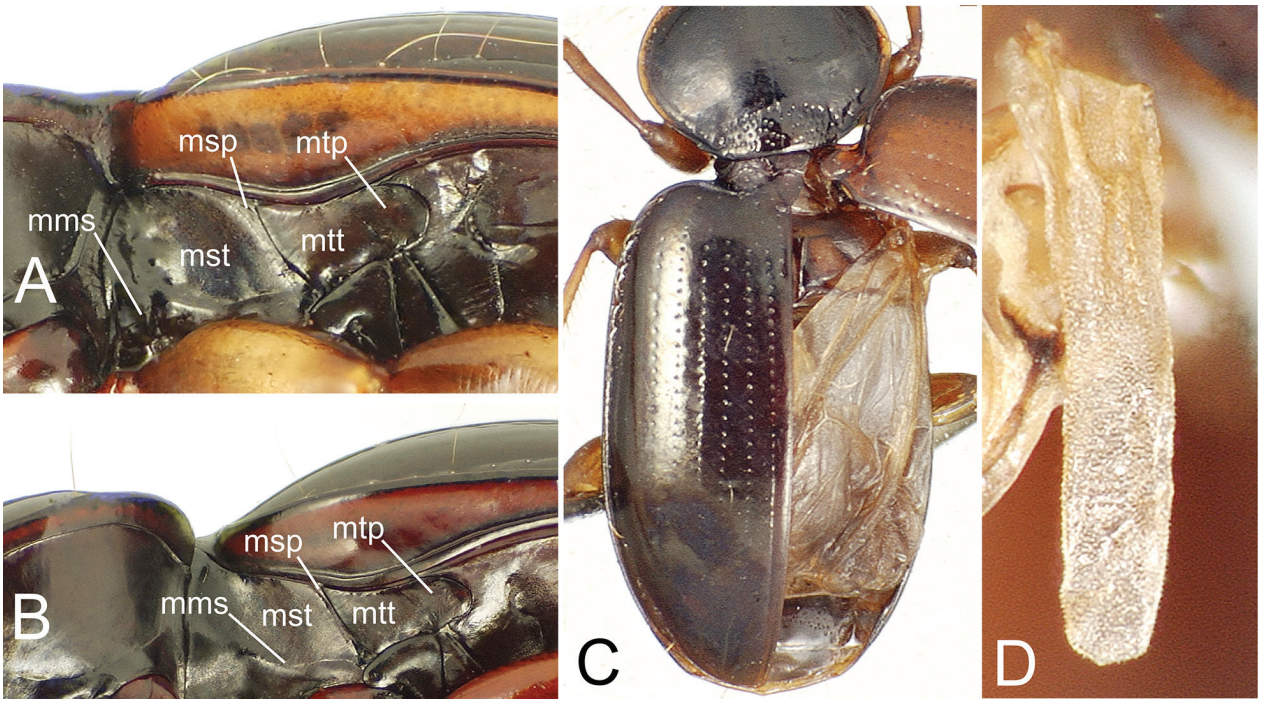

Figure 3. Thoracic structures of *Mecyclothorax* spp. **A–B**. Lateral view of elytral epipleuron and meso-and metapleurites: **A**, *M. laterorectus*; **B**, *M. fleutiauxi*. **C–D**. Metathoracic flight wing: **C**, *M. punctipennis*, showing fully developed flight wing folded under elytron; **D**, *M. lissus*, stenopterous wing rudiment that extends beyond metanotum, rudimentary wing venation present at base of strap. Abbreviations include: **mms**, mesepisternal-mesosternal suture; **msp**, mesepimeron; **mst**, mesepisternum; **mtp**, metepimeron; **mtt**, metepisternum.

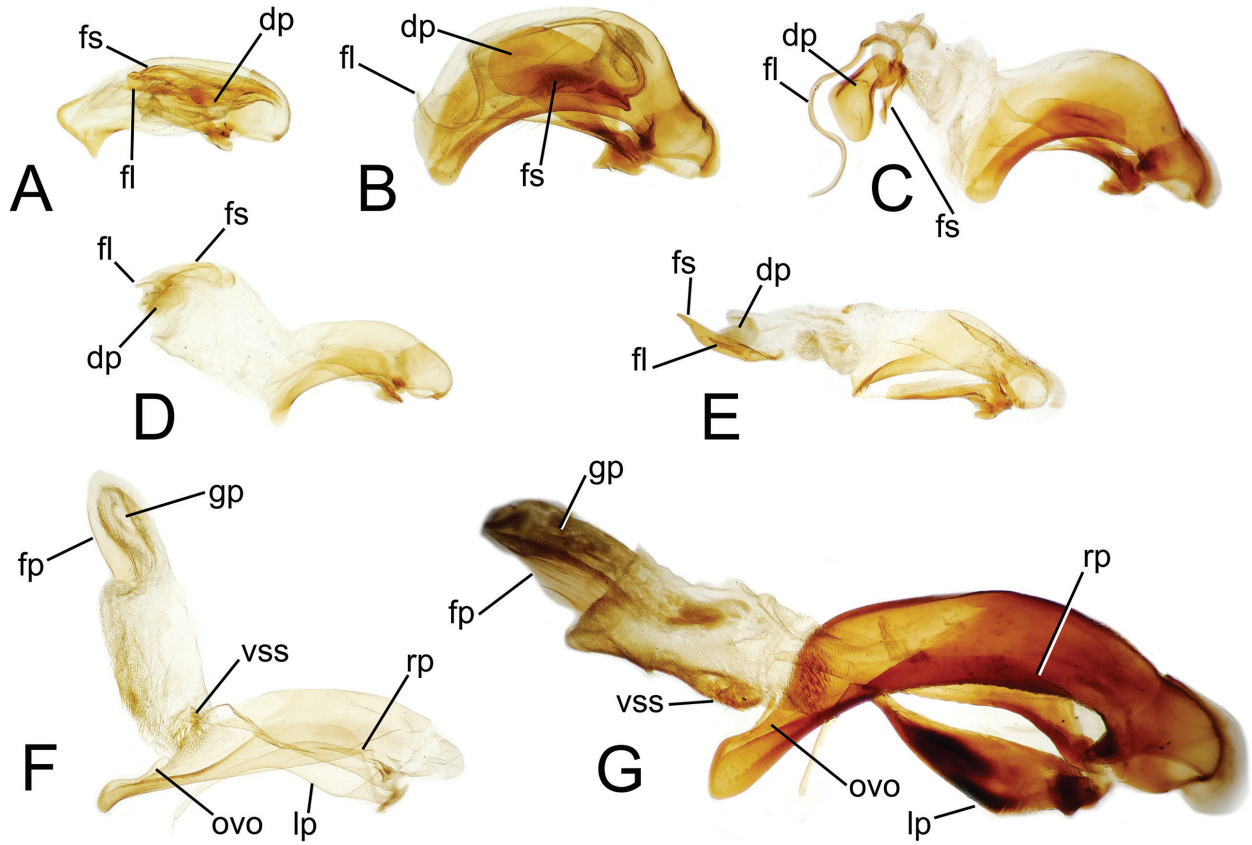

Figure 4. Male aedeagal median lobe and parameres of *Mecyclothorax* spp., right lateral view, internal sac everted in **C–G**: **A**, *M. blackburni*; **B–C**, *M. peryphoides*; **D**, *M. moorei*; **E**, *M. lewisensis*; **F**, *M. punctipennis*; **G**, *M. montivagus*. See Table 2 for abbreviations.

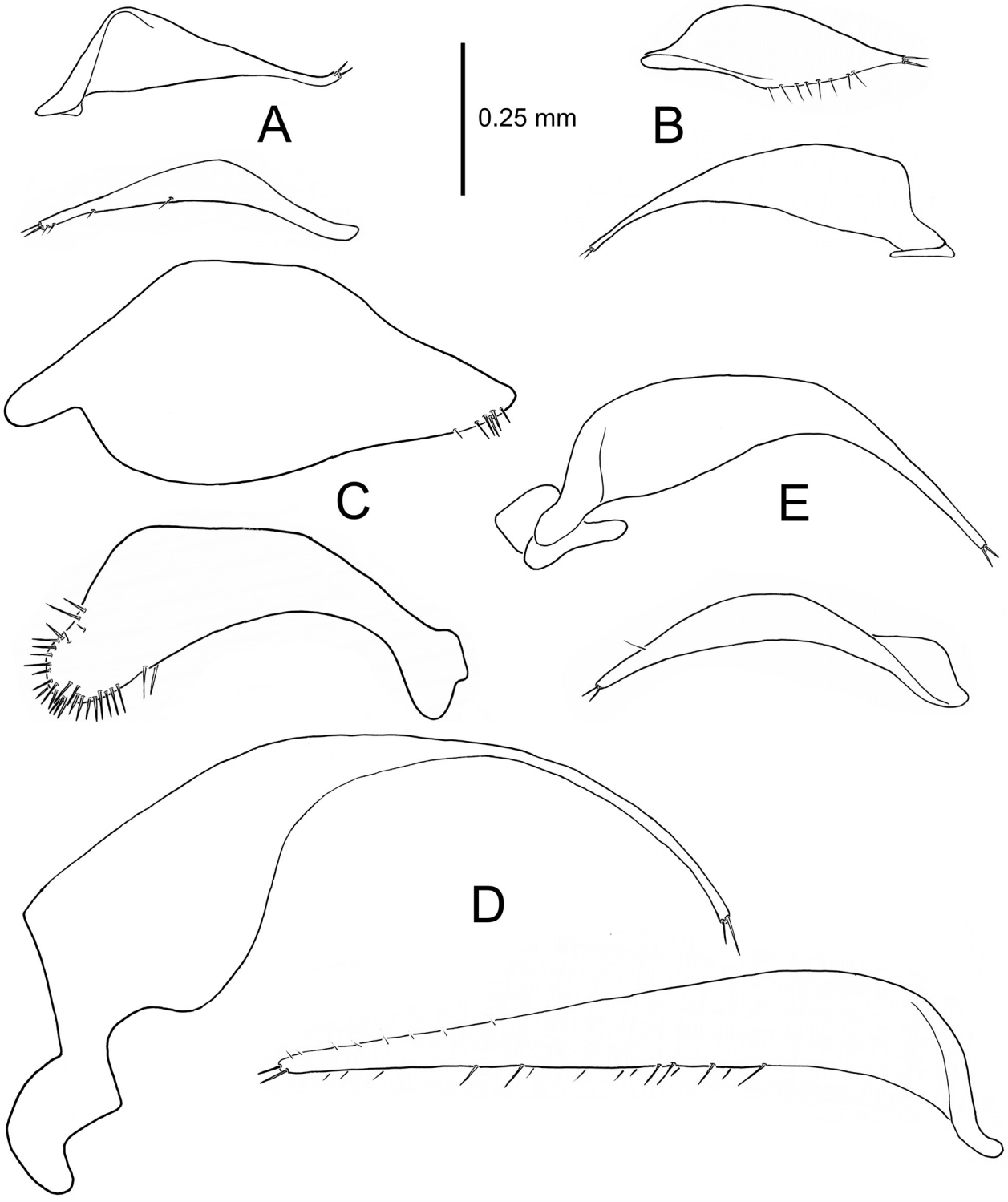

Figure 5. Paired left (above) and right (below) parameres of *Mecyclothorax* spp. (ectal view): **A**, *M. blackburni*; **B**, *M. storeyi*; **C**, *M. amplipennis*; **D**, *M. montivagus*; **E**, *M. laterobustus.* As the aedeagal assembly of *M. storeyi* males is inverted relative to other *Mecyclothorax* species (Moore 1984), the configuration of the upper, or right paramere of *M. storeyi* should be compared to the ventral, or left parameres of the other species, and vice versa.

broad as long, these mixed with isodiametric sculpticells on vertex; pronotal disc and base covered with elongate transverse mesh plus transverse lines, surface iridescent; elytral iridescent, disc with loose elongate transverse mesh, apex with very elongate transverse mesh, sculpticell breadth 3–4× length.

Male genitalia (n = 1). Antecostal margin of male mediotergite IX distally angulate, little extended (Fig. 10B);

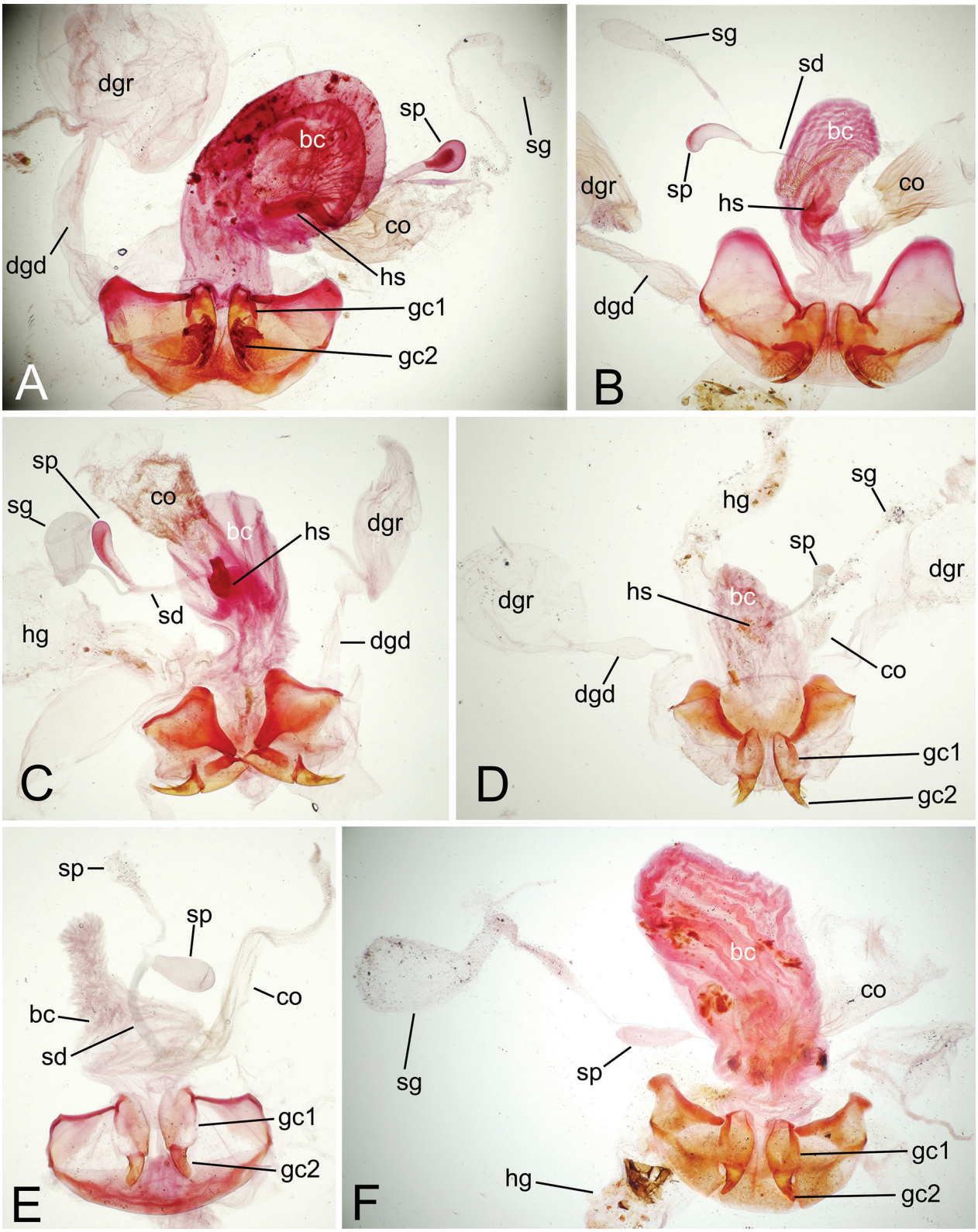

Figure 6. Female reproductive tract, gonocoxites and associated laterotergites, *Amblytelus* and *Mecyclothorax* spp: **A**, *A. matthewsi*; **B**, *A. brevis*; **C**, *M. blackburni*; **D**, *M. storeyi*; **E**, *M. minutus*; **F**, *M. rectangulus*. See Table 2 for abbreviations.

right paramere very elongate, moderately narrow, with a single seta on dorsal margin distant from two apical setae (Fig. 5E); left paramere narrow basally, evenly narrowed to a whip-shaped apex, two longer setae at apex; aedeagal median lobe shaft robust, broad dorsoventrally (Fig. 10A), median lobe apex broad, sides subparallel, with tip broadly rounded; aedeagal internal sac with flagellum, flagellar sheath, and sclerotized dorsal plate.

Female reproductive tract (n = 1). Bursa copulatrix elongate, length more than twice circumference, surface translucent, membranous (Fig. 12A); spermathecal duct entering near bursa-common oviduct juncture with duct oriented toward right side of bursa, duct longer than spermathecal reservoir; a rounded laminar helminthoid sclerite present at base of spermathecal duct; spermatheca fusiform on narrow duct, spermathecal gland duct entering at base of spermathecal reservoir; basal gonocoxite 1 with apical fringe of two setae near medial margin, a series of small setae lining medial margin (Fig. 13A); gonocoxite 2 moderately broad basally, basal width about half medial length; two gracile lateral ensiform setae of moderate length present.

Types – Holotype male (MNHN): NEW CALEDONIA / Ningua Res.camp / 12-13Nov 2001 / G.B.Monteith // QM Berlesate 1039 / 21°45'Sx166°09'E / Rainforest, 1100m / Sieved litter // QUEENSLAND / MUSEUM LOAN / Date: Nov. 2003 / No. LEN-1686 (green label) // HOLOTYPE / Mecyclothorax / laterobustus / J.K.Liebherr 2017 (black-bordered red label).

Paratypes (10 specimens). NEW CALEDONIA: Ningua Reserve, camp, 1100 m el., 21°45'S 166°09'E, rainforest, sieved litter, 12-13-xi-2001, lot 1039, Monteith (QMB, 4), near summit, rainforest, 1300 m el., 21°45'S 166°09'E, berlesate, sieved litter, 13-xi-2001, lot 1052, Monteith (QMB, 3); Plateau de Dogny, rainforest, 910 m el., 21°37'S, 165°53'E, berlesate sieved litter, 16-xi-2002, lot 1085, Burwell (QMB, 3).

Etymology. The very broad and robust body form of these beetles (Fig. 9A) suggests the compound, adjectival species epithet laterorobustus.

Distribution and habitat. This species is known from two localities, Ningua Reserve and Plateau de Dogny (Fig. 14), and specimens have been collected from 900–1300 m elevation. The three collecting events are all based on recovering specimens from sieved litter, consistent with an interpretation that these beetles occupy ground-level microhabitats.

2. *Mecyclothorax laterosinuatus* Liebherr, sp. n.

http://zoobank.org/BC6BAC70-3131-45CD-B8DE-0D72BB0D70A3
Figures 9B, 10C–E, 11A, 12B, 13B, 14

Diagnosis. These beetles are very similar in external appearance to those of *M. laterorectus* (Fig. 9B–C) below, sharing the moderately robust body form and cordate pronotum, though the pronotal base is slightly broader relative to the maximal pronotal width in this species: MPW/BPW = 1.28–1.33. This species also differs from *M. laterorectus* in the very shallow second elytral stria contrasted to the deeper sutural stria and striae 3–6. Like the preceding *M. laterobustus*, the pronotal hind angles protrude, with the pronotal lateral margin concave before the angle, but in this species and the following, the pronotal lateral seta is present. Also, this and the following species exhibit both anterior and posterior supraorbital setae. Standardized body length 3.7–4.3 mm. Chaetotaxy +/+//+/–//+/2/+/+.

Description (n = 5). Head capsule broad, eyes convex, ocular lobe meeting gena at obtuse angle very close to eye posterior margin; 12–14 ommatidia along horizontal diameter of eye; ocular ratio 1.43–1.50, ocular lobe ratio 0.84–0.89, EyL/EyD = 2.50–2.65; frontal grooves nearly straight from posterior terminus inside anterior supraorbital seta to deepest point just posterad clypeus, briefly and shallowly extended onto clypeus; mandibles moderately elongate, mandibular ratio 1.8; ligular anterior margin narrowly rounded to ligular seta, concave between setae, the two setae separated by two setal diameters; paraglossae thin, extended as far beyond ligular margin as their basal length to margin; antennae elongate, antennomere 9 length 2.25× maximal breadth; antennomere 3 glabrous except for apical ring of setae. Pronotum distinctly constricted basally, cordate, hind angles obtuse rounded, lateral pronotal margins subparallel anterad hind angles, then distinctly divergent anteriorly (Fig. 9B); MPW/BPW = 1.37–1.40, MPW/PL = 1.24–1.27; front angles protruded, obtusely angulate, APW/BPW = 0.75–0.78; basal margin slightly convex, nearly straight between broadly upraised hind margins posterad broad laterobasal depressions; laterobasal depression with longitudinal tubercle inside hind angle, and broad furrowlike longitudinal extension onto disc; median longitudinal impression fine and shallow on disc, with deep longitudinal pitlike depression anterad median base, absent anterad very broad and shallow anterior transverse impression; proepisternum separated anteriorly from prosternum by fine shallow groove, distinctly separated ventrally by smooth, deep groove; prosternal process deeply, narrowly between procoxae, that deep depression extended 1/3 distance toward anterior prothoracic margin. Elytra broadly ellipsoid, humeri extended laterally, humeral angle obtusely rounded outside pronotal hind angles; MEW/EL = 0.81–0.86; basal groove evenly arcuate from scutellum to humeral angles, with depressions at bases of sutural and elytral striae 3–5; sutural stria deep throughout length, stria 2 shallow, obsolete on disc, striae 3–5 deep, stria 6 shallow, and stria 7 obsolete in basal half; striae 1–2, 7 and 8 evident apically, elytra appressed and conjoined apically, sutural intervals narrower and upraised at apex. Pterothoracic mesepisternal anterior furrow with five broad depressions in one to two vertical rows; metepisternum maximum width/lateral length = 1.1; mesosternal-mesepisternal suture complete (as in Fig. 3A); metepisternal-metepimeral suture incomplete, shallower and incomplete laterally. Abdomen with deep crescent-shaped depression along suture between first and second ventrite, second ventrite depressed within crescent; suture between second and third ventrites reduced, incomplete laterally; ventrites 2–6 with broad, shallow, linear plaques near lateral margin. Microsculpture of frons an evident transverse mesh, transverse sculpticells mixed with isodiametric sculpticells on vertex; pronotal disc and base covered with elongate transverse mesh plus transverse lines,

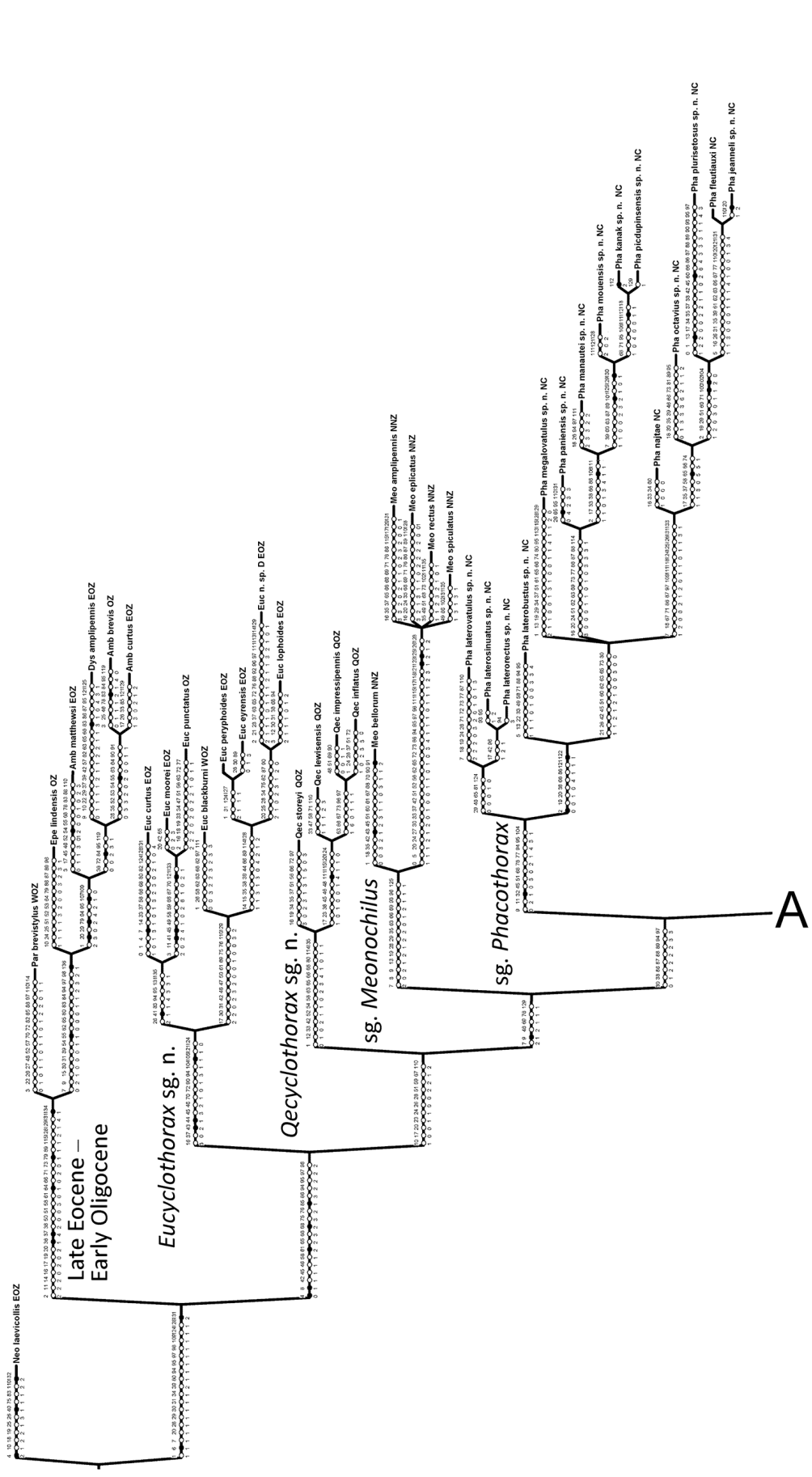

Figure 7. Strict consensus cladogram of 16 equally most-parsimonious trees derived from cladistic analysis of 65 moriomorphine taxa, including the secondary outgroup *Neonomius laevicollis*, six primary outgroup taxa in *Ambbytelus* and allied genera, and 58 ingroup terminals; 57 *Mecyclothorax* species plus two genitalic forms of *M. andersoni*. Species terminals are labeled with species name and three-letter abbreviation of relevant generic or subgeneric name. Full listing of included taxa along with subgeneric assignments is presented in Table 2. Cladistic analysis is based on 137 characters (see character descriptions for nature of each character Areas occupied by the included taxa indicated by abbreviations following species epithets: **Bo**, Borneo; **EOZ**, eastern Australia, i.e. east of the Nullarbor Plain; **FP**, French Polynesia, Tahiti; **HI**, Hawaiian Islands, Maui; **Jv**, Java; **LH**, Lord Howe Island; **NC**, New Caledonia; **Nf**, Norfolk Island; **NNZ**, North Island of New Zealand; **NZ**, generally distributed across New Zealand; **OZ**, generally distributed across Australia; **PNG**, Papua New Guinea; **QOZ**, restricted to Queensland, Australia; **SNZ**, South Island of New Zealand plus Chatham Islands; **SP&A**, St. Paul and Amsterdam Islands; **WOZ**, western Australia, i.e. west of the Nullarbor Plain.

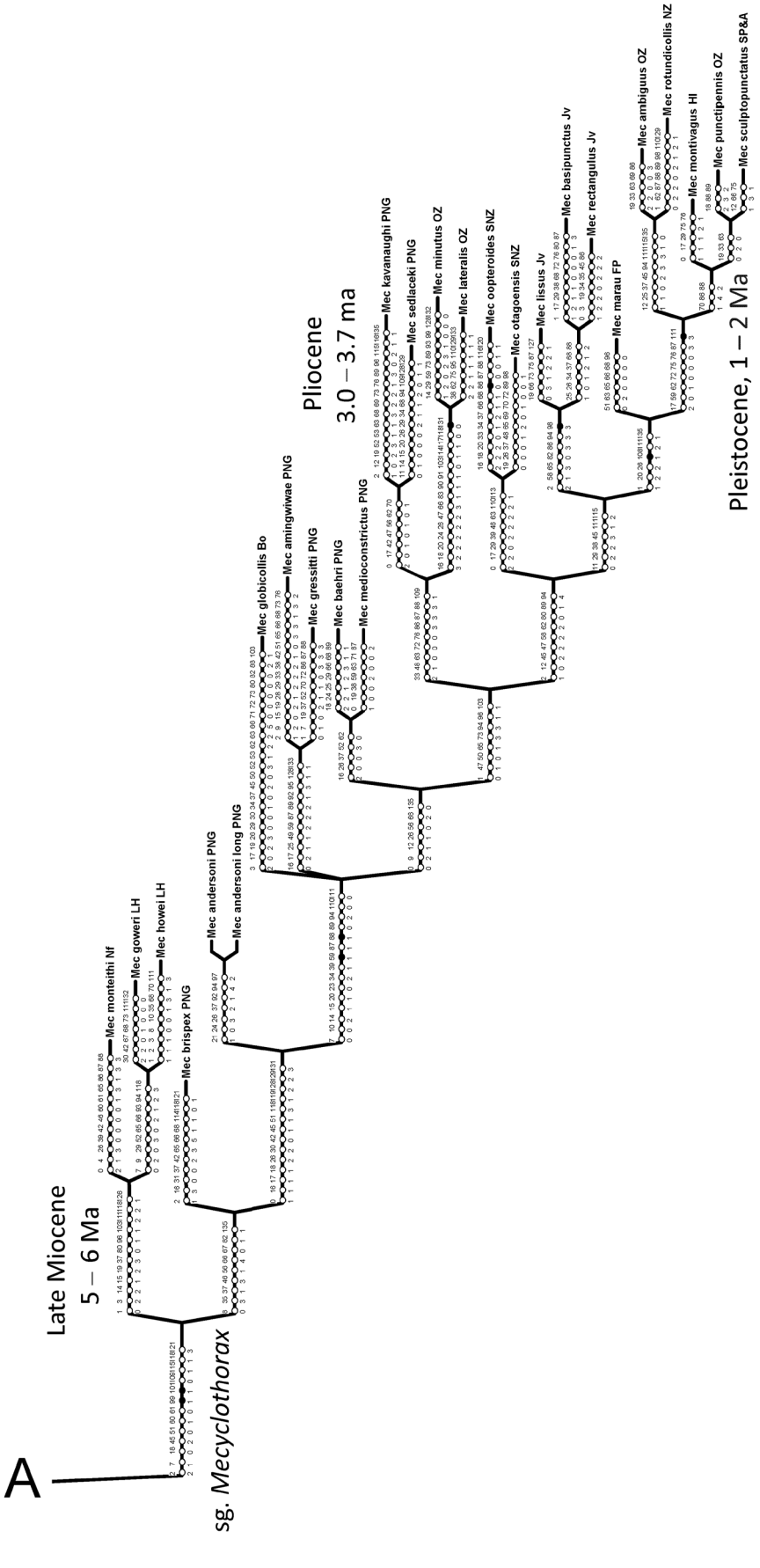

Figure 7. Continue.

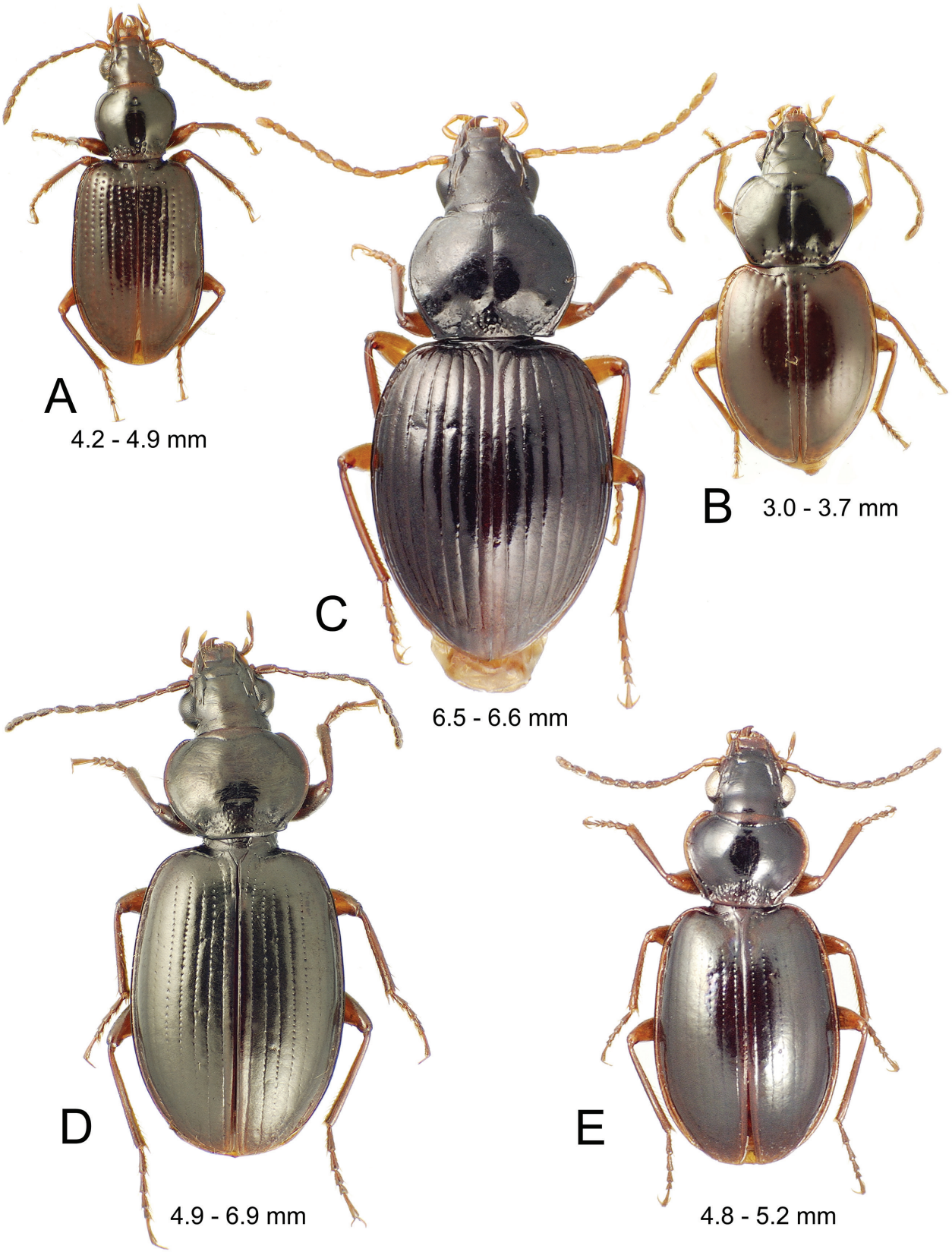

Figure 8. *Mecyclothorax* spp., dorsal view, with subgeneric assignments: **A**, *M.* (*Eucyclothorax*, subgen. n.) *blackburni* (type species); **B**, *M.* (*Qecyclothorax*, subgen. n.) *storeyi* (type species); **C**, *M.* (*Meonochilus*, status n.) *amplipennis* (type species); **D**, *M.* (*Mecyclothorax*) *montivagus* (type species); **E**, *M.* (*Mecyclothorax*) *lissus*.

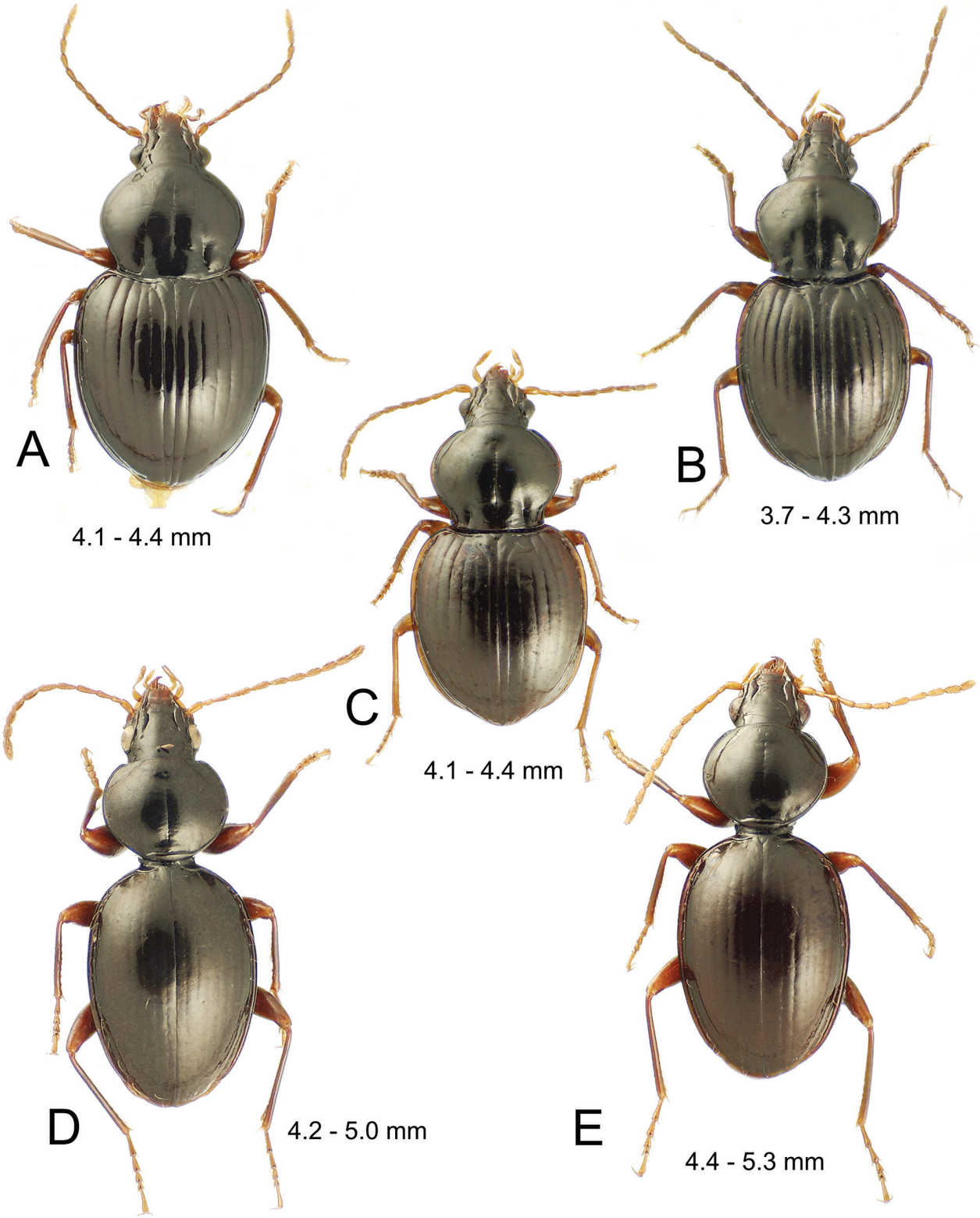

Figure 9. New Caledonian *Mecyclothorax* (*Phacothorax*) spp., dorsal view: **A**, *M. laterobustus*; **B**, *M. laterosinuatus*; **C**, *M. laterorectus*; **D**, *M. fleutiauxi*; **E**, *M. jeanneli*.

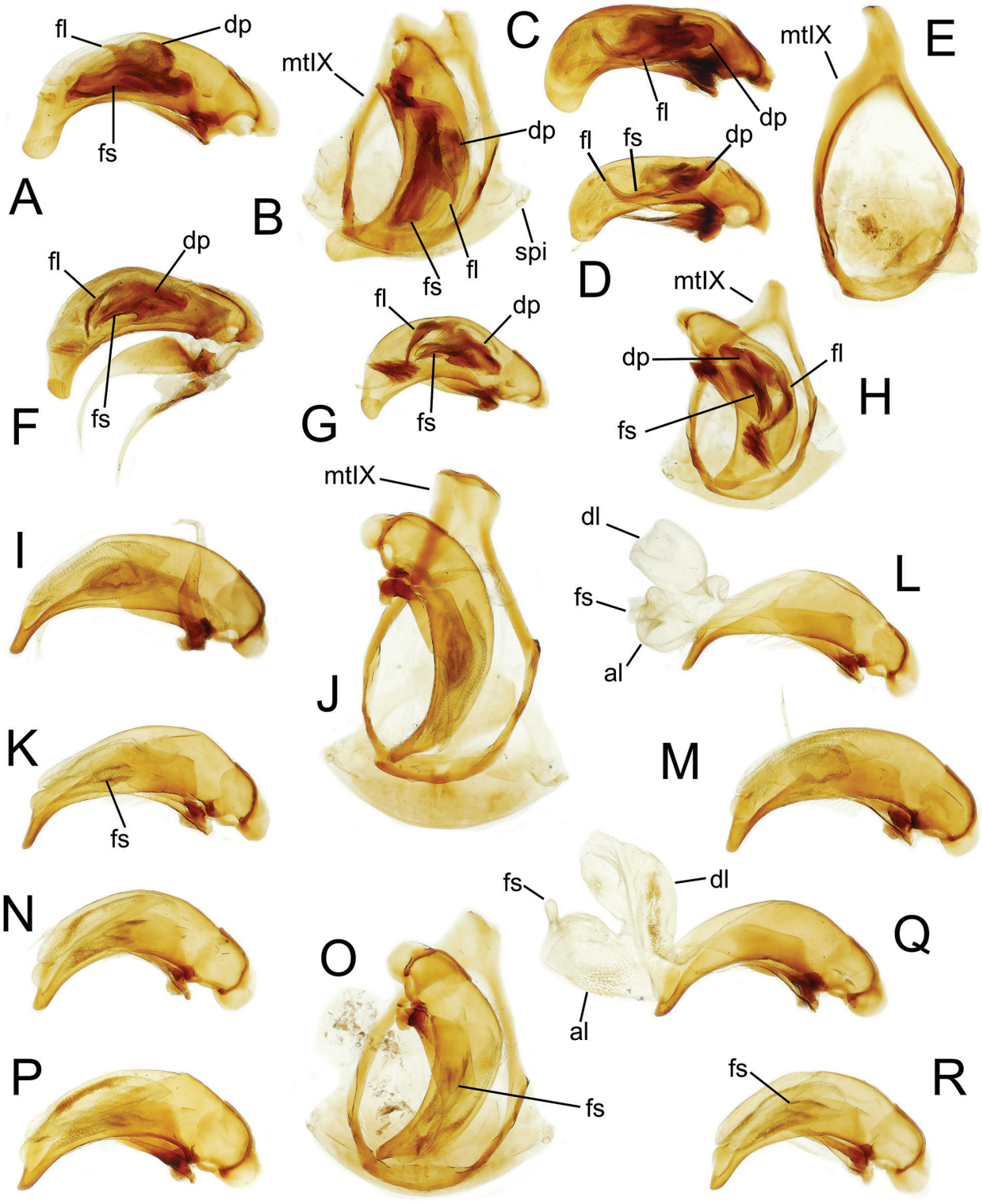

Figure 10. Male aedeagal median lobe and parameres, and ring sclerite–mediotergite plus antecostal margin, tergite IX–of *Mecyclothorax* (*Phacothorax*) spp.: **A–B**, *M. laterorobustus*, right view, dorsal view in situ (Ningua); **C**, *M. laterosinuatus*, right view (Col d'Amieu); **D**, *M. laterosinuatus*, right view (Touho TV tower); **E**, *M. laterosinuatus* ring, dorsal view; **F**, *M. laterorectus*, right view (Mt. Panié); **G–H**, *M. laterorectus*, right vew, dorsal view in situ (Mandjélia); **I–J**, *M. fleutiauxi*, right view, dorsal view in situ (Mt. Do); **K–L**, *M. fleutiauxi*, right view, sac inverted and everted (Me Maoya); **M**, *M. fleutiauxi*, right view (Ningua); **N–O**, *M. jeanneli*, right view, dorsal view in situ (Mt. Humboldt, 1350 m); **P**, *M. jeanneli*, right view (Mt. Humboldt, 1300 m); **Q**, *M. jeanneli*, right view, sac everted (Mt. Dzumac); **R**, *M. jeanneli*, right view (Rivière Bleue). See Table 2 for abbreviations.

surface iridescent; elytra iridescent, disc with loose elongate transverse mesh, apex with very elongate transverse mesh, sculpticell breadth 3–4× length. Femora rufobrunneous basally, with a broad flavous band in apical third.

Male genitalia (n = 5). Antecostal margin of abdominal mediotergite IX angulate distally, an elongate distal extension present (Fig. 10E); right paramere very elongate, apical half narrowed into a whiplike extension (Fig. 11A), with 10 setae on ventral surface complementing the two apical setae, dorsal surface with four small setae; left paramere narrow basally, evenly extended to whiplike apex, surfaces glabrous except for two apical setae; aedeagal median lobe robust, broad dorsoapically, apex broadly curved ventrally with tip rounded (Fig. 10C–D); aedeagal median lobe internal sac with flagellum, flagellar sheath, and dorsal plate, the former two structures curved dorsad apically. The median lobes of the two figured males–Col d'Amieu (Fig. 10C) and Touho TV Tower (Fig. 10D) – differ about 10% in length, whereas the males themselves are nearly identical in standardized body length; 4.0 versus 4.05 mm. As the internal sac structures do not appear to differ except in the basal shape of the dorsal plate (differing orientation inside median lobe?), these two populations are considered conspecific.

Female reproductive tract (n = 2). Bursa copulatrix elongate, length about twice circumference, surface translucent, membranous (Fig. 12B); spermathecal duct entering near bursa-common oviduct juncture with duct oriented toward right side of bursa, duct as long as spermathecal reservoir; an elongate laminar helminthoid sclerite present at base of spermathecal duct; spermatheca fusiform on narrow duct, spermathecal gland duct entering at base of spermathecal reservoir; ligular apophysis present near base of common oviduct; basal gonocoxite 1 with apical fringe of one to two short setae laterally on apical margin, smaller microsetae scattered along apical margin, and a series of small setae lining medial margin (Fig. 13B); gonocoxite 2 broad basally, basal width slightly more than half medial length; two short, gracile lateral ensiform setae present.

Types – Holotype male (MNHN): NEW CALEDONIA / Aoupinie top camp / 2-3Nov 2001 / G.B.Monteith // QM Berlesate 1060 / 21°11'Sx165°18'E / Rainforest, 850m / Sieved litter // QUEENSLAND / MUSEUM LOAN / DATE: Nov. 2003 / No. LEN-1686 (green label) // *New Caledonia Mecyclothorax* revision / measured specimen 2 / J.K. Liebherr 2016 // HOLOTYPE / Mecyclothorax / laterosinuatus / J.K.Liebherr 2017 (black-bordered red label).

Paratypes (83 specimens; BPBM, MNHW, PMGC, QMB): see Suppl. material 2.

Etymology. Like the preceding and immediately following species, beetles of this species exhibit a basally broad pronotum (Fig. 9A–C). In this species, the distinctly sinuate lateral pronotal margin leads to the compound adjectival species epithet laterosinuatus.

Distribution and habitat. This species is broadly distributed along mid-latitudinal Grand Terre, from Touho TV tower on the north to Mt. Rembai on the south (Fig. 14), with beetles found from 400 m elevation to the summits of the occupied uplands. Of the 76 known specimens, 67 have been collected from sieved litter, indicating occupation of the ground-level microhabitat. Exceptions with situational label data include a singleton found via headlamp search at night (Will, EMEC), and two beetles collected from two flight-intercept traps (Monteith, QMB; Théry, MNMH), no doubt after crawling into the collecting tray.

3. *Mecyclothorax laterorectus* Liebherr, sp. n.

http://zoobank.org/B689EE86-804C-491D-8790-A6E9CAA437D3
Figures 1C, 2A, 2H, 3A, 9C, 10F–H, 11B, 12C, 13C, 14

Diagnosis. This third of the species characterized by robust body and a cordate, broad-based pronotum with well-defined hind angles (Fig. 9A–C), can be diagnosed by the relatively narrower pronotal base: MPW/BPW = 1.37–1.40 (Fig. 2A). Like the immediately preceding *M. laterosinuatus* there are two supraorbital setae each side, and the pronotal lateral seta is present, but the discal elytral striae 3–5 are much shallower here, only slightly deeper than the shallow stria 2. The pronotal lateral margins are subparallel basally, with the pronotal hind angle obtuse, its apex not projected. Standardized body length 4.1–4.4 mm. Chaetotaxy +/+//+/–//+/2/+/+.

Description (n = 5). Head capsule broad, eyes very convex, popeyed, ocular lobe meeting gena at obtuse angle close to eye posterior margin; 14 ommatidia along horizontal diameter of eye; ocular ratio 1.37–1.45, ocular lobe ratio 0.81–0.90, EyL/EyD = 2.56–2.89; frontal grooves nearly straight from posterior terminus inside anterior supraorbital seta to deepest point just posterad clypeus, briefly and shallowly extended onto clypeus; mandibles moderately elongate, mandibular ratio 1.7; ligular anterior margin narrowly rounded to ligular seta, concave between setae, the two setae separated by one to two setal diameters; paraglossae thin, extended as far beyond ligular margin as their basal length to margin; antennae moderately elongate, antennomere 9 length 2.0× maximal breadth; antennomere 3 glabrous except for apical ring of setae. Pronotum distinctly constricted basally, cordate, hind angles protruded and nearly right, lateral margins distinctly, briefly sinuate anterad angles (Figs 2A, 9B); MPW/BPW = 1.37–1.40, MPW/PL = 1.19–1.25; front angles only slightly protruded, rounded, APW/BPW = 0.72–0.77; basal margin broadly convex, margin broadly upraised behind broad laterobasal depression, the depression extended longitudinally onto disc as a broad sinuous furrow; median longitudinal impression fine and shallow on disc, continued to basal margin (a shallow transverse impression inside basal margin), absent anterad very shallow anterior transverse impression; proepisternum incompletely separated anteriorly from prosternum, but by a deep, smooth groove ventrally; prosternal process broadly, shallowly depressed between procoxae, that depression extended 1/3 distance to anterior prothoracic margin. Elytra

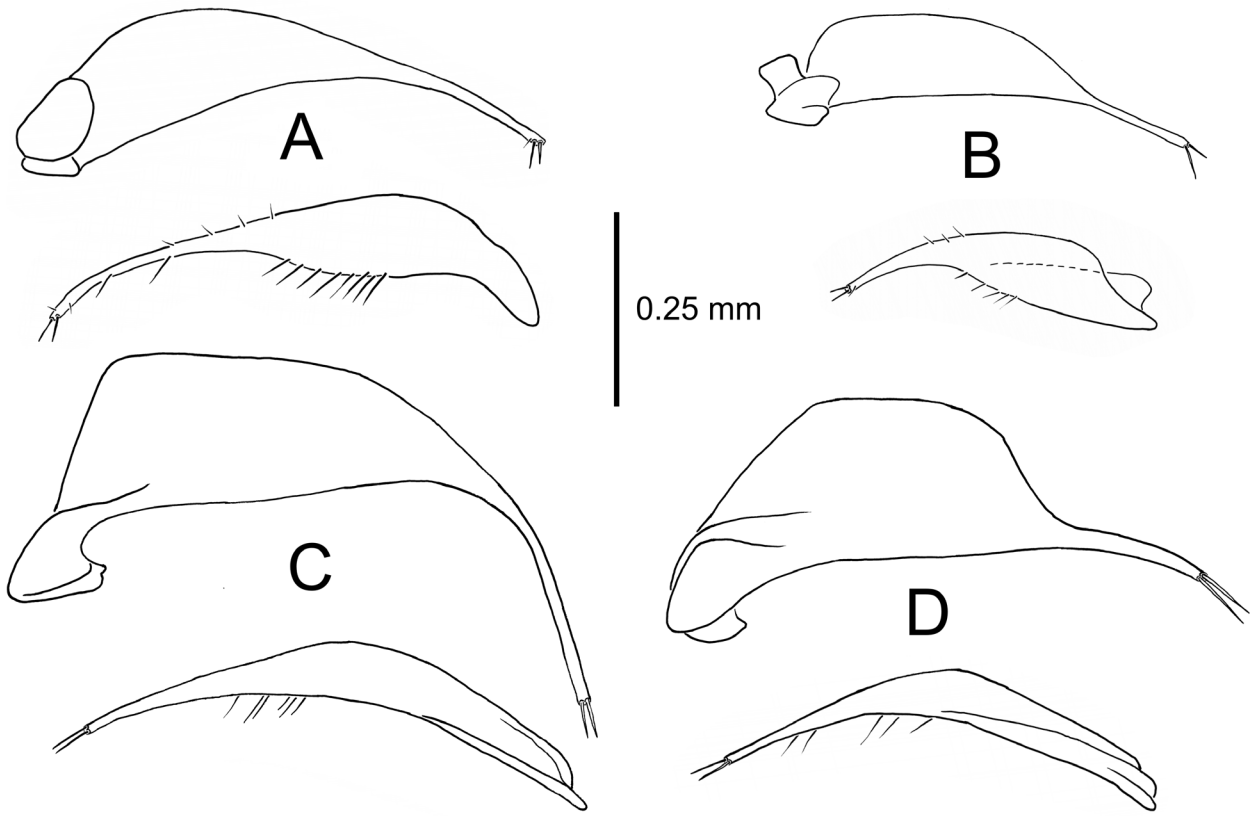

Figure 11. Paired left (above) and right (below) parameres of *Mecyclothorax* (*Phacothorax*) spp. (ectal view): **A**, *M. laterosinuatus*; **B**, *M. laterorectus*; **C**, *M. fleutiauxi*; **D**, *M. jeanneli.*

broadly ellipsoid to obovoid, humeri narrow, humeral angle obtusely rounded behind pronotal hind angles; MEW/EL = 0.82–0.86; basal groove evenly arcuate from scutellum to humeral angles, with depressions at bases of the sutural and elytral striae 4–5; sutural stria deep throughout length, striae 2–3 shallow but evident on disc, striae 4–7 deep in basal half; striae 1–2, 7 and 8 evident apically, elytra appressed and conjoined apically, sutural intervals narrower and upraised at apex. Pterothoracic mesepisternal anterior furrow with 5 broad depressions in 1–2 vertical rows; metepisternum maximum width/lateral length = 1.0; mesosternal-mesepisternal suture complete (as in Fig. 3A); metepisternal-metepimeral suture incomplete, shallower and incomplete laterally. Abdomen with deep crescent-shaped depression along suture between first and second ventrite, the second ventrite depressed within crescent; suture between second and third ventrites reduced, incomplete laterally; ventrites 2–6 with broad, shallow, linear plaques near lateral margin. Microsculpture of frons an evident transverse mesh, transverse sculpticells mixed with isodiametric sculpticells on vertex; pronotal disc and base covered with elongate transverse mesh plus transverse lines, surface of tubercle in laterobasal depression with less transverse sculpticells, surface iridescent; elytra iridescent, disc with loose elongate transverse mesh, apex with very elongate transverse mesh, sculpticell breadth 3–4× length. Femora rufobrunneous basally, with a broad flavous band in apical third.

Male genitalia (n = 3). Antecostal margin of abdominal mediotergite IX angulate, little extended distally (Fig. 10H); right paramere narrowly extended apically (Fig. 11B), with five setae on ventral margin and three on dorsal margin complementing two apical setae; left paramere narrow basally, evenly narrowed to a whiplike apex; aedeagal median lobe robust, broad dorsoventrally, apex distinctly curved ventrad to a narrowly rounded tip, its apical face slightly flattened; aedeagal median lobe internal sac with flagellum, flagellar sheath, and dorsal plate, flagellum and flagellar sheath curved ventrad apically (Fig. 10F–G), a patch of stout macrospicules present just inside ostial opening apicad flagellar structures. The median lobe apex is extended more in the specimen from Mt. Panié (Fig. 10F) than in the Mandjélia male (Fig. 10G). A third male from Mandjélia summit, 750–780 m elevation (MNHW) exhibits a lobe apex of intermediate extension. This continuous variation coupled with the extreme similarity of internal sac structures argues for conspecificity of these populations.

Female reproductive tract (n = 1). Bursa copulatrix elongate, length more than twice circumference, surface translucent, wrinkled, membranous (Fig. 12C); spermathecal duct entering near bursa-common oviduct juncture with duct oriented toward right side of bursa, duct as long as spermathecal reservoir; an elongate laminar helminthoid sclerite present near base of spermathecal duct; spermatheca fusiform on narrow duct, spermathecal gland

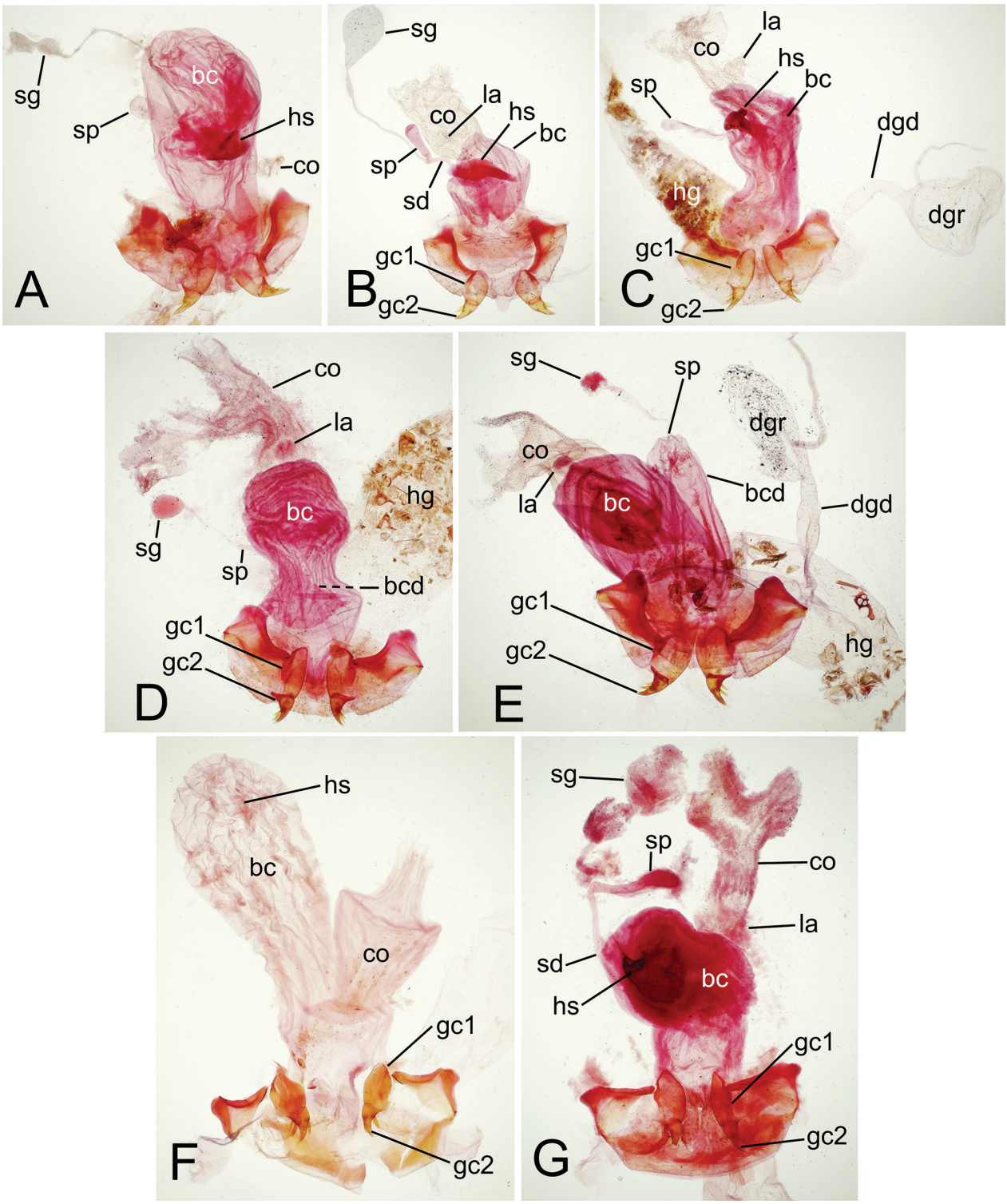

Figure 12. Female reproductive tract, gonocoxites and associated laterotergites, *Mecyclothorax* (*Phacothorax*) spp: **A**, *M. laterobustus*; **B**, *M. laterosinuatus*; **C**, *M. laterorectus*; **D**, *M. fleutiauxi*; **E**, *M. jeanneli*; **F**, *M. plurisetosus*; **G**, *M. megalovatulus*. See Table 2 for abbreviations.

duct entering at base of spermathecal reservoir; ligular apophysis present near base of common oviduct; basal gonocoxite 1 with apical fringe of two to three setae laterally on apical margin, middle seta of series largest, several small setae scattered along medial margin (Fig. 13C); gonocoxite 2 moderately narrow basally, medial length more than twice basal width; two broad lateral ensiform setae present, apical seta larger.

Types – Holotype male (MNHN): NEW CALEDONIA / Mt. Panié / 16 May 1984 / G. monteith & D. Cook // Q.M. BERLESATE No. 650 / 20.35S X 164.47E / Rainforest, 900 m / Litter // QUEENSLAND / MUSEUM

LOAN / DATE: Nov. 2003 / No. LEN-1686 (green label) // genitalia in polyethylene vial with glycerine // HOLOTYPE / Mecyclothorax / laterorectus / J.K.Liebherr 2017 (black-bordered red label).

Paratypes (21 specimens). NEW CALEDONIA: Hienghène [vicinity, code PA 63], 150 m el., 20°41'S 164°57'E, 02-ix-1970, Franz (NHMW, 4); Mandjélia, 700 m el., 20°24'S 164°32'E, 12-v-1984, rainforest, Q.M. berlesate 648, sieved litter, Monteith & Cook (QMB, 2), montane rainforest, 700-780 m el., 20°24'S 164°32'E, *Pandanus,* 20-xi-2008, Wanat (MNHW, 1), 750-780 m el., 20°24'S 164°32'E, 01-xi-2007, sieved litter, Wanat (MNHW, 5), summit, 750 m el., 20°24'S 164°32'E, hand collecting, 06-07-xi-2001, lot 8750, Burwell & /Monteith (QMB, 1), rainforest, sieved litter, 06-07-xi-2001, lot 1055, Monteith (QMB, 3), flight intercept trap, 29-xi-2003–11-i-2004, lot 11486, Monteith (QMB, 1), 780 m el., 20°24'S 164°32'E, berlesate, sieved litter, 12-xii-2004, lot 11941, Monteith (QMB, 2); Mt. Panié, rainforest, 900 m el., 20°33'S 164°45'E, Q.M. berlesate 650, litter, 16-v-1984, Monteith & Cook (QMB, 1); Roche d'Ouaïème, near Hienghène [PA 65], 500-700 m el., 20°37'S 164°52'E, 03-ix-1970, Franz (NHMW, 1).

Etymology. As in the preceding two species (Fig. 9A–C), the broad pronotal base leads to the use of latero- to modify the adjectival rectus, which denotes the right pronotal hind angles of these beetles.

Distribution and habitat. This species is distributed in the northern reaches of the Chaîne Centrale, from Mandjélia south to near Hienghène (Fig. 14). Elevations range 700–900 m for credible collecting localities where complete information was provided on the specimen label. Of the 22 specimens known, 14 were recovered from sieved litter. Other collecting situations include hand collecting (1, QMB), flight intercept trap (1, QMB), and association with *Pandanus* (Pandanaceae) screw palm (1, MNHW).

4. *Mecyclothorax fleutiauxi* (Jeannel)

Figures 1B, 1I, 2C, 2G, 3B, 9D, 10I–M, 11C, 12D, 13D, 15

Phacothorax fleutiauxi Jeannel 1944: 85.
Mecyclothorax fleutiauxi, Liebherr & Marris 2009: 10.

Diagnosis. Though markedly different from all other New Caledonian species, this and the following *M. jeanneli* (Fig. 9D–E) are indistinguishable externally. Both species are characterized by presence of only the single posterior supraorbital seta (Fig. 1B), and by the orbicular pronotum with a broadly margined base, and evenly ellipsoid elytra. The elytral striae are very shallow, though traceable to the fifth stria. That this and the following species are distinct is supported by characters of the male and female genitalia. In the males, the aedeagal median lobe has the apex elongate, variably extended beyond the apical margin of the ostium (Fig. 10I–M). The female reproductive tract in this species is characterized by presence of a short dorsal lobe of the bursa copulatrix, with the spermathecal duct joined to the lobe's apex (Fig. 12D). Standardized body length 4.2–5.0 mm. Chaetotaxy –/+//+/–//+/1–2/+–/+.

Description (n = 10). The description for *M. jeanneli* (below) serves to describe the external anatomy of this species, with the following exceptions: 18–20 ommatidia along horizontal diameter of eye; ocular ratio 1.43–1.52, ocular lobe ratio 0.89–0.94, EyL/EyD = 3.09–3.33; MPW/PL = 1.24–1.30; MEW/EL = 0.68–0.73; either one or two dorsal elytral setae associated with third interval; if one, the posterior seta is absent (in 2 of 10 specimens scored).

Male genitalia (n = 17). Antecostal margin of abdominal mediotergite IX robust distally, broadly angulate and truncate (Fig. 10J); right paramere very elongate, apical half narrowed to a whiplike extension (Fig. 11C), six setae along ventral margin well separated from apical pair of setae, dorsal surface glabrous; left paramere broad basally, distinctly narrowed to a whiplike extension; aedeagal median lobe moderately gracile, apical half evenly narrowed to extended tip that protrudes at least twice its dorsoventral dimension beyond the apex of the ostial opening (Fig. 10I–M); aedeagal internal sac bilobed, the dorsal lobe much larger than apical lobe (Fig. 10L), a small crescent-shaped structure with lightly sclerotized outer margin–interpreted as a reduced flagellar sheath–dorsad gonopore on apical lobe. Although there is variation in the amount of apical extension and apical curvature of the median lobe among males assigned to this species (Fig. 15), that variation occurs both within and between populational samples indicating that the variation is infraspecific.

Female reproductive tract (n = 5). Bursa copulatrix bilobate, an elongate ventral lobe with length more than twice circumference, and a short dorsal lobe that is about as long as broad and which bears the spermathecal duct at its apex (Fig. 12D); bursal walls moderately thick, wrinkled, semitranslucent; spermathecal duct that enters apex of bursal dorsal lobe about half the diameter of spermathecal reservoir, and about twice length of reservoir, spermathecal gland duct entering onto apex of spermathecal reservoir; well-developed ligular apophysis present on common oviduct as far distant from base of common oviduct as apex of ventral bursal lobe; basal gonocoxite 1 with apical fringe of two setae, a few microsetae near apicomedial margin of gonocoxite complementing very few medial setae (Fig. 13D); apical gonocoxite 2 falciform with an elongate laterobasal extension, basal width more than 0.75× length; two lateral ensiform setae elongate.

Type – Holotype male (MNHN): La Foa à Canala / fev. 1907 La Foa // TYPE (red label) // Phacothorax / Fleutiauxi / Jeannel (male dissected with genitalia separately mounted on card with label "Phacothorax / fleutiauxi ? Jeann."). So that the separated genitalia can remain unambiguously associated with the male holotype body, a black-bordered red holotype label has been added to that pin.

Additional taxonomic material (145 specimens; EMEC, MNHW, QMB): see Suppl. material 2.

Distribution and habitat. This species is recorded from middle latitudes of Grand Terre, from Aoupinié on the north to Ningua Reserve on the south (Fig. 15), its range a northerly parapatric disjunct to the range of its adelphotaxon, *M. jeanneli*. Species records indicate a broad altitudinal range among populations, from 485–1400 m elevation. Of 135 specimens with detailed ecological data, 127 have been collected via application of pyrethrin spray to tree trunks or downed logs, whereas none have been recovered from sieved litter. Thus this species is associated with epiphytic growth, bark, or loose bark on plants. That these beetles climb is shown by a record of one taken in an axil of a *Freycinetia* (Pandanaceae) plant (QMB).

5. *Mecyclothorax jeanneli* Liebherr, sp. n.

http://zoobank.org/834CBF6A-2041-4A93-B068-5CDE22913FB5
Figures 9E, 10N–R, 11D, 12E, 13E, 15

Diagnosis. The diagnosis for *M. fleutiauxi* serves to summarize external diagnostic characters for this species (Fig. 9D–E). Internally, the male aedeagal median lobe has a much shorter apex in beetles of this species, with the tip extended beyond the apical ostial margin only as much as the width of the median lobe at that point (Fig. 10N–R). The female reproductive tract differs in that the dorsal lobe of the bursa copulatrix is as long as the ventral or principal lobe (Fig. 12E), with the spermathecal duct again entering at its apex. Standardized body length 4.4–5.3 mm. Chaetotaxy –/+//+/–//+/1–2/+/+.

Description (n = 10). Head capsule narrowly elongate, with large, moderately convex eyes, ocular lobe meeting gena at obtuse angle, a broad shallow groove indicating juncture; 20 ommatidia along horizontal diameter of eye; ocular ratio 1.42–1.51, EyL/EyD = 2.8–3.4; frontal grooves sinuously canaliculate, deepest posterad frontoclypeal suture at a line between posterior margin of antennal fossae, briefly prolonged onto clypeus (as in Fig. 1B); mandibles elongate, mandibular ratio 1.9; ligular anterior margin angularly rounded to ligular seta, concave between setae, the two setae separated by two setal diameters (as in Fig. 1I); paraglossae thin, extended as far beyond ligular margin as half of basal length to margin; antennae moderately elongate, antennomere 9 length 2.05× maximal breadth; antennomere 3 glabrous except for apical ring of setae. Pronotum vase-shaped, lateral margins meeting base in a smooth convex curve, hind angles nonexistent (Fig. 9E); MPW/PL = 1.23–1.30; front angles protruded, obtusely rounded; basal margin bordered by broadly convex marginal bead that joins fine lateral marginal beads at very small, shallow laterobasal depressions; median longitudinal impression fine and shallow on disc, terminated anteriorly at a small depression at position of anterior transverse impression; anterior transverse impression broad, very shallow, traceable to front angles; proepisternum separated from prosternum by a broad shallow groove both anteriorly and ventrally; prosternum with shallow anteapical impression laterally, impression absent from ventral 2/3 of circumference; prosternal process broadly depressed between procoxae, that depression extended anteriorly where it broadens to a depressed anterior face extended nearly to prothoracic anterior margin. Elytra elongate, ovoid, humeri quickly sloping posterad outside humeral angles; MEW/EL = 0.70–0.75; basal groove very briefly recurved laterad scutellum, humeral angle tightly rounded; all striae broad and shallow on disc, intervening intervals only slightly convex; one to two dorsal elytral setae present in third interval, if one, the posterior seta is absent (in 3 of 10 specimens scored); shallow remnants of the sutural stria plus striae 2 and 7 traceable at apex; elytra appressed and conjoined apically, sutural intervals narrower and distinctly upraised at apex. Pterothoracic mesepisternal anterior surface smooth; mesosternal-mesepisternal suture incomplete, obsolete to absent anteriorly (as in Fig. 3B); metepisternum very foreshortened, maximum width/lateral length = 1.3; metepisternal-metepimeral suture complete. Abdomen with broad crescent-shaped depression along suture between first and second ventrite, second ventrite broadly depressed behind crescent; suture between second and third ventrites reduced though traceable laterally; ventrites 2–6 with broad, shallow, linear plaques near lateral margin. Microsculpture of frons distinct, a mix of isodiametric and transverse sculpticells; pronotal disc and base covered with elongate transverse mesh, sculpticells on disc 3–4× broad as long, those on base somewhat less broad, surface iridescent; elytra iridescent, disc covered with transverse-line microsculpture, apex with transverse lines loosely joined into a transverse mesh.

Male genitalia (n = 23). Antecostal margin of abdominal mediotergite IX robust distally, broadly angulate and obliquely truncate (Fig. 10O); right paramere very elongate, apical half narrowed to a whiplike extension (Fig. 11D), five setae along ventral margin well separated from apical pair of setae, dorsal surface glabrous; left paramere broadly quadrate basally, distinctly narrowed to a whiplike extension; aedeagal median lobe moderately gracile, apical half evenly narrowed to tip that protrudes less than its dorsoventral dimension beyond the apex of the ostial opening (Fig. 10N–R); aedeagal internal sac bilobed, the dorsal lobe subequal to the apical lobe (Fig. 10Q), a small crescent-shaped structure with lightly sclerotized outer margin–interpreted as a reduced flagellar sheath–dorsad gonopore on apical lobe. There is less variation among males with regard to extension of the median lobe apex (Fig. 15) – understandable due to the generally shorter extension–and this variation is not geographically associated. Thus the species geographic limits include all populations lying south and east of Mt. Humboldt (Fig. 15).

Female reproductive tract (n = 8). Bursa copulatrix bilobate, a broad ventral lobe complemented by narrower dorsal lobe of subequal length, dorsal lobe bearing spermathecal duct at apex (Fig. 12E); bursal walls moderately thick, wrinkled, semitranslucent; spermathecal duct that enters apex of bursal dorsal lobe slightly broader

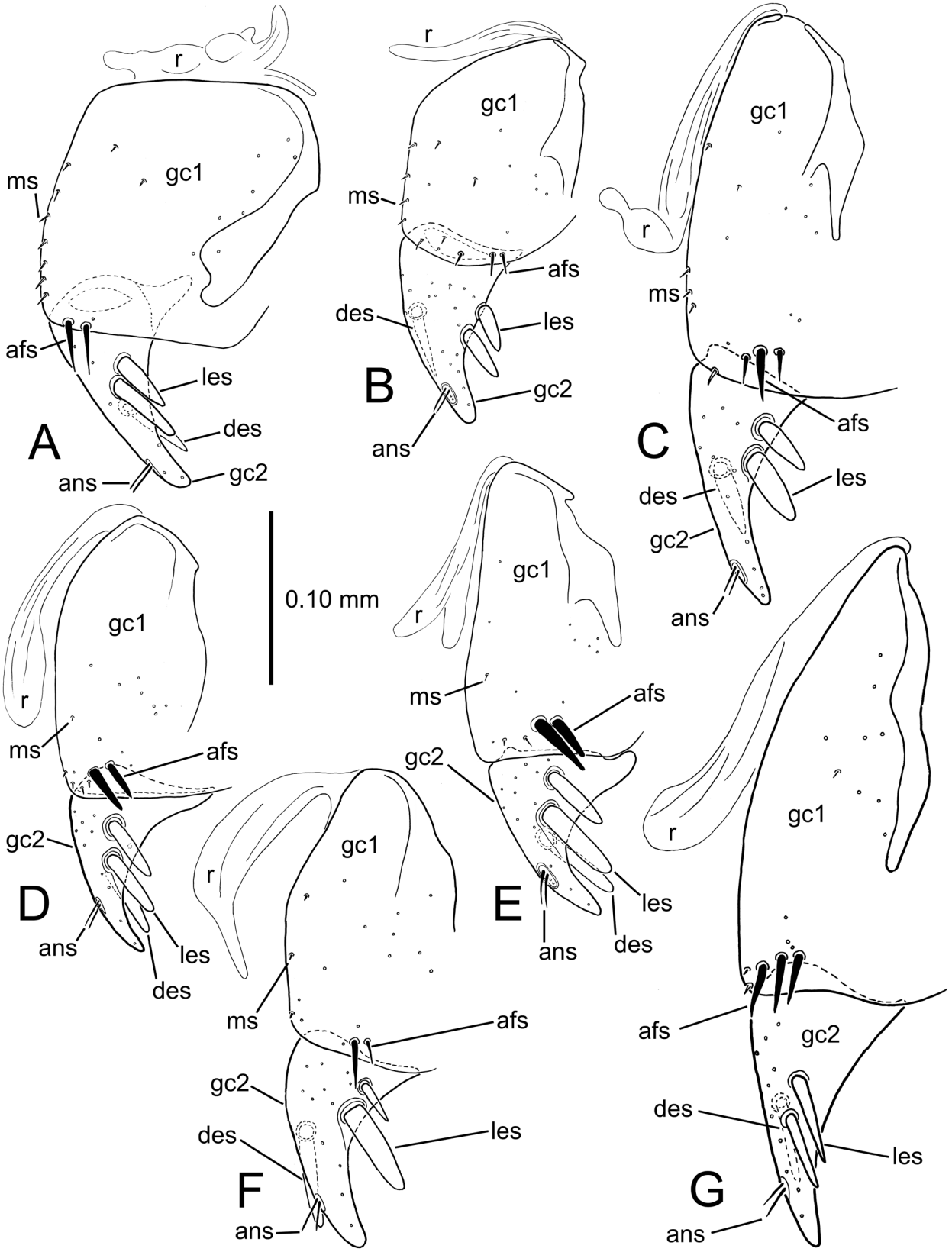

Figure 13. Left female gonocoxa, ventral view, *Mecyclothorax* (*Phacothorax*) spp.: **A**, *M. laterobustus*; **B**, *M. laterosinuatus*; **C**, *M. laterorectus*; **D**, *M. fleutiauxi*; **E**, *M. jeanneli* ; **F**, *M. plurisetosus*; **G**, *M. megalovatulus*. See Table 2 for abbreviations.

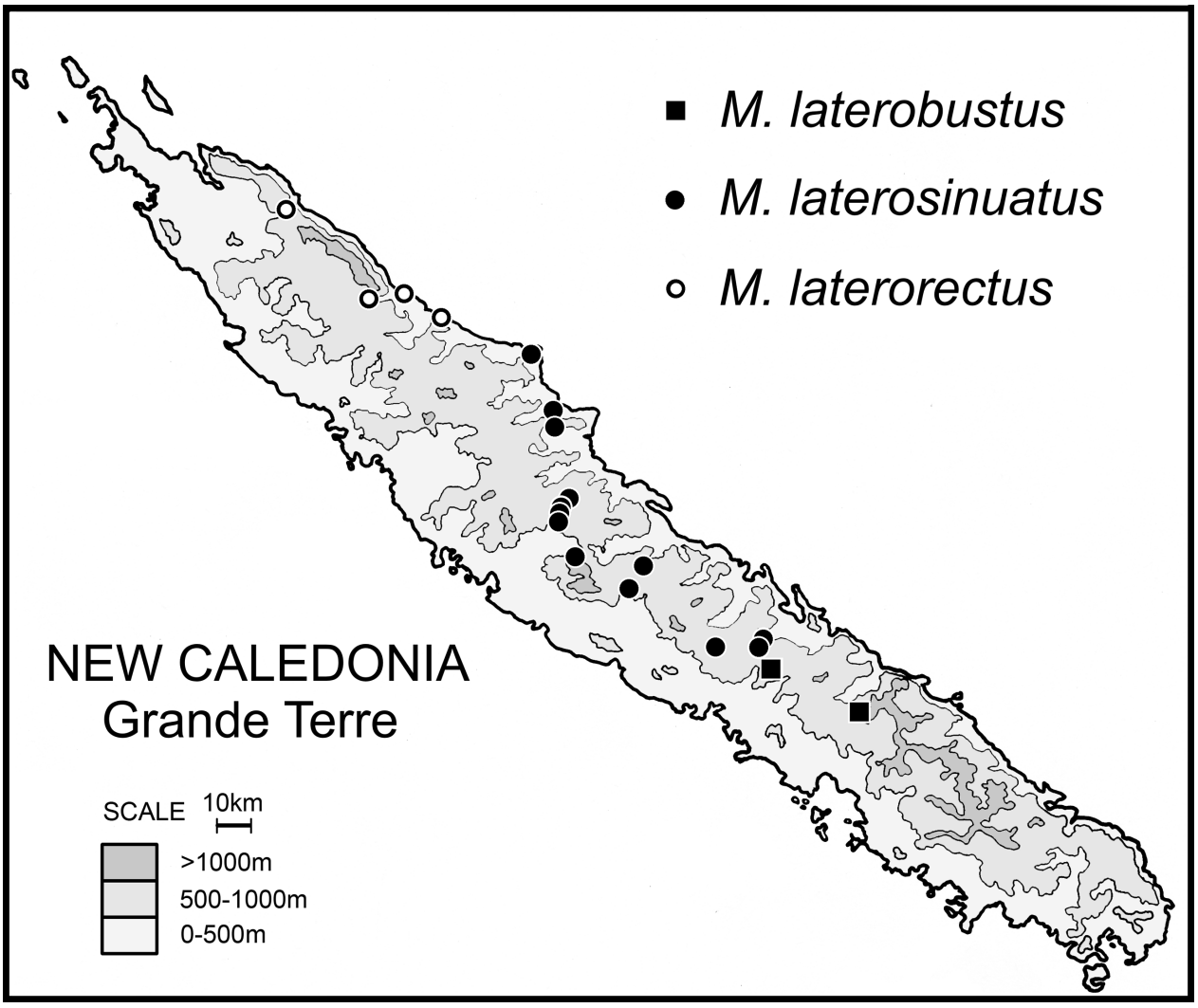

Figure 14. Geographical distributions of *Mecyclothorax* (*Phacothorax*) spp.

than spermathecal reservoir, and about twice length of reservoir, spermathecal gland duct entering onto apex of spermathecal reservoir; well-developed ligular apophysis present on common oviduct as far distant from base of common oviduct as apex of ventral bursal lobe; basal gonocoxite 1 with apical fringe of two setae, a few microsetae near apicomedial margin of gonocoxite complementing very few medial setae (Fig. 13E); apical gonocoxite 2 falciform with an elongate laterobasal extension, basal width more than 0.75× length; lateral ensiform setae elongate and broad.

Types – Holotype male (MNHN): NEW CALEDONIA.9944 / 22°11'Sx166°01'E [sic, crossed out and hand corrected to 31'E] / Mt Koghi, 750m / 29Nov2000.GB Monteith / Pyrethrum, trunks&logs // QUEENSLAND / MUSEUM LOAN / DATE: Nov. 2003 / No. LEN-1686 (green label) // HOLOTYPE / Mecyclothorax / jeanneli / J.K.Liebherr 2017 (black-bordered red label). The type locality longitude is incorrect on the label, and is corrected (Google Earth Pro 2017).

Paratypes (156 specimens; EMEC, HNHM, MNHW, NHMW, QMB): see Suppl. material 2.

Etymology. This species epithet is a patronym honoring Dr. René Jeannel, whose extensive body of literature dominates 20th Century carabidology. Dr. Jeannel's early and perspicacious appreciation of Wegenerian historical biogeography was ground breaking in Entomology (Jeannel 1942), and we have yet to test fully the biogeographic hypotheses he proposed in his many contributions. More close to home, the necessity of examining the male genitalia to determine *M. jeanneli* versus its sister species, *M. fleutiauxi*, reiterates Dr. Jeannel's pioneering research on the underlying homologies of insect genitalia (Jeannel 1955) and his extensive use of insect genitalia to diagnose species (e.g. Jeannel 1944).

Distribution and habitat. This species is distributed in the southern end of Grand Terre, from Mt. Humboldt on the north to Forêt Nord on the south (Fig. 15), allopatric to the northerly range of its adelphotaxon, *M. fleutiauxi*. These beetles are known from any even greater altitudinal range than *M. jeanneli*, with recorded elevations ranging 160–1600 m. As with *M. jeanneli*, the vast majority (150 of 156 specimens) have been collected on

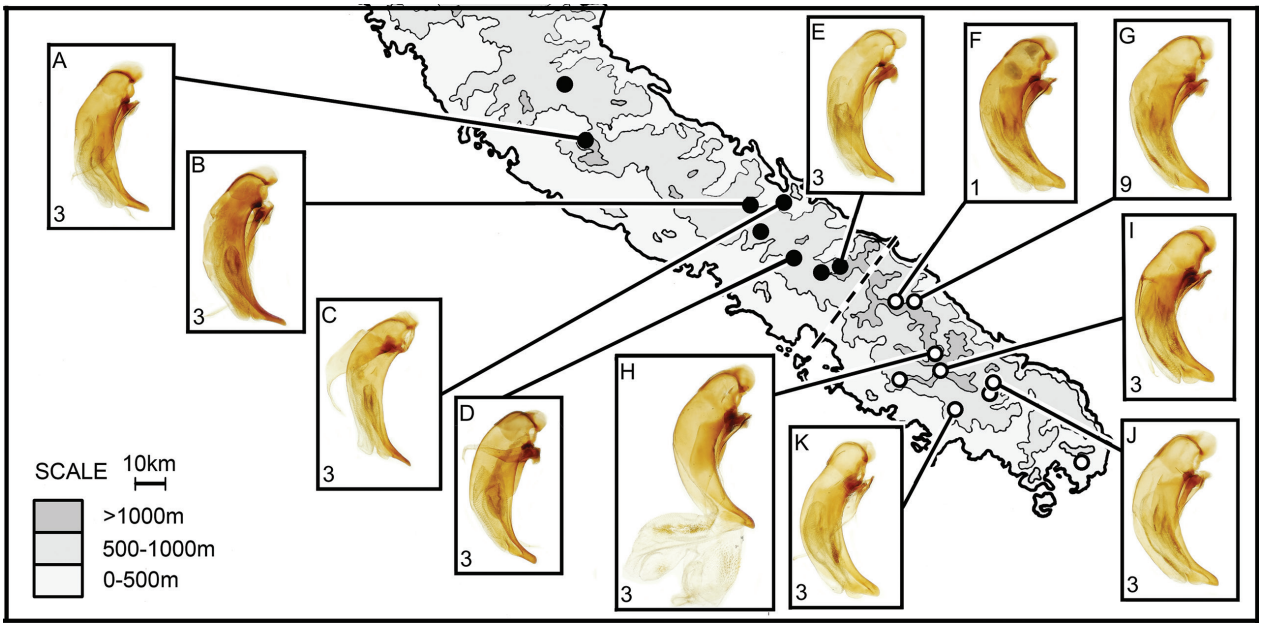

Figure 15. Recorded geographical distribution of *M. fleutiauxi* (including population samples **A–E** northwest of dashed boundary) and *M. jeanneli* (including population samples **F–K** southeast of dashed boundary): numbers of males sampled for each locality indicated in lower left of boxes. Sampled population localities for *M. fleutiauxi* include: **A**, Me Maoya; **B**, Rembai; **C**, Gelima; **D**, Mt. Do; **E**, Ningua. Sampled population localities for *M. jeanneli* include: **F**, Mt. Humboldt, 600 m; **G**, Mt. Humboldt, 1300–1600 m; **H**, Mt. Ouin; **I**, Mt. Dzumac; **J**, Rivière Bleue; **K**, Mts. Koghis.

tree trunks or downed logs, most via application of pyrethrin spray. A series of 31specimens was taken during one collecting event through spray application onto a moss-covered trunk (QMB). Thus, like *M. jeanneli*, this species is associated with emergent plant substrates, not the ground-level litter microhabitat.

6. *Mecyclothorax plurisetosus* Liebherr, sp. n.

http://zoobank.org/CE1562F9-33FE-440C-AE08-E6B1DFF160B0
Figures 12F, 13F, 16A, 17A–B, 18A, 19

Diagnosis. These beetles (Fig. 16A) share an orbicular pronotum and smooth ovoid elytra with the previous two species, *M. fleutiauxi* and *M. jeanneli* (Fig. 9D–E). This similarity in body form is indicative of phylogenetic relationship, as *M. plurisetosus* comprises the adelphotaxon to those species two (Fig. 7). However this species can be diagnosed from all others by the presence of extra setae on the pronotum. In addition to the large setae homologized with the lateral pronotal setae, there are 9–11 smaller setae in the marginal depression anterad the lateral seta, and 4–5 setae in the depression behind the lateral seta. The prosternum also bears a sparse pelage of elongate setae, with the anterior surfaces of the femora also so covered. The elytral striae are totally reduced in this species, and the cuticular microsculpture also totally absent from head capsule, pronotum, elytra, and ventrites. Standardized body length 4.7–5.1 mm. Chaetotaxy +/+//2+11/–5//+/2/+/+, signifying that the lateral pronotal seta has been doubled, with up to 11 microsetae lining the lateral marginal depression anterad those setae. Also, though the basal pronotal seta is absent, up to 5 microsetae lie along the lateral margin near the pronotal base. The two lateral pronotal setae are longer and stouter than the anterior 11 and posterior 5 microsetae, supporting homology of the double setae with the single lateral pronotal seta of the other species, and the autapomorphic status of the numerous and variable microsetae.

Description (n = 3). Head capsule trapezoidal, neck broad, with small, moderately convex eyes, ocular lobe meeting gena at obtuse angle very close to eye posterior margin; 18–19 ommatidia along horizontal diameter of eye; ocular ratio 1.28–1.42, ocular lobe ratio 0.88–0.91, EyL/EyD = 2.9–3.1; frontal grooves very deep, arcuately convergent at midlength, extended deeply onto clypeus; mandibles moderately elongate, mandibular ratio 1.8; ligular lateroanterior margin rounded to ligular seta, the two setae separated by one to two setal diameters; paraglossae thin, extended as far beyond ligular margin as half of basal length to margin; antennae very elongate, antennomere 9 length 3.4× maximal breadth; antennomere 3 with sparse fine setae near apex in addition to apical ring of longer setae. Pronotum transversely ovoid, median base depressed relative to disc, lateral margins evenly curved to meet narrow median peduncular collar, pronotal lateral margin obtusely concave at the juncture (Fig. 16A); MPW/BPW = 3.6–3.9, MPW/PL = 1.23–1.25; front angles protruded, obtusely rounded, the apex broad to match broad base of head, APW/BPW = 2.1–2.3; basal margin bordered by broadly convex marginal bead that joins lateral marginal bead at sinuate margin, three deep pits anterad median marginal bead; median longitudinal impression very finely incised on disc, terminated ante-

riorly at position of anterior transverse impression; anterior transverse impression very broad, very shallow, indistinctly traceable to front angles; proepisternum separated from prosternum by a narrow, shallow groove both anteriorly and ventrally; prosternum without anteapical impression, though anterior margin is irregularly punctate; prosternal process narrowly depressed between procoxae, that depression not extended anteriorly, but venter of prosternum is flattened toward front of prothorax (as in *M. fleutiauxi* and *M. jeanneli*). Elytra ovate, broadest in basal half and narrowed apically; MEW/EL = 0.81–0.85; basal groove very briefly extended laterad scutellum, the only indication of humeral angle being the basal groove's juncture with the broader lateral marginal depression; striae 1–7 absent, only striae 8 and 9 (i.e. the inner portion of the elytral lateral marginal depression) present; only an obsolete vestige of the sutural stria evident at apex; elytra appressed and conjoined at apex where the sutural margin is narrowly and distinctly upraised. Pterothoracic mesepisternal anterior surface smooth except for a broad deep pit ventrally near prosternum; mesosternal-mesepisternal suture incomplete, obsolete to absent anteriorly (as in Fig. 3B); metepisternum foreshortened, maximum width/lateral length = 1.0; metepisternal-metepimeral suture incomplete, obsolete laterally. Abdomen with only a shallow crescent-shaped depression along suture between first and second ventrite, second ventrite little depressed posterad crescent; suture between second and third ventrites reduced though traceable laterally; ventrites 2–6 with broad, shallow, linear plaques near lateral margin. Microsculpture of frons reduced, surface glossy; pronotal disc and base with shallow transverse mesh, sculpticell breadth 3–4× length; elytra glossy, only patchy indications of transverse microsculpture visible.

Male genitalia (n = 1). Antecostal margin of abdominal mediotergite IX angulate, an elongate "butterfly-net handle" extension distally (Fig. 17B); right paramere elongate, slightly convex dorsally near base, narrowly extended to apex (Fig. 18A), dorsal and ventral surfaces glabrous, two apical setae present; left paramere narrow basally, evenly constricted to a narrow, porrect apex, also glabrous except for two apical setae; aedeagal median love gracile, parallel-sided at midlength, the apex expanded dorsally to an acuminate point, and ventrally as a rounded projection (Fig. 17A); median lobe internal sac with evident crescent-shaped structure (Fig. 17A) homologous with flagellar sheath of above two species; folds of internal sac visible in the single uneverted type specimen interpreted as a bilobed sac as per the previous two species.

Female reproductive tract (n = 1). Bursa copulatrix unilobate, elongate, length about 3× circumference, walls thin, slightly wrinkled (Fig. 12F); the only evidence of spermathecal configuration is a lightly sclerotized helminthoid sclerite near apex of bursa, spermatheca lost in single dissected female; basal gonocoxite 1 with apical fringe of 2 setae, lateral seta smaller, a few medial setae scattered along median margin (Fig. 13F); apical gonocoxite 2 moderately broad basally, breadth less than half of length; two lateral ensiform setae, apical seta much longer and broader than basal seta.

Types – Holotype male (MNHN): NEW CALEDONIA 8716 / 21°11'Sx165°18'E.850m / Aoupinie, top camp, / 2-3Nov2001.C.Burwell& / GMonteith.pyr.trees,logs // QUEENSLAND / MUSEUM LOAN / DATE: Nov. 2003 / No. LEN-1686 (green label) // *New Caledonia Mecyclothorax* revision / measured specimen 3 / J.K. Liebherr 2016 // HOLOTYPE / Mecyclothorax / plurisetosus / J.K.Liebherr 2017 (black-bordered red label).

Paratypes (2 specimens): same locality and labeling as holotype (QMB, 1); Aoupinié summit, 1000 m el. [984 m; Google Earth Pro 2017], 21°11'S 165°16'E, pyrethrum trees & logs, 02-x-2004, lot 11665, Monteith (QMB, 1).

Etymology. The presence of accessory setae on the pronotal lateral margins (Fig. 16A), prosternum, legs, and ventral body surface supports application of the compound adjectival epithet plurisetosus.

Distribution and habitat. This species is known only from the upper elevations of Mt. Aoupinié (Fig. 19), either from the vicinity of the summit transmitting station, or along the approach road at 850 m elevation. The four specimens were all collected via the application of pyrethrin spray to standing trees or downed logs. As this species is the adelphotaxon to *M. fleutiauxi* + *M. jeanneli*, finding it in this arboreal microhabitat supports the phylogenetic retention of preferred microhabitat among this triplet of species.

7. *Mecyclothorax megalovatulus* Liebherr, sp. n.

http://zoobank.org/75E12733-B4D0-463E-957C-368853BD124C
Figures 12G, 13G, 16B, 17C–D, 18B, 19

Diagnosis. This and the following species, *M. octavius*, can be diagnosed by their large body size; in this species standardized body length = 5.4–5.8 mm. Individuals of this species have the elytral striae well developed, with striae 1–8 deep and continuous throughout their length (Fig. 16B) in contrast to the obsolete striae and smooth elytra of *M. octavius* (Fig. 16 C). The elytra are narrowly ellipsoid with very narrow humeri. The pronotal hind angles are obtuse but rounded at the apex of the angle, and the pronotal base is unmargined. Chaetotaxy +/+//+/–//+/2/+/+.

Description (n = 4). Head capsule trapezoidal, neck broad, eyes broad and little convex, ocular lobe meeting gena at very obtuse angle well behind eye posterior margin; 20 ommatidia along horizontal diameter of eye; ocular ratio 1.37–1.44, ocular lobe ratio 0.74–0.82, EyL/EyD = 2.81–2.86; frontal grooves narrow, well incised, sinuously convergent to just posterad clypeus, extended briefly onto clypeus; mandibles moderately elongate, mandibular ratio 1.83; ligular margin rounded to ligular seta, concave between the two setae, setae separated by one to two setal diameters; paraglossae thin, extended as far beyond ligular margin as half of basal length to margin;

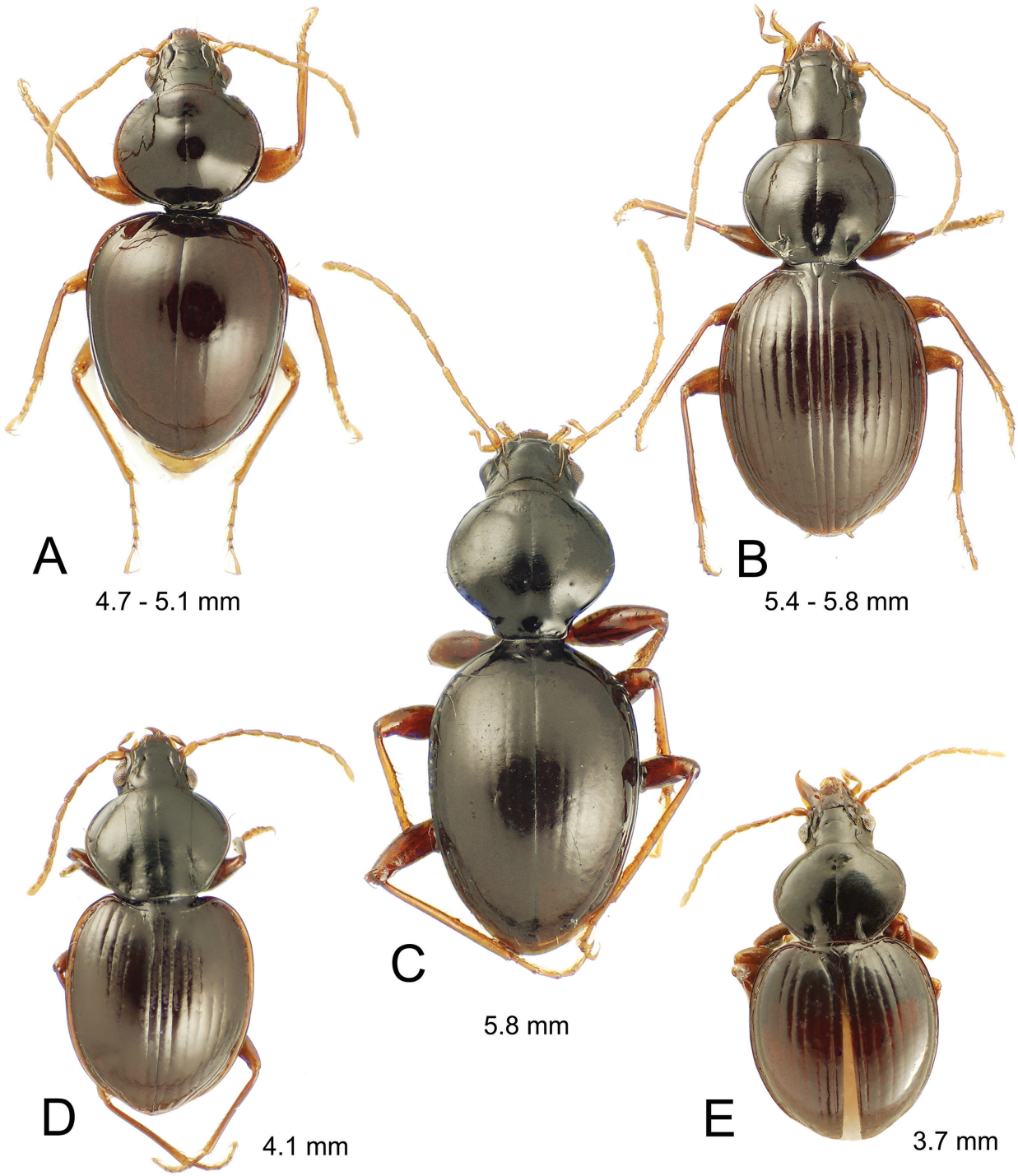

Figure 16. New Caledonian *Mecyclothorax* (*Phacothorax*) spp., dorsal view: **A**, *M. plurisetosus*; **B**, *M. megalovatulus*; **C**, *M. octavius*; **D**, *M. laterovatulus*; **E**, *M. najtae*.

antennae elongate, antennomere 9 length 2.9× maximal breadth; antennomere 3 glabrous except for apical ring of setae. Pronotum vase-shaped, narrow basally, lateral margins only slight concave anterad rounded hind angles, median base convex, not depressed relative to disc, without marginal bead (Fig. 16B); MPW/BPW = 2.56–2.83, MPW/PL = 1.21–1.28; front angles protruded, obtuse, pronotal apex distinctly broader than base, APW/BPW = 1.65–1.74; median longitudinal impression shallowly and very finely incised on disc, intermittently extended in front of evident anterior transverse impression, terminated posteriorly in deep ellipsoid pit situated medially between the anterior margins of laterobasal depressions; anterior transverse impression broad and shallow but easily traceable to front angles; laterobasal depressions flat, triangular, defined medially by a longitudinal crease laterad median base and

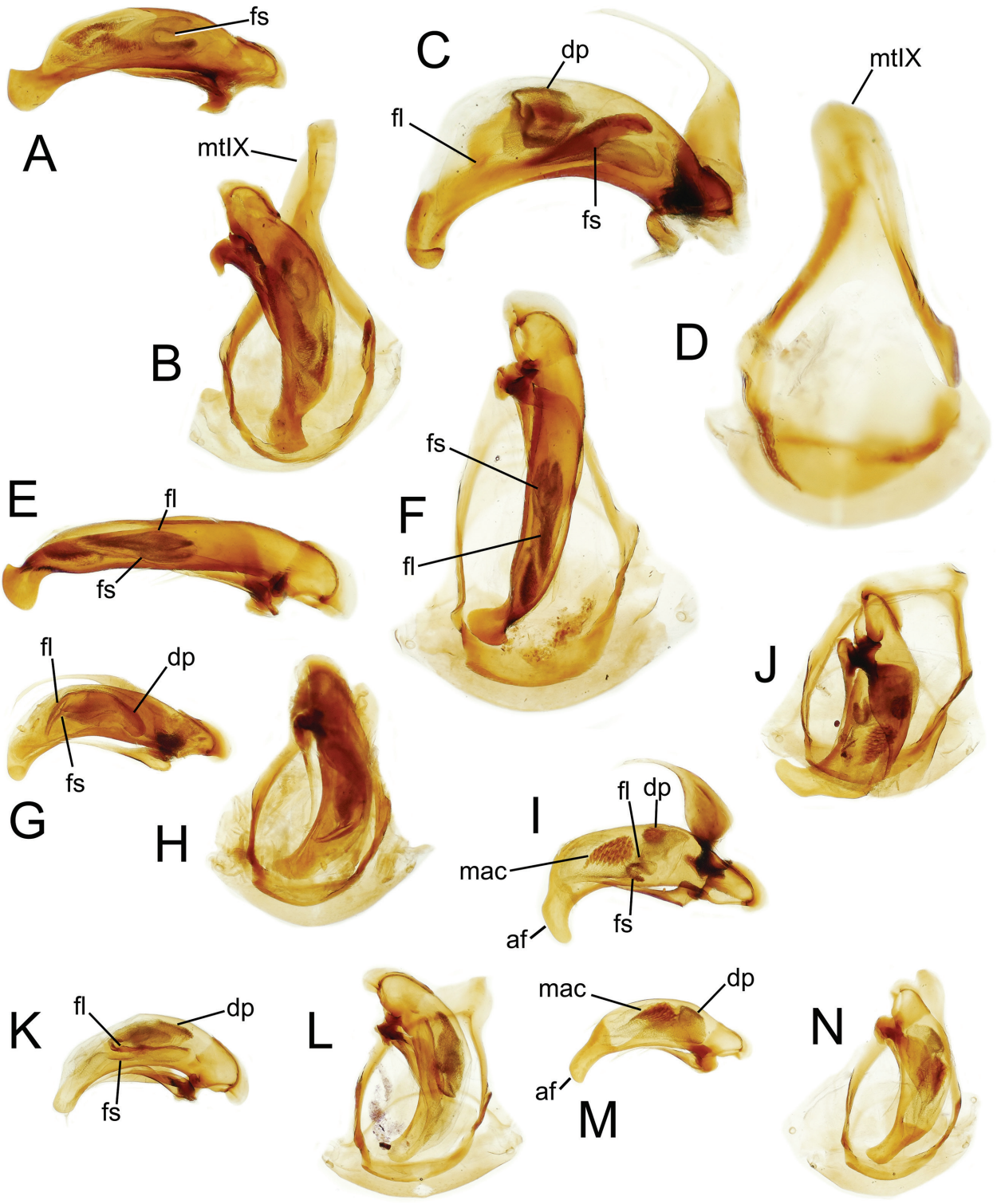

Figure 17. Male aedeagal median lobe and parameres, and ring sclerite–mediotergite plus antecostal margin, tergite IX–of *Mecyclothorax* (*Phacothorax*) spp.: **A–B**, *M. plurisetosus*, right view, dorsal view in situ (Aoupinié); **C–D**, *M. megalovatulus*, right view, dorsal view of righ sclerite (Mt. Panié); **E–F**, *M. octavius*, right view, dorsal view in situ (Me Maoya); **G–H**, *M. laterovatulus*, right view, dorsal view in situ (Aoupinié); **I–J**, *M. manautei*, right view, dorsal view in situ (Mt. Humboldt, 1400 m); **K–L**, *M. paniensis*, right view, dorsal view in situ (Mt. Panié); **M–N**, *M. mouensis*, right view, dorsal view in situ (Mt. Mou). See Table 2 for abbreviations.

anteriorly by a transverse crease bordering pronotal disc; proepisternum separated from prosternum by a shallow groove both anteriorly and ventrally; prosternum with well-defined anteapical impression laterally, the impression shallower though complete ventrally; prosternal process shallowly and broadly depressed between procoxae,

prosternum medially flattened anterad procoxae with an ovoid pitlike depression medially about 1/3 distance to anterior prosternal margin. Elytra ellipsoid, broadest about midlength, humeri distinctly sloping posterad humeral angle; MEW/EL = 0.74–0.81; basal groove briefly extended laterad scutellum, four-punctate at bases of abbreviated parascutellar striole, sutural and striae 3 and 4; intervals 3 and 8 more convex than the others at elytral apex, though all intervals are at least moderately convex; elytra appressed and conjoined at apex , sutural intervals slightly narrowed there. Pterothoracic mesepisternal anterior surface smooth except for a vertical furrow ventrally near prosternum; mesosternal-mesepisternal suture incomplete, obsolete to absent near anterior margin of mesothorax (as in Fig. 3B); metepisternum very short, maximum width/lateral length = 1.73, metepisternal-metepimeral suture incomplete, obsolete laterally. Abdomen with distinct, well-defined crescent-shaped depression along suture between first and second ventrite, second ventrite little depressed posterad crescent; suture between second and third ventrites reduced though traceable laterally; ventrites 2–6 with broad, shallow, linear plaques near lateral margin. Microsculpture of frons and vertex a well-defined, transversely-stretched isodiametric mesh; pronotal disc and base with shallow transverse mesh, sculpticell breadth 3–4× length, surface glossy, sculpticells arranged as a distinct transverse mesh in laterobasal depressions; elytral disc with shallow transverse lines, the surface glossy, subiridescent, the apex covered with indistinct transverse lines.

Male genitalia (n = 1). Antecostal margin of abdominal mediotergite IX angulate, broad and little distended (Fig. 17D); right paramere with broad base, apex elongate, narrowly extended and membranous, with two very short apical setae (Fig. 18B); left paramere broad basally, evenly narrowed in basal half to an elongate whiplike extension, two elongate setae apically; aedeagal median lobe robust, broad dorsoventrally, distinctly curved both dorsally and ventrally to a subparallel, extended apex, the tip of apex laterally curved into an apical hooklike crease (Fig. 17C); aedeagal internal sac with flagellum, flagellar sheath, and dorsal plate (Fig. 17C).

Female reproductive tract (n = 1). Bursa copulatrix elongate, length more than twice basal circumference, apical portion expanded laterally toward right, surface thick apically, wrinkled, densely stained relative to bursal base (Fig. 12G); spermathecal duct entering near bursa-common oviduct juncture with duct oriented toward right side of bursa, duct as long as spermathecal reservoir; a heavily sclerotized, triangular helminthoid sclerite present near base of spermathecal duct; spermatheca fusiform on narrow duct, spermathecal gland duct entering at base of spermathecal reservoir; ligular apophysis present near base of common oviduct; basal gonocoxite 1 with apical fringe of three setae situated near apicomedial angle, medial surface of gonocoxite 1 glabrous (Fig. 13G); gonocoxite 2 narrow basally, basal width about 2/3 medial length; two very gracile lateral ensiform setae present.

Types – Holotype male (MNHN): NEW CALEDONIA 8764 / 20°34'Sx164°46'E / Mt Panie refuge, 1300 m / 8-9Nov.2001.C.Burwell / Pyrethrum, trees & logs // QUEENSLAND / MUSEUM LOAN / DATE: Sept 2002 No. LE 02.43 (green label) // *New Caledonia Mecyclothorax* revision / measured specimen 3 / J.K. Liebherr 2016 ♂1 // genitalia in polyethylene vial with glycerine // HOLOTYPE / Mecyclothorax / megalovatulus / J.K.Liebherr 2017 (black-bordered red label).

Paratypes (3 specimens). NEW CALEDONIA: Mt. Panié, 1300-1600 m el., 20°35'S 164°46'E, 15-v-1984, Monteith & Cook (QMB, 1), refuge, 1300 m el., summit, 1600 m el., 20°34'S 164°46'E, rainforest, sieved litter, 9-xi-2001 lot 8769, Burwell (QMB, 1), track, 1500 m el., 20°34'S 164°46'E, pyrethrum trees & logs, 09-xi-2001, lot 8768, Burwell (QMB, 1).

Etymology. Large body size and ovoid pronotum and elytra (Fig. 16B) suggested the compound adjectival epithet megalovatulus.

Distribution and habitat. This species is only known from 1300–1600 m elevation on Mt. Panié, in the northern portion of the Chaîne Centrale (Fig. 19). Three of the six specimens have been recovered from sieved litter, whereas one was collected via pyrethrin spray application to trees and logs, supporting occupation of ground-level litter as well as plant-based, mossy microhabitats.

8. *Mecyclothorax octavius* Liebherr, sp. n.

http://zoobank.org/003616EF-AF92-4481-864C-A91512EC417E
Figures 16C, 17E–F, 18C, 19

Diagnosis. This species (Fig. 16C) exhibits superficial similarity to *M. fleutiauxi* and *M. jeanneli* (Fig. 9D–E), but differs in: 1, larger body size, standardized body length 5.8 mm; 2, presence of both anterior and posterior supraorbital setae; 3, an unmargined and depressed pronotal median base with sinuate lateral margins anterad the obtusely rounded hind angles; and 4, eyes of very small diameter, i.e. ocular lobe ratio = 0.71 versus ratios of 0.89–0.94 for individuals of the former two species. The male aedeagus is completely different, exhibiting a flagellum and flagellar sheath, and a dorsoventrally expanded apex (Fig. 17E). Chaetotaxy +/+//+/–//+/2/+/+.

Description (n = 1). Head capsule elongate, distinctly broader at the small, moderately convex eyes, ocular lobe gradually curving to meet gena well behind eye posterior margin; 20 ommatidia along horizontal diameter of eye; ocular ratio 1.45, ocular lobe ratio 0.71, EyL/EyD = 2.4; frontal grooves deep, sinuously convergent to just posterad clypeus, extended deeply onto clypeus; mandibles moderately elongate, mandibular ratio 1.8; ligular lateroanterior margin rounded to ligular seta, the two setae separated by one to two setal diameters; paraglossae thin, extended twice as far beyond ligular margin as their basal length to margin, apex observably spiculate (100×); antennae elongate, antennomere 9 length 2.3× maximal breadth; antennomere 3 with glabrous except for apical

ring of setae. Pronotum transverse, vase-shaped, median base depressed relative to broadly convex disc, lateral margins evenly curved until joined to long median peduncular collar, pronotal lateral margin obtusely concave at the juncture (Fig. 16C); MPW/BPW = 2.4, MPW/PL = 1.1; front angles narrowly protruded, obtuse, pronotal apex constricted, APW/BPW = 1.35; median base trapezoidally depressed relative to convex disc, 8–10 small punctures present each side, lateral marginal bead continued along anterior half of basal peduncle, terminated at base of peduncle, median base unmargined posteriorly; median longitudinal impression very finely incised on disc, extended briefly anterad broad and shallow anterior transverse impression; anterior transverse impression very broad, very shallow, indistinctly traceable to front angles; proepisternum separated from prosternum by a deep, sinuous groove both anteriorly and ventrally; prosternum with anteapical impression that is continuous ventrally; prosternal process narrowly and deeply depressed between procoxae, depression extended anteriorly half the distance to prothoracic anterior margin, the depression broadest at anterior terminus. Elytra ellipsoid, broadest just anterad midlength; MEW/EL = 0.72; basal groove absent from very narrowly pedunculate elytral base, the very narrow lateral marginal depressions converging on posterior margin of pronotum; striae 1–7 very shallow though traceable , stria 8 deep, diverging from stria 9 just posterad anterior series of lateral elytral setae; all striae except 8 absent from elytral apex; apical elytral setae positioned only slightly nearer to suture than subapical seta; elytra appressed and conjoined at apex, the upraised sutural margin forming an elongate isosceles triangle connected to the narrowly beaded elytral apical margin. Pterothoracic mesepisternal anterior surface with eight broad punctures, the largest anterior puncture separated from the remainder by a vertical ridge; mesosternal-mesepisternal suture incomplete, obsolete to absent anteriorly (as in Fig. 3B); metepisternum very short, maximum width/lateral length = 1.46 (difficult to measure due to fusion of metepisternum and metepimeron). Abdomen with first and second ventrites fused laterally, not suture visible; suture between second and third ventrites reduced though traceable laterally; ventrites 2–6 with broad, shallow, linear plaques near lateral margin. Microsculpture of frons reduced, an indistinct transverse mesh on a glossy surface, microsculpture on vertex an evident transverse mesh with some isodiametric sculpticells; pronotal disc and base with fine, elongate transverse mesh, sculpticell breadth 3–4× length, surface iridescent; elytra with evident transverse mesh, sculpticell breadth 2–3×length; elytral apex with elongate transverse mesh, sculpticell breadth 3–4× length where traceable.

Male genitalia (n = 1). Antecostal margin of abdominal mediotergite IX angulate, not extended (Fig. 17F); right paramere elongate, slightly expanded dorsally in basal half, narrowly extended apically (Fig. 18C), with 13 setae along the apical 2/3 of the ventral margin, those setae complementing two elongate apical setae; left paramere moderately broad basally, evenly narrowed to a moderately extended, narrow apex, two small setae present apically; aedeagal median lobe gracile, tubular, straight at midlength, with apex broadly expanded dorsoventrally, dorsally to am obtuse point, ventrally in a tightly rounded and projected margin; aedeagal median lobe internal sac with flagellum and flagellar sheath, apparently unilobate based on interpretation of uneverted unique type male (Fig. 17E), a diffuse spicular patch apicad flagellar apparatus, no structure present at position of dorsal plate.

Type –Holotype male (MNHN): NEW CALEDONIA / Me Maoya, summit / plateau.12Nov2002. / Monteith & Burwell // QM Berlesate 1080 / 21°22'Sx165°20'E / rainforest, 1400 m/ / sieved litter // QUEENSLAND / MUSEUM LOAN / DATE: Nov. 2003 / No. LEN-1686 (green label) // *New Caledonia Mecyclothorax* revision / measured specimen 1 / J.K. Liebherr 2016 ♂1 // genitalia in polyethylene vial with glycerine // HOLOTYPE / Mecyclothorax / megalovatulus / J.K.Liebherr 2017 (black-bordered red label) .

Etymology. Given that the body form comprises a pair of ovoids (Fig. 16C) suggesting the numeral eight, this species is given the epithet octavius. As a Latin personal name, denoting the eighth-born son, or a son born in the eighth month, the species name is to be treated as a noun.

Distribution and habitat. The single specimen of this species was collected from sieved litter collected at the 1400 m summit of Mt. Maoya (Fig. 19). This species is adelphotaxon to the species triplet *M. plurisetosus* (*M. fleutiauxi* + *M. jeanneli*), all of whom are most commonly found in arboreal microhabitats, supporting transformation of habitat preference to the arboreal realm in their common ancestor.

9. *Mecyclothorax laterovatulus* Liebherr, sp. n.

http://zoobank.org/A6065519-5F9F-4AE9-8BD3-F5A0A46CF137
Figures 16D, 17G–H, 18D, 19

Diagnosis. This and the following species *M. najtae* (Fig. 16D–E) are characterized by very obtuse pronotal hind angles that are rounded apically, pronotal lateral margins straight to only indistinctly concave before the very obtuse angles. The elytra are broader basally in beetles of this species, with the humeri extended anterad and the basal groove narrowly rounded near the base of stria 6, and elytral length is relatively longer than in *M. najtae*, with MEW/EL = 0.85. The outer elytral striae 5–7 are well impressed at midlength in this species, versus obsolete to entire absent laterally in *M. najtae*. The configuration of the male aedeagal internal sac–with elongate, curved flagellum and flagellar sheath and a dorsal plate (Fig. 17G) – indicates this species' true relatives (Fig. 7); *M. laterorectus* (Fig. 10F) and *M. laterosinuatus* (Fig. 10C–D). Chaetotaxy +/+//+/–//+/2/+/+.

Standardized body length 4.1 mm.

Description (n = 1). Head capsule broad, foreshortened, eyes small, moderately convex, ocular lobe meeting

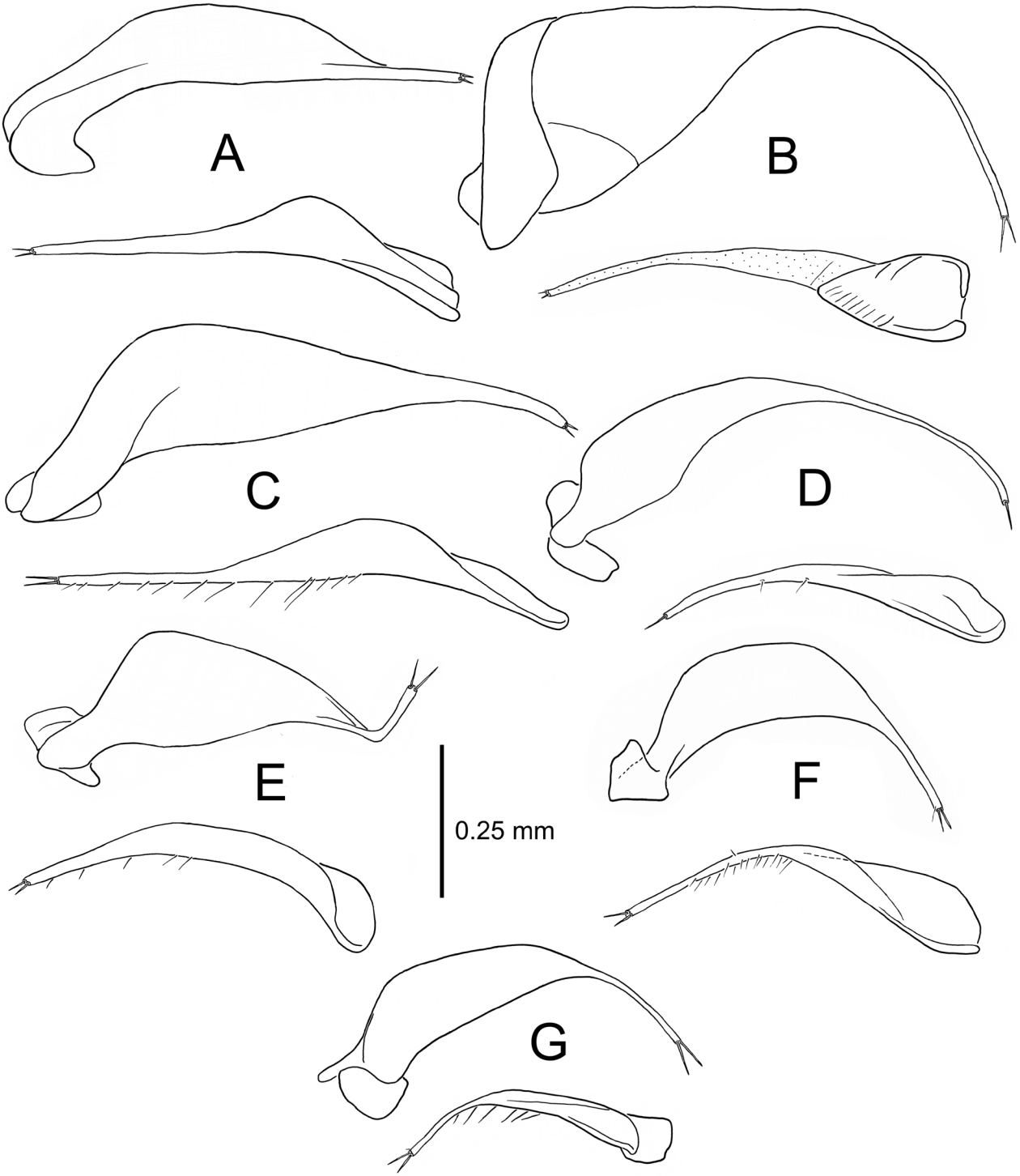

Figure 18. Paired left (above) and right (below) parameres of *Mecyclothorax* (*Phacothorax*) spp. (ectal view): **A**, *M. plurisetosus*; **B**, *M. megalovatulus*; **C**, *M. octavius*; **D**, *M. laterovatulus*; **E**, *M. manautei*; **F**, *M. paniensis*; **G**, *M. mouensis*.

gena at very obtuse angle; 15–16 ommatidia along horizontal diameter of eye; ocular ratio 1.39, ocular lobe ratio 0.89, EyL/EyD = 3.13; frontal grooves nearly straight from posterior terminus inside anterior supraorbital seta to deepest point just posterad clypeus, briefly and shallowly extended onto clypeus; mandibles moderately elongate, mandibular ratio 1.8; ligular anterior margin narrowly rounded to ligular seta, concave between setae, the two setae separated by one to two setal diameters; paraglossae thin, extended as far beyond ligular margin as their basal length to margin; antennae elongate, antennomere 9 length 2.5× maximal breadth; antennomere 3 glabrous except for apical ring of setae. Pronotum vase-shaped, hind angles broadly subangulate, lateral margins only slightly concave anterad angles (Fig. 16D); MPW/

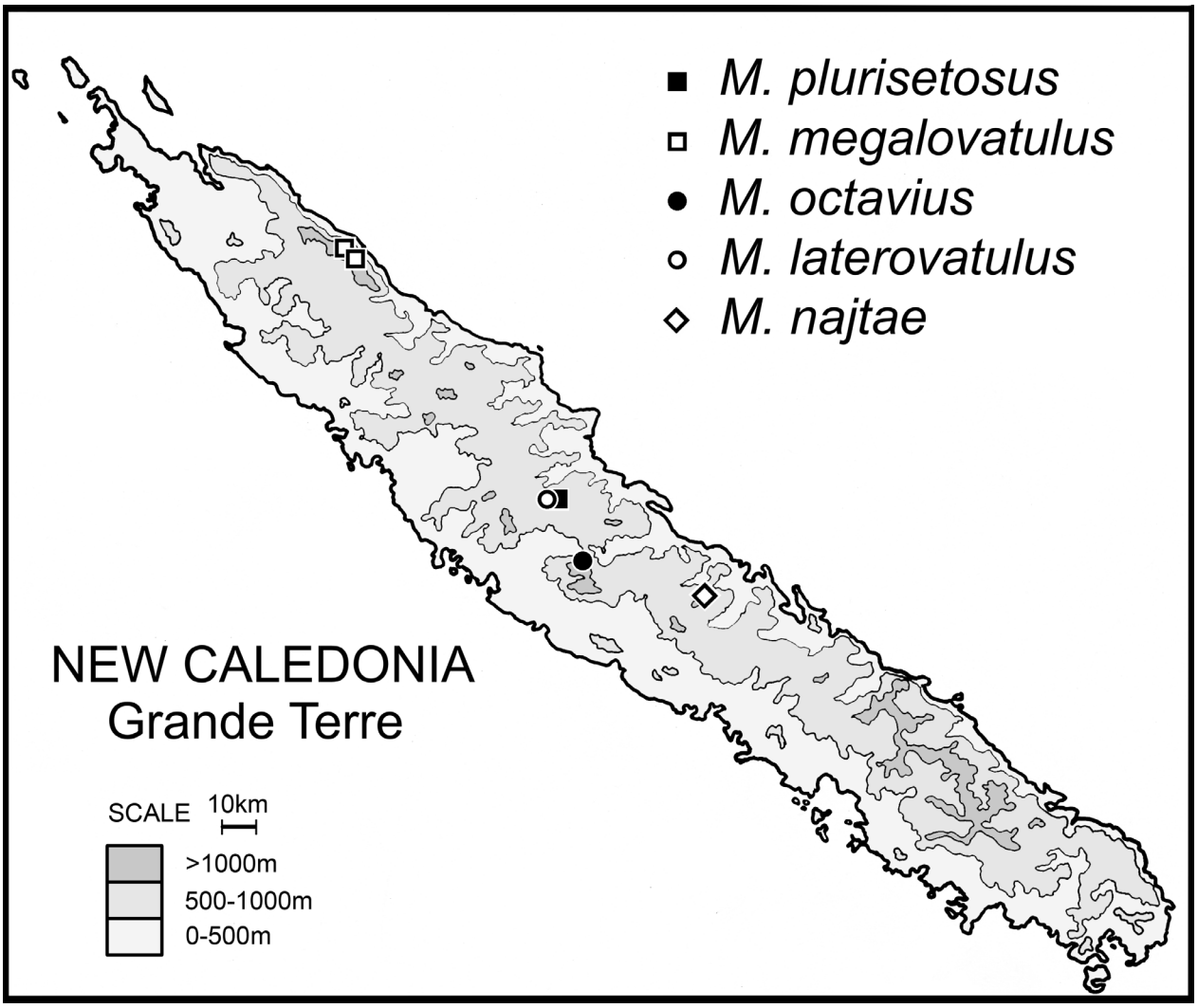

Figure 19. Geographical distributions of *Mecyclothorax* (*Phacothorax*) spp.

BPW = 1.66, MPW/PL = 1.24; front angles only slightly protruded, broadly obtuse, APW/BPW = 0.93; median base coplanar relative to disc, unmargined; laterobasal depression with longitudinal tubercle inside hind angle, defined medially by longitudinal border with median base; median longitudinal impression fine and shallow on disc, posteriorly terminated at deep lenticular pit anterad median base, terminated anteriorly at very broad and shallow anterior transverse impression; proepisternum separated anteriorly from prosternum by fine shallow groove, distinctly separated ventrally by smooth, deep groove; prosternal process deeply, narrowly depressed between procoxae, that depression extended 1/4 distance toward anterior prothoracic margin. Elytra broadly ellipsoid to hemiovoid, humeri extended laterally, humeral angle rounded outside pronotal hind angles; MEW/EL = 0.85; basal groove extended anterad from scutellum to humerus, with depressions at bases of sutural and elytral striae 4–5; sutural stria deep throughout length, striae 2 and 5–7 almost as well developed, striae 3–4 shallower though still evident; striae 1–2 and 7 evident apically, elytra appressed and conjoined apically, sutural intervals narrower and upraised at apex. Pterothoracic mesepisternal anterior furrow with five pitlike depressions in one vertical row; metepisternum maximum width/lateral length = 0.88; mesosternal-mesepisternal suture complete (as in Fig. 3A); metepisternal-metepimeral suture incomplete, shallower and incomplete laterally. Abdomen with deep crescent-shaped depression along suture between first and second ventrite, second ventrite depressed within crescent; suture between second and third ventrites reduced, incomplete laterally; ventrites 2–6 with broad, shallow, linear plaques near lateral margin. Microsculpture of frons and vertex an evident transversely stretched isodiametric mesh; pronotal disc and base covered with elongate transverse mesh, sculpticell breadth 3–4× length, surface iridescent, sculpticells in laterobasal depressions less transverse, breadth 2–3× length; elytra iridescent, disc with dense transverse lines loosely connected into a mesh, apex covered with transverse lines. Femora rufobrunneous, a piceous cloud in basal 2/3.

Male genitalia (n = 1). Antecostal margin of abdominal mediotergite IX angulate, not extended (Fig. 17H); right paramere narrow, narrowly extended apically (Fig.

18D), with two setae on the ventral margin complementing a single apical seta; left paramere narrow basally, extended as an elongate, whiplike extension with a single apical seta; aedeagal median lobe robust, broad dorsoventrally, apex evenly narrowed dorsally and ventrally to a narrowed rounded tip (Fig. 17G); aedeagal median lobe internal sac with dorsal plate, dorsally curved flagellum and flagellar sheath.

Type – Holotype male (MNHN): NEW CALEDONIA 11665 / 21°11'S 165°16'E. / Aoupinie, summit. 1000 m / 2Oct2004. G.Monteith / pyrethrum, trees&logs // QUEENSLAND / MUSEUM LOAN / DATE: July 2005 / No. LE 05.24 // *New Caledonia Mecyclothorax* revision / measured specimen 1 / J.K. Liebherr 2016 ♂1 // genitalia in polyethylene vial with glycerine // HOLOTYPE / Mecyclothorax / laterovatulus / J.K.Liebherr 2017 (black-bordered red label) /

Etymology. Though this species is separated in the dichotomous key and therefore in the species treatment sequence from its broad-bodied phylogenetic relatives (Fig. 9A-C), this species is given the compound adjectival epithet laterovatulus to signify the broad body and ovoid pronotum coupled with rounded pronotal hind angles (Fig. 16D), thereby making the species name reiterate the names of those other species; *M. laterobustus*, *M. laterorectus*, and *M. laterosinuatus*.

Distribution and habitat. The lone holotype of this species was collected on Aoupinié summit at 1000 m elevation via application of pyrethrin spray to trees and logs (Fig. 19). Based on restriction of its adelphotaxon, *M. laterorectus* + *M. laterosinuatus*, as well as the closely related *M. laterorobustus* (Fig. 7) to ground-level microhabitats, it is predicted that additional specimens of this species will be collected predominantly in ground level litter, or from mossy subcortical microhabitats.

10. *Mecyclothorax najtae* Deuve

Figures 16E, 19

Mecyclothorax najtae Deuve 1987: 144.

Diagnosis. This, the second of the small-bodied species with very obtuse pronotal hind angles and basally straight lateral pronotal margins (Fig. 16D–E) can be diagnosed by the unique elytral configuration with elytral length only slightly greater than breadth: MEW/EL = 0.96. This species is also characterized by extremely convex eyes, with the eye convexity ratio, EyL/EyD = 2.0. Standardized body length 3.7 mm. Chaetotaxy +/+//+/–//+/2/+/+.

Description (n = 1). As a complement to Deuve's (1987) description, we may add: 14 ommatidia along horizontal diameter of eye; ligular apex rounded, the two ligular setae separated by two setal diameters; paraglossae thin, extended beyond ligular margin 1/2 distance from their base to ligular margin; antennae moderately elongate, antennomere 9 length 2.25× maximal breadth. Pronotum transverse, hind angles very obtuse, the lateral margins only slightly concave anterad angles (Fig. 16E); MPW/BPW = 2.0, MPW/PL = 1.32; front angles only slightly protruded, broadly obtuse, pronotal apex and base subequal, APW/BPW = 1.05; proepisternum separated anteriorly from prosternum by fine shallow groove, distinctly separated ventrally by deep, indistinctly punctate groove; prosternal process deeply depressed between procoxae, that depression extended 1/2 distance toward anterior prothoracic margin. Abdomen with deep crescent-shaped depression along suture between first and second ventrite, second ventrite depressed within crescent; suture between second and third ventrites reduced, incomplete laterally; ventrites 2–6 with broad, shallow, linear plaques near lateral margin. Microsculpture of frons and vertex a shallow transversely stretched isodiametric mesh; pronotal disc covered with elongate transverse mesh, sculpticell breadth 2–3× length, surface subiridescent, sculpticells on median base and in laterobasal depressions less transverse, breadth 2× length; elytra iridescent, disc with dense transverse lines loosely connected into a mesh, apex covered with transverse lines.

Type – Holotype female (MNHN): HOLOTYPE (red label) // Nouvelle-Caledonie / Menazi 1020 m / 18.x84 Tillier"/"Bouchet // Mecyclothorax / najtae sp. n. / det. T. Deuve // *New Caledonia Mecyclothorax* revision / measured specimen 1 / J.K. Liebherr 2016. The specimen is mounted on two platens: 1, head, prothorax, and pterothorax separated from elytra; 2, abdominal ventrites. No female genitalic structures were available for study in this specimen.

Distribution and habitat. The type locality northwest of the summit of Menazi (Fig. 19) is situated at 21°26.83'S × 165°41.75'E. Deuve (1987) reported the microhabitat as humid *Auracaria* forest on peridotite; i.e. igneous, ultramafic rock.

11. *Mecyclothorax manautei* Liebherr, sp. n.

http://zoobank.org/0A0B84B4-7BC4-4925-B2DE-6AAF3582A1BF

Figures 17I–J, 18E, 20A, 23A, 24A, 25

Diagnosis. This species can be diagnosed by small body size–standardized body length 3.5–3.9 mm–and the transversely ovoid pronotum with evenly convex lateral margins basally, i.e., hind angles lacking (Fig. 20A). The elytral striae are much more reduced than in the prior two species–*M. laterovatulus* and *M. najtae*–with the sutural stria obsolete at midlength, and only striae 2–3 evident there, though very shallow. The eyes broadly cover the ocular lobe, ocular lobe ratio 0.88–0.89, and are very convex, i.e. "popeyed", with EyL/EyD = 2.2–2.4. Chaetotaxy +/+//+/–//+/2/+/+.

Description (n = 4). Head capsule quadrate, eyes very convex, popeyed, ocular lobe meeting gena at obtuse angle close to eye posterior margin; 14 ommatidia along horizontal diameter of eye; ocular ratio 1.48–1.52, ocular lobe ratio 0.88–0.89, EyL/EyD = 2.2–2.4; frontal grooves deep, slightly convergent to deepest portion just posterad clypeus, deeply extended onto clypeus; mandibles elongate, mandibular ratio 1.92; ligular anterior margin rounded to

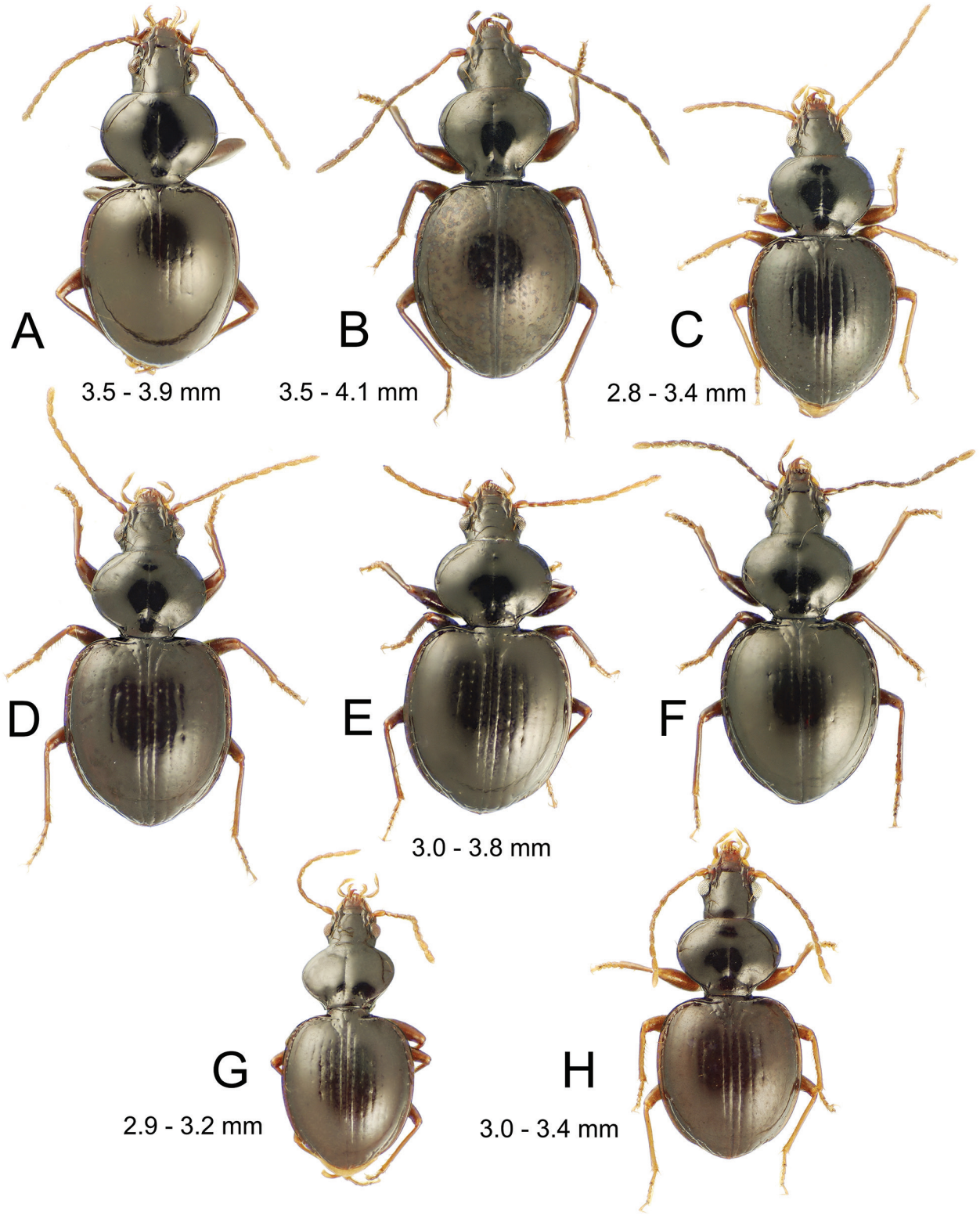

Figure 20. New Caledonian *Mecyclothorax* (*Phacothorax*) spp., dorsal view: **A**, *M. manautei*; **B**, *M. paniensis*; **C**, *M. mouensis*; **D**, *M. kanak* (Mt. Humboldt, 580 m); **E**, *M. kanak* (Mt. Humboldt, 630 m); **F**, *M. kanak* (Mt. Dzumac); **G**, *M. kanak* (Col de Yaté); **H**, *M. picdupinsensis*.

ligular seta, concave between setae, the two setae separated by one to two setal diameters; paraglossae thin, extended twice as far beyond ligular margin as their basal length to margin; antennae elongate, antennomere 9 length 2.25× maximal breadth; antennomere 3 glabrous except for apical ring of setae. Pronotum transversely ovoid, lateral margin evenly convex anterad base, hind angles absent though suggested by presence of short peduncular collar at base of

pronotum (Fig. 20A), MPW/BPW = 2.46–2.55, MPW/PL = 1.29–1.31; front angles slightly protruded, obtuse-rounded, APW/BPW = 1.39–1.48; median base unmargined basally, trapezoidally depressed relative to disc, the median longitudinal impression divided basally into two transverse impressions that isolate disc from base, each transverse basal impression terminated laterally in pitlike laterobasal depression; median longitudinal impression finely incised on disc, terminated anteriorly just anterad anterior transverse impression, a lenticular fovea at posterior juncture with basal transverse impressions; anterior transverse impression shallow, broad, but traceable to front angles; proepisternum separated from prosternum by a distinct groove both anteriorly and ventrally; smooth anteapical impression well developed laterally, continuous though shallower ventrally; prosternal process deeply and broadly depressed between procoxae, that depression extended 2/3 distance toward anterior prothoracic margin, the depression broadest at its anterior terminus. Elytra broadly ovoid, humeri sloped posteriorly laterad scutellum, humeral angle indicated only by slight change in curvature at juncture of narrow basal elytral groove and broader lateral marginal depression; MEW/EL = 0.79–0.94; all striae reduced on disc, stria 3 and 6 more evident, but intervening intervals at most slightly convex; only stria 8 evident apically, stria 2 present as very broad and shallow depression; elytra appressed and conjoined apically, the suture upraised at apex. Pterothoracic mesepisternal anterior furrow with 5 punctures in a curved line; mesosternal-mesepisternal suture complete (as in Fig. 3A); metepisternum maximum width/lateral length = 1.08; metepisternal-metepimeral suture complete. Abdomen with broad crescent-shaped depression along suture between first and second ventrite, second ventrite only slightly depressed within crescent; suture between second and third ventrites reduced though traceable laterally; ventrites 2–6 with broad, shallow, linear plaques near lateral margin. Microsculpture of frons reduced, surface glossy, indistinct transversely stretched sculpticells evident on vertex; pronotal disc glossy, transverse-line microsculpture visible over portions of surface depending on direction of light reflection, trapezoidal median base with only indistinct indications of transverse microsculpture; elytra iridescent, disc with elongate transverse mesh mixed with transverse lines, elytral apex covered with elongate transverse-mesh microsculpture.

Male genitalia (n = 1). Antecostal margin of abdominal mediotergite IX broadly angulate, not extended (Fig. 17J); right paramere narrow basally, evenly narrowed to apex, with 5 setae along ventral margin and two short apical setae (Fig. 18E); left paramere broad basally, narrowed to a dorsally twisted apex, parameral apex flexibly articulating with base, two elongate apical setae present; aedeagal median lobe robust, broad dorsoventrally, with apex distinctly down-curved relative to the expanded shaft and flattened into an apical face (Fig. 17I); male aedeagal internal sac with short flagellum and flagellar sheath present, a dorsal plate dorsad and basad flagellar complex, and a large dorsoapical field of macrospicules.

Female reproductive tract (n = 1). Bursa copulatrix length slightly greater than circumference, its surface thin, translucent, only slightly wrinkled (Fig. 23A); spermathecal duct entering near bursa-common oviduct juncture with duct oriented toward right side of bursa, duct length about 1.25× length of spermathecal reservoir; laminar helminthoid sclerite with rounded apex present at base of spermathecal duct; spermatheca fusiform on narrow duct, spermathecal gland duct entering at base of spermathecal reservoir; ligular apophysis present near base of common oviduct; basal gonocoxite 1 with apical fringe of two setae laterally–a smaller seta may be present medially–and several small setae near apex of medial margin (Fig. 24A); gonocoxite 2 moderately broad basally, basal width 0.6× medial length; two gracile lateral ensiform setae of moderate length present.

Types – Holotype male (MNHN): NEW CALEDONIA 11138 / 21°53'SX166°24'E.1400m. / Mt Humboldt, moss forest. / 6-7Nov2002. Monteith & / Burwell.pyreth,trees&logs // QUEENSLAND / MUSEUM LOAN / DATE: Nov. 2003 / No. LEN-1686 (green label) // *New Caledonia Mecyclothorax* revision / measured specimen 1 / J.K. Liebherr 2016 // HOLOTYPE / Mecyclothorax / manautei / J.K.Liebherr 2017 (black-bordered red label).

Paratypes (3 specimens). NEW CALEDONIA: Mt. Humboldt, moss forest, 1400 m el., 21°53'S 166°24'E, pyrethrum trees & logs, 06-07-xi-2002, lot 11138, Monteith/Burwell (QMB, 2), beyond summit, 1500 m el., 21°53'S 166°25'E, 07-xi-2002, lot 11122, Burwell (QMB, 1).

Etymology. This species epithet is a patronym honoring Joseph Manauté, Directeur du Parc Provincial de la Rivière Bleue chez Province Sud, who provided helicopter support for the Queensland Museum expedition to Mt. Humboldt, allowing Geoff Monteith and Chris Burwell to collect the type series of this species as well as other interesting and important taxa (Reid and Smith 2004).

Distribution and habitat. The species is known only from elevations 1400–1500 on Mt. Humboldt (Fig. 25). The four specimens were all collected via application of pyrethrin spray to tree trunks and downed logs.

12. *Mecyclothorax paniensis* Liebherr, sp. n.

http://zoobank.org/E2C4B0A1-CF5D-4890-AF6B-EA86F9D0F9CF
Figures 17K–L, 18F, 20B, 23B, 24B, 25

Diagnosis. These beetles can be diagnosed by the parallel lateral margins at the base of the pronotum, resulting in very slightly obtuse hind angles that protrude laterally (Fig. 20B). The elytral striae are much reduced, with the sutural striae only evident basally where it comprises a series of shallow, disconnected, elongate depressions. The elytra are broadly ovoid, with the humeri very reduced, with the elytral basal groove angulate posterad the protruded pronotal hind angles. Standardized body length 3.5–4.1 mm. Chaetotaxy +/+//+/–//+/2/+/+.

Description (n = 5). Head capsule elongate, eyes small, convex, ocular lobe-genal juncture evenly curved,

a very shallow groove indicating limit of ocular lobe; 14 ommatidia along horizontal diameter of eye; ocular ratio 1.35–1.42, ocular lobe ratio 0.77–0.82, EyL/EyD = 2.0–2.49; frontal grooves narrowly incised, straight and convergent to deepest portion at frontoclypeal suture, deeply extended onto clypeus; mandibles moderately elongate, mandibular ratio 1.71; ligular anterior margin narrowly rounded, the two ligular setae separated by one to two setal diameters; paraglossae thin, extended twice as far beyond ligular margin as their basal length to margin; antennae elongate, antennomere 9 length 2.62× maximal breadth; antennomere 3 glabrous except for apical ring of setae. Pronotum distinctly cordate, lateral margins slightly convergent anterad protruded, obtusely-angulate hind angles, the lateral margin immediately divergent anterad subparallel lateral margins at pronotal base (Fig. 20B), MPW/BPW = 1.83–1.88, MPW/PL = 1.13–1.26; front angles slightly protruded, obtuse, APW/BPW = 1.11–1.16; median base unmargined basally, trapezoidally depressed relative to disc, the median longitudinal impression divided basally into two transverse impressions that isolate disc from base, each transverse basal impression terminated laterally in a longitudinally arcuate laterobasal depression; median longitudinal impression finely incised on disc, terminated anteriorly just anterad anterior transverse impression, a lenticular fovea at posterior juncture with basal transverse impressions; anterior transverse impression shallow, broad, intermittently traceable to front angles; proepisternum separated from prosternum by a shallow groove anteriorly, and deep, distinct groove ventrally; smooth anteapical impression well developed laterally, continuous though shallower ventrally; prosternal process broadly depressed between procoxae, that depression extended 1/2 distance toward anterior prothoracic margin, the depression broadest at its anterior terminus. Elytra broadly ovoid, humeri extended laterally before sloping posteriorly laterad distinct, obtuse humeral angle; MEW/EL = 0.80–0.88; all striae reduced on disc, sutural and fourth stria most evident, but intervening intervals flat; sutural stria distinctly impressed apically to complement deep stria 8; elytra appressed and conjoined apically, the sutural margin upraised at apex. Pterothoracic mesepisternal anterior furrow with 2–3 irregular pits in deepest portion of furrow; mesosternal-mesepisternal suture complete (as in Fig. 3A); metepisternum slightly longer than broad, maximum width/lateral length = 0.92; metepisternal-metepimeral suture complete. Abdomen with broad crescent-shaped depression along suture between first and second ventrite, second ventrite only slightly depressed within crescent; suture between second and third ventrites reduced though traceable laterally; ventrites 2–6 with broad, shallow, linear to circular plaques near lateral margin. Microsculpture of frons reduced, surface glossy, indistinct transverse mesh visible over portions of vertex; pronotal disc glossy but with transverse sculpticells, breadth 4× length, and transverse lines over surface, trapezoidal median base with transverse sculpticells, breadth 3× length visible in areas of no reflection; elytra distinctly iridescent, disc covered with transverse lines, elytral apex covered with elongate transverse sculpticells and lines.

Male genitalia (n = 1). Antecostal margin broadly angulate, not extended (Fig. 17L); right paramere narrow basally, apical half narrowed into a narrow whiplike extension, its ventral surface bearing 15 setae near midlength distant from elongate pair of apical setae (Fig. 18F); left paramere narrow basally, evenly narrowed to a whiplike apex, two apical setae present; aedeagal median lobe robust, broad dorsoventrally, the ventral and dorsal margins evenly curved to a broadly rounded apex that extends moderately beyond ostial opening (Fig. 17K); aedeagal median lobe internal sac with elongate flagellum and flagellar sheath plus dorsal plate.

Female reproductive tract (n = 1). Bursa copulatrix length slightly greater than circumference, its surface thin, translucent, not wrinkled (Fig. 23B); spermathecal duct entering near bursa-common oviduct juncture with duct oriented toward right side of bursa, duct length twice length of spermathecal reservoir; knoblike helminthoid sclerite present at base of spermathecal duct; spermatheca fusiform on narrow duct, spermathecal gland duct entering at base of spermathecal reservoir; ligular apophysis present on common oviduct; basal gonocoxite 1 with apical fringe of two setae laterally and several smaller setae medially, a series of small setae lining medial margin (Fig. 24B); gonocoxite 2 moderately broad basally, basal width half medial length; two gracile lateral ensiform setae of moderate length present, the apical seta slightly broader.

Types – Holotype male (MNHN): NEW CALEDONIA / Mt Panie summit / Nov 2001 / C. Burwell // QM Berlesate 1058 / 20°34’Sx164°46’E / Rainforest, 1600m / Sieved litter // QUEENSLAND / MUSEUM LOAN / DATE: Sept 2002 No. LE 02.43 (green label) // HOLOTYPE / Mecyclothorax / paniensis / J.K.Liebherr 2017 (black-bordered red label).

Paratypes (11 specimens). NEW CALEDONIA: Mt. Panié, 20°34’S 164°46’E, 08-x-1977, J. Balogh (HNHM, 1), 1300-1600 m, 15-v-1984, Monteith & Cook (QMB, 1), E trail, 1350–1629 m el., 20°35.3’S 164°46.2’E, rainforest, 24-xi-2010, Wanat & Ruta (MNHW, 3), refuge, 1300 m el., 20°34’S 164°46’E, rainforest, sieved litter, 8–9–xi–2001, lot 1056, Burwell (QMB, 2), summit, 1600 m el., 20°34’S 164°46’E, rainforest, sieved litter, xi-2001, lot 1058, Burwell (QMB, 2), summit, 1600, 20°35’S 164°46’E, 18-xi-2000, 9939, Bouchard, Burwell & Monteith (QMB, 2).

Etymology. The adjectival ending -ensis is elided with the type locality Mt. Panié to obtain the species epithet paniensis, an adjective in the genitive case.

Distribution and habitat. This species’ distribution is restricted to Mt. Panié (Fig. 25). Collecting localities are in the higher reaches of the mountain, 1300–1629 m elevation, with recorded microhabitats or collecting situations including rainforest and sieved litter. As such it appears beetles of this species occupy the ground-level litter layer.

13. *Mecyclothorax mouensis* Moore & Liebherr, sp. n.

http://zoobank.org/572EF2F8-5BF7-4663-8F53-74100E27DF5E
Figures 2B, 17M–N, 18G, 20C, 23C, 24C, 25

Diagnosis. This species, along with *M. kanak* and *M. picdupinsensis*, comprises a triplet of cryptic sibling species best determined using the male aedeagal median lobe. To that end, this species is characterized by a median lobe with the apex dorsally and ventrally subparallel beyond the ostial opening, and with the lobe's apical face narrowly flattened (Fig. 17M). All three species share broadly hemiovoid elytra, with this species exhibiting a broadly rounded basal groove across the humerus. Individuals of this species can be best diagnosed externally from those of the following two species by the broader elytral lateral marginal depression outside the anterior series of lateral elytral setae (Fig. 20C). The anterior lateral elytral setae are situated in the lateral depression in beetles of this species, whereas they lie on the upraised lateral reaches of the elytral disc in *M. kanak* and *M. picdupinsensis*. Also the sutural stria is deep and smooth on the disc and striae 2–3 are evident and traceable to nearly obsolete in *M. mouensis*. This differs from the sutural stria in beetles of the following two species where the sutural stria is crenulate to indistinctly punctate on the disc. Standardized body length 2.8–3.4 mm. Chaetotaxy +/+//+/–//+/2/+/+.

Description (n = 5). Head capsule elongate, eyes small, very convex, ocular lobe-genal juncture evenly curved, a very shallow groove indicating limit of ocular lobe; 11 ommatidia along horizontal diameter of eye; ocular ratio 1.43–1.48, ocular lobe ratio 0.73–0.77, EyL/EyD = 2.17–2.38; frontal grooves narrowly incised, sinuously convergent to pit at frontoclypeal suture, briefly extended onto clypeus; mandibles moderately elongate, mandibular ratio 1.73; ligula narrowed to a moderately broad, slightly convex anterior margin, the two ligular setae separated by one setal diameter; paraglossae thin, extended twice as far beyond ligular margin as their basal length to margin, apex visibly spiculate (100×); antennae moderately elongate, antennomere 9 length 2.0× maximal breadth; antennomere 3 glabrous except for apical ring of setae. Pronotum very transverse, distinctly cordate, lateral margins sinuately concave anterad obtuse-rounded hind angles (Figs 2B, 20C), MPW/BPW = 2.43–2.82, MPW/PL = 1.35–1.39; front angles slightly protruded, obtuse, APW/BPW = 1.42–1.50; median base unmargined basally, trapezoidally depressed relative to disc, the median longitudinal impression divided basally into two transverse impressions that isolate disc from base, each transverse basal impression terminated laterally in a short laterally arcuate laterobasal depression; median longitudinal impression finely incised on disc, terminated anteriorly at anterior transverse impression, a narrow fovea at posterior juncture with basal transverse impressions; anterior transverse impression shallow, broad, traceable to front angles; proepisternum separated from prosternum by a shallow groove anteriorly, and deep, distinct groove ventrally; smooth anteapical impression well developed laterally, continuous though shallower ventrally; prosternal process broadly, shallowly depressed between procoxae, the shallow depression extended 1/2 distance toward anterior prothoracic margin. Elytra broadly hemiovoid, humeri well-extended laterally before lateral margins curve posteriorly; basal elytral groove posteriorly curved laterad obtuse humeral angle; MEW/EL = 0.85–0.91; sutural stria well developed in basal 2/3, striae 2–3 traceable on disc near positions of dorsal elytral setae, stria 4 indicated by an series of intermittent longitudinal depressions; only stria 8 evident on elytral apex; elytra appressed and conjoined apically, the sutural margin upraised at apex. Pterothoracic mesepisternal anterior furrow with five to six depressions in one to two irregular rows; mesosternal-mesepisternal suture complete (as in Fig. 3a); metepisternum length and breadth subequal; metepisternal-metepimeral suture complete though fine laterally. Abdomen with elongate crescent-shaped depression along suture between first and second ventrite, second ventrite only slightly depressed within crescent; suture between second and third ventrites reduced though traceable laterally; ventrites 3–6 with broad, shallow, linear plaques near lateral margin. Microsculpture of frons reduced, surface glossy, indistinct transverse mesh–sculpticell breadth 2× length–visible over portions of vertex; pronotal disc glossy but with transverse sculpticells visible outside areas of reflection, trapezoidal median base glossy with indistinct transverse mesh anterad laterobasal depression; elytra opalescent, disc covered with very finely separated transverse lines, elytral apex covered with elongate transverse sculpticells and lines.

Male genitalia (n = 8). Antecostal margin of mediotergite IX angulate, not extended (Fig. 17N); right paramere narrow, with basal cuff articulating with elongate, whiplike apical extension (Fig. 18G), six setae along ventral margin to complement to longer apical setae; left paramere narrow basally, evenly narrowed to whiplike apex; aedeagal median lobe robust, broadest medially basad apex of ostial opening, apex subparallel dorsoventrally beyond ostium, with apical face somewhat flattened (Fig. 17M); aedeagal median lobe internal sac with broad, basal dorsal plate and a large field of macrospicules apicad the plate, but flagellum and flagellar sheath not present.

Female reproductive tract (n = 1). Bursa copulatrix length subequal to circumference, its surface thin, translucent, slightly wrinkled (Fig. 23C); spermathecal duct entering near bursa-common oviduct juncture with duct oriented toward right side of bursa; elongate laminar helminthoid sclerite present at base of spermathecal duct; spermatheca of only slightly greater circumference than spermathecal duct, spermathecal gland duct entering at base of spermathecal reservoir; ligular apophysis present on common oviduct; basal gonocoxite 1 with apical fringe of two setae laterally, a very small setae may be present immediately mesad, and several smaller setae along medial margin (Fig. 24C); medial margin bearing a dense field of microtrichia basally, this field about 3–4

microtrichia broad and appearing like the hooklike surface of a Velcro® closure; gonocoxite 2 moderately broad basally, basal width 0.6× medial length; two gracile lateral ensiform setae of moderate length present.

Types – Holotype male (MNHN): NEW CALEDONIA / Mt Mou summit / 24 May 1984 / G. Monteith & D. Cook // Q.M. Berlesate 659 / 22.04S X 166.21E / Rainforest, 1200 n / Litter // QUEENSLAND / MUSEUM LOAN / DATE: Nov. 2003 / No. LEN-1686 (green label) // HOLOTYPE / Mecyclothorax / mouensis / B.P. Moore & J.K. / Liebherr 2017 (black-bordered red label).

Paratypes (33 specimens). NEW CALEDONIA: Mts. Koghis, [code PA 58], 22°11'S 166°31'E, 30-viii-1970, Franz (NHMW, 3), ~5 km N Noumea, 550 m el., 22 10.5'S, 166 30.3'E, forest litter, 25-xi-2009, Schuh (NHMW, 1), forest, 520 m el., 22°10.7'S 166°30.3'E, sifted litter, 25-x-2008, Wanat (MNHW, 9), La Roussette, 600 m el., 22°10.8'S 166°30.7'E, sifted litter, 27-x-2008, Wanat (MNHW, 4), track entrance, 500 m el., 22°11'S 166°31'E, berlesate, 06-v-2005, lot 12264, Monteith (QMB, 4), 500 m el., 22°10'S 166°31'E, 26-viii-1978, S. & J. Peck (CNC, 1), 400-500 m el., 22°11'S 166°31'E, primary forest, 18–19-x-1998, Löbl (MBC, 1; MHNG, 6); Mt. Mou, summit, 1200 m el., 22°04'S, 166°21'E, rainforest litter, 24-v-1984, Monteith & Cook (QMB, 2), top camp, 1150 m el., 22°04'S, 166°21'E, berlesate, sieved litter, 27-xii-2004, lot 12013, Monteith (QMB, 2). Non-type female specimen: Forêt Cachée, 250 m el., 22°11.5'S 166°47.2'E, sifted litter, 26-x-2008, Wanat (MNHW, 1).

Etymology. As in the species above, this species epithet elides the type locality, Mt. Mou, with the genitive, adjectival ending -ensis. As Dr. Barry P. Moore had both diagnosed this species from the following *M. kanak* through the use of male genitalic characters, and had chosen a holotype specimen, he is given senior author status for this species.

Distribution and habitat. This species is restricted to the southern portion of Grande Terre, from Mt. Mou on the west, Mts. Koghis north of Noumea, and with a easternmost record from Forêt Cachée based on a single non-type female specimen (Fig. 25). Collection localities range 250–1200 m elevation. Given that 24 of the 35 specimens are labeled from Berlese samples or sieved litter, and another 7 specimens (1, S. & J. Peck, CNC; 6, Löbl, MHNG) were collected by coleopterists studying the microcoleopteran litter fauna, it can be concluded that this species occupies the ground-level litter layer.

14. *Mecyclothorax kanak* Moore & Liebherr, sp. n.

http://zoobank.org/062E8A3B-6762-429F-B2D7-669FB5A2AE14
Figures 1H, 20D–G, 21A–K, 22A, 23D–E, 24D, 26

Diagnosis. This second of the species triplet also including *M. mouensis* and *M. picdupinsensis* can be diagnosed externally by characters listed in the *M. mouensis* diagnosis. This species and the following *M. picdupinsensis* are adelphotaxa based on possession of the synapomorphous hitch on the apical surface of the male aedeagal median lobe (Fig. 7, character 112, state 1). This species can be diagnosed from *M. picdupinsensis* by the hitch configuration being a well-developed apical invagination (Fig. 21A–D, F–K), the level of invagination, curvature and length of the apex varying among populations assigned to this species (Fig. 26). In these instances the apical invagination is much more developed than in the sister species below (Fig. 21L–N). Much like the externally-cryptic species pair *M. fleutiauxi* and *M. jeanneli* (Fig. 9D–E), these two species are indistinguishable based on external characters. They are treated as distinct species because just as in the *M. fleutiauxi* + *M. jeanneli* pair, female reproductive tract characters also differ between the two taxa. In *M. kanak* females, the bursa copulatrix is more parallel-sided in ventral view, with the apex narrowed (Fig. 23D–E). Also, the basal gonocoxites bear a narrow, spiculate mediobasal band of fine, setose spicules (Fig. 24D), versus basal gonocoxites with a broader spiculate mediobasal band of spatulate spicules in *M. picdupensis* (Fig. 24E). Standardized body length 3.0–3.8 mm (Fig. 20D–F) for all population samples except that from Col de Yaté, for which the three specimens range 2.9–3.2 mm length (Fig. 20G). Chaetotaxy +/+//+/–//+/2/+/+.

Description (n = 24). Head capsule elongate, eyes small, very convex, ocular lobe-genal juncture evenly curved, a very shallow groove indicating limit of ocular lobe; 12–14 ommatidia along horizontal diameter of eye; ocular ratio 1.41–1.54, ocular lobe ratio 0.74–0.81, EyL/EyD = 2.16–2.45; frontal grooves narrowly incised, sinuously convergent to pit at frontoclypeal suture, extended onto clypeus; mandibles moderately elongate, mandibular ratio 1.60; ligula narrowed to a moderately broad, slightly convex anterior margin, the two ligular setae separated by 1–2 setal diameters; paraglossae thin, extended twice as far beyond ligular margin as their basal length to margin, apex visibly spiculate (100×); antennae moderately elongate, antennomere 9 length 2.1× maximal breadth; antennomere 3 glabrous except for apical ring of setae. Pronotum very transverse, distinctly cordate, lateral margins sinuately concave anterad obtuse-rounded hind angles (Fig. 20D–G), MPW/BPW = 2.31–2.64, MPW/PL = 1.27–1.37; front angles slightly protruded, obtuse, APW/BPW = 1.27–1.48; median base unmargined basally, trapezoidally depressed relative to disc, the median longitudinal impression divided basally into two transverse impressions that isolate disc from base, each transverse basal impression terminated laterally in a short linear laterobasal depression; median longitudinal impression finely incised on disc, terminated anteriorly just anterad anterior transverse impression, a narrow fovea at posterior juncture with basal transverse impressions; anterior transverse impression shallow, broad, traceable to front angles; proepisternum separated from prosternum by a shallow groove anteriorly, and deep, distinct groove ventrally; smooth anteapical impression well developed laterally, continuous though shallower ventrally; prosternal pro-

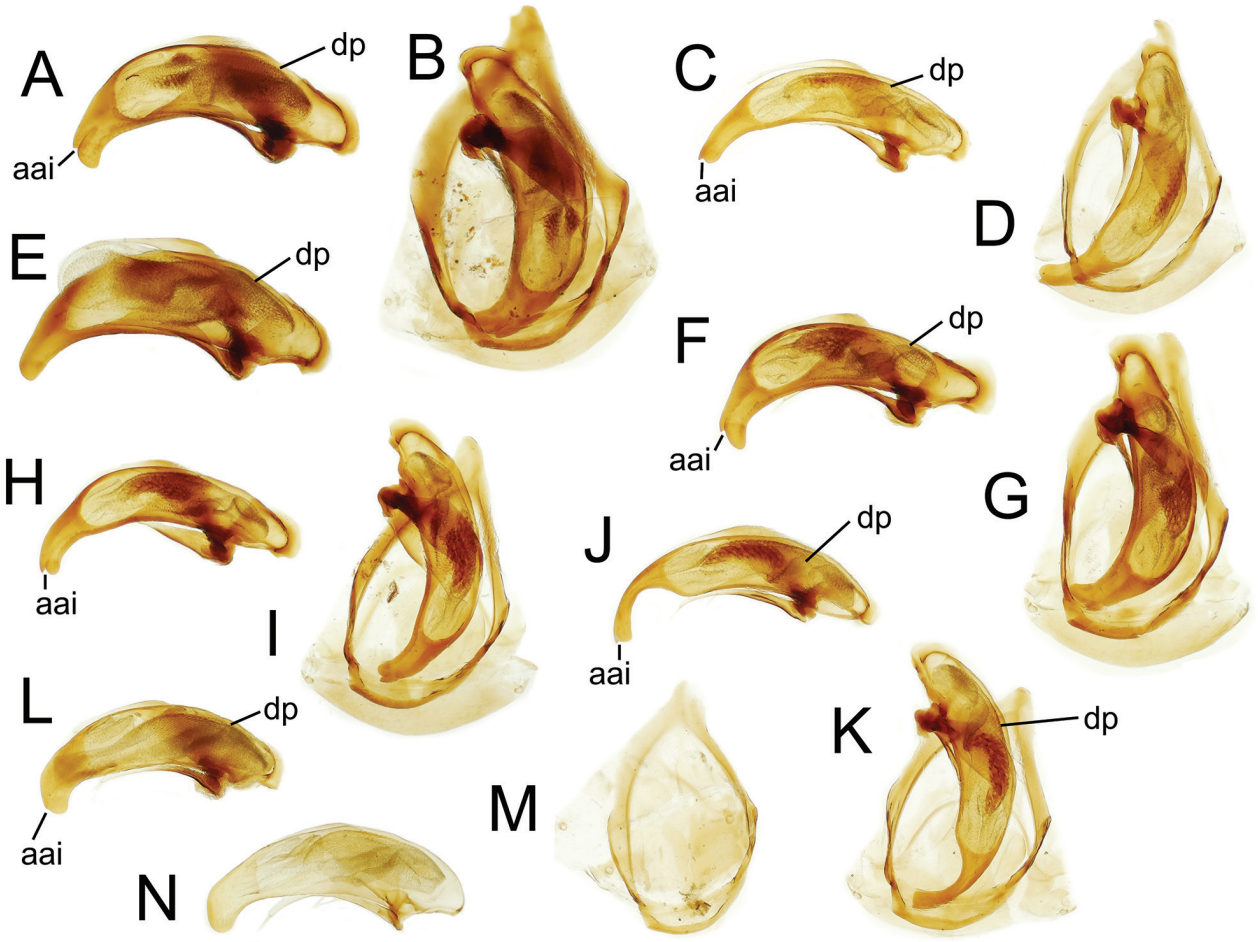

Figure 21. Male aedeagal median lobe and parameres, and ring sclerite–mediotergite plus antecostal margin, tergite IX–of *Mecyclothorax* (*Phacothorax*) spp.: **A–B**, *M. kanak*, right view, dorsal view in situ (Mt. Humboldt, 630 m); **C–D**, *M. kanak*, right view, dorsal view in situ (Mt. Humboldt, 1400 m); **E**, *M. kanak*, form Q, right view (Mt. Humboldt, 1300 m); **F–G**, *M. kanak*, right view, dorsal view in situ (Mt. Dzumac); **H–I**, *M. kanak*, right view, dorsal view in situ (Rivière Bleue); **J–K**, *M. kanak*, right view, dorsal view in situ (Col de Yaté); **L–N**, *M. picdupinsensis*, right views, dorsal view of ring sclerite. See Table 2 for abbreviations.

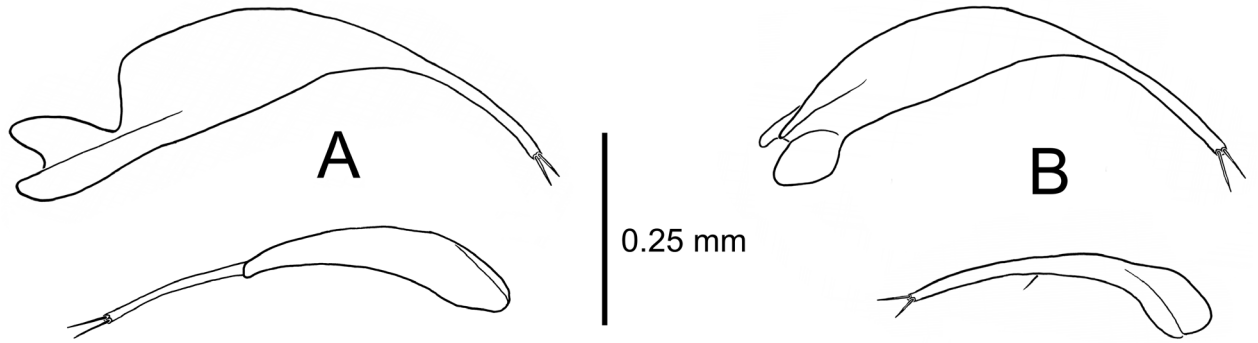

Figure 22. Paired left (above) and right (below) parameres of *Mecyclothorax* (*Phacothorax*) spp. (ectal view): **A**, *M. kanak*; **B**, *M. picdupinsensis*.

cess broadly, shallowly depressed between procoxae, the shallow depression extended 1/3 distance toward anterior prothoracic margin. Elytra broadly hemiovoid, humeri well-extended laterally before lateral margins curve posteriorly; basal elytral groove posteriorly curved laterad obtuse humeral angle, with three punctate depressions at the base of sutural and striae 5 and 5; MEW/EL = 0.81–0.93; sutural stria well developed in basal 2/3, striae 2–3 traceable on disc near positions of dorsal elytral setae, all three irregularly depressed with intermittent crenulations or elongate punctures along their length; stria 4 indicated by an intermittent series of shallow longitudinal depressions;

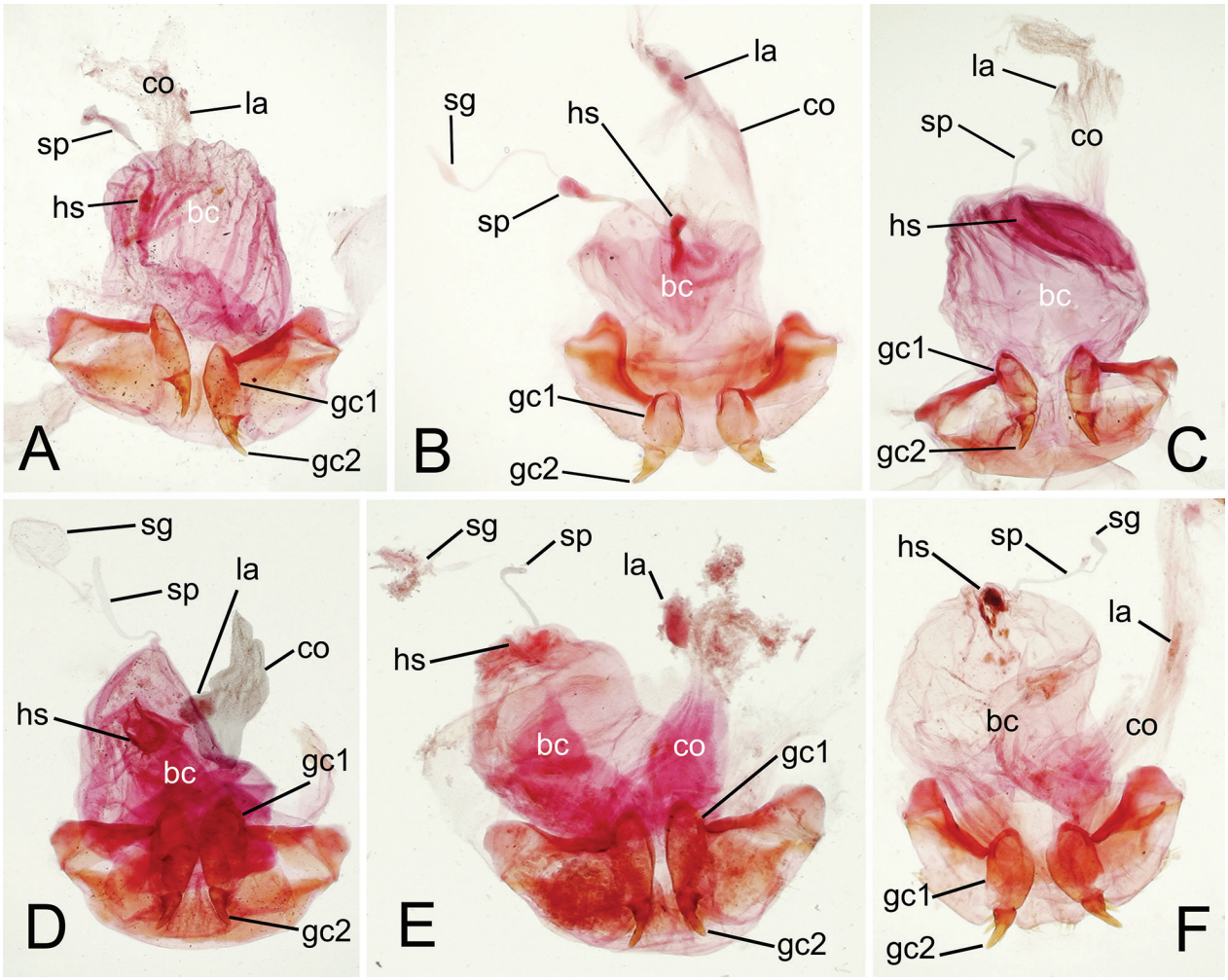

Figure 23. Female reproductive tract, gonocoxites and associated laterotergites, *Mecyclothorax* (*Phacothorax*) spp: **A**, *M. manautei*; **B**, *M. paniensis*; **C**, *M. mouensis*; **D**, *M. kanak* (Mt. Dzumac; common oviduct artificially darkened to show configuration); **E**, *M. kanak* (Pic du Grand Kaori); **F**, *M. picdupinsensis*. See Table 2 for abbreviations.

striae 1 and 2 shallow and traceable, and stria 8 evident on elytral apex; elytra appressed and conjoined apically, the sutural margin upraised at apex. Pterothoracic mesepisternal anterior furrow with 5 depressions in 1–2 irregular rows; mesosternal-mesepisternal suture complete (as in Fig. 3A); metepisternum foreshortened, lateral length/maximum width = 1.1–1.25; metepisternal-metepimeral suture complete though fine laterally. Abdomen with very elongate, shallowly curved crescent-like depression along suture between first and second ventrite, second ventrite only slightly depressed within crescent; suture between second and third ventrites reduced though traceable laterally; ventrites 3–6 with broad, shallow, linear plaques near lateral margin. Microsculpture of frons reduced, surface glossy, indistinct transverse mesh–sculpticell breadth 2× length–visible over portions of vertex; pronotal disc glossy but with transverse sculpticells visible outside areas of reflection, trapezoidal median base glossy with indistinct transverse mesh anterad laterobasal depression; elytra opalescent, disc covered with very finely separated transverse lines, elytral apex covered with elongate transverse sculpticells and lines.

Male genitalia (n = 25). Antecostal margin of abdominal mediotergite IX angulate, not extended (Fig. 21B, D, G, I); right paramere narrow, extended as a very narrow whiplike extension which flexibly articulates with the base, both ventral and dorsal margins glabrous, with two apical setae (Fig. 22A); left paramere moderately broad basally, evenly narrowed to a whiplike apex, two longer apical setae present; aedeagal median lobe variously robust, broader relative to length in specimens with a shorter aedeagal apex (Fig. 21A, F), and narrower relative to length in males with more gracile median lobes (Fig. 21C, H, J); median lobe apex variously bifurcate–except for the infraspecific variant, form Q discussed below (Fig. 21E)–with an apical aedeagal invagination laterally splitting the tip, that invagination continued laterally on the median lobe toward the ostial opening (Fig. 21A, C, F, H, J); aedeagal apex variously extended and curved, from short and broad, and briefly extended beyond the ostial opening (Fig. 21A, F), to more elongate broadly extended and slightly downturned (Fig. 21H), to more elongate and narrowly extended (Fig. 21C), to very narrowly extended and distinctly curved (Fig. 21J); median lobe internal sac

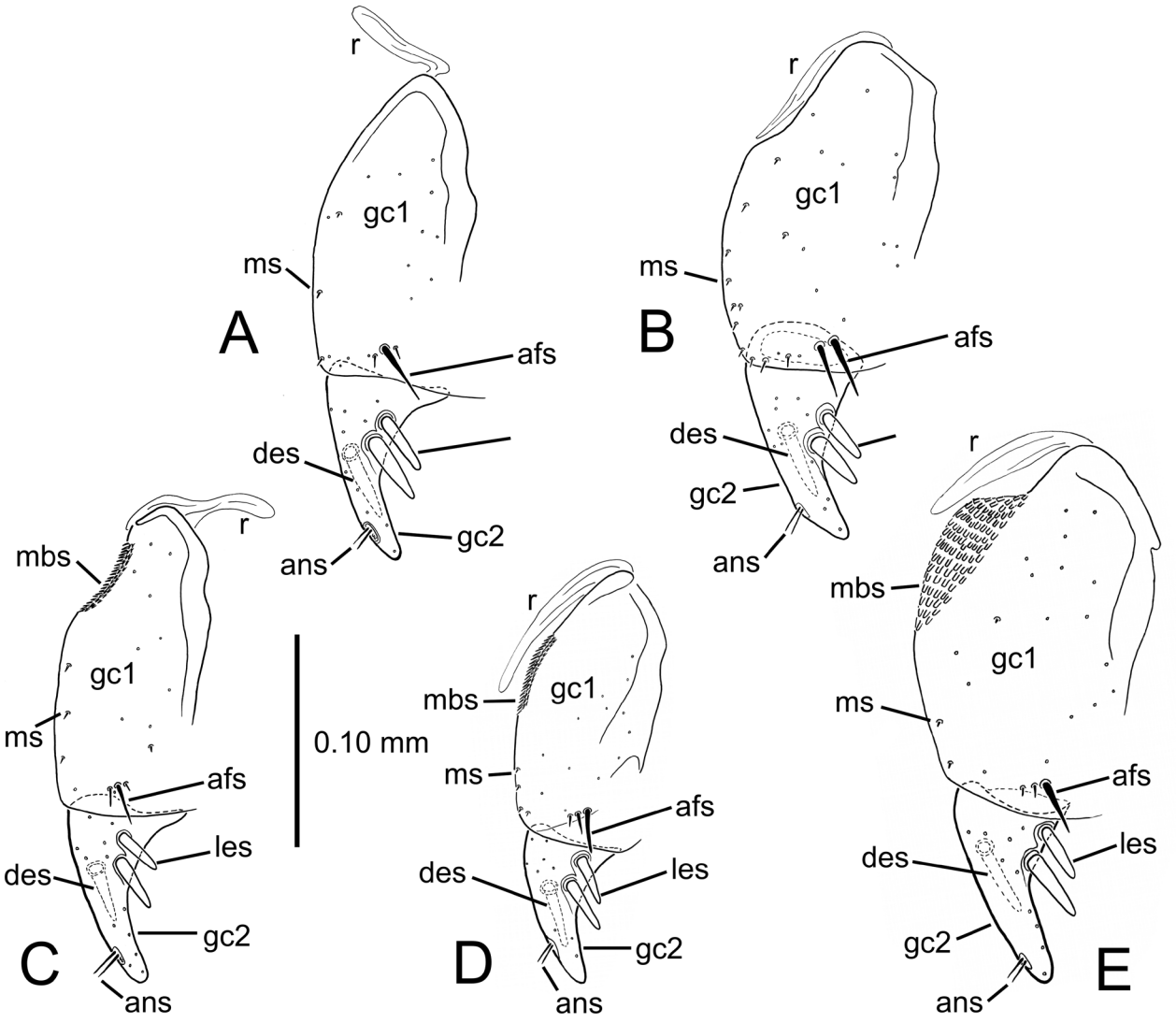

Figure 24. Left female gonocoxa of *Mecyclothorax* (*Phacothorax*) spp., ventral view: **A**, *M. manautei*; **B**, *M. paniensis*; **C**, *M. mouensis*; **D**, *M. kanak*; **E**, *M. picdupinsensis*. See Table 2 for abbreviations.

with translucent dorsal plate, most visible in well-sclerotized specimens (Fig. 21A, E, J), and a longitudinal apical field of microspicules (Fig. 21A, J).

One of a series of nine males from Mt. Humboldt, 1300 m el., 6–7-xi-2002, Monteith & Wright, lot 1076 (QMB) exhibits a broad aedeagus with a rounded tip, the ostial opening more asymmetrical apically (Fig. 21E), herein dubbed form Q. The other eight males of this particular collecting series all exhibit aedeagal apices similar to those from Mt. Humboldt, 1400 m (Fig. 21C). There are no external differences discernible among the males of this series, and no other examined male from Mt. Humboldt or anywhere else across the distributional range exhibits the "form Q" aedeagal configuration. Therefore this form is considered an infraspecific variant without nomenclatural status, with its evolutionary basis requiring further study.

The geographic pattern of aedeagal configuration shows that populations in the southern end of the range include males with a longer, narrower, and more curved aedeagal apex (Fig. 26, populations G, H, I). The extreme of this trend is observed in two males from Col de Yaté (Fig. 26, population G). The beetles comprising the Col de Yaté sample also tend to be smaller, though the size range of the three specimens of this population sample overlap the ranges of other populations, precluding diagnosis by size. Given the trend toward longer, narrower aedeagal apices in the south, and the demonstrated variation in aedeagal apices among other population samples (e.g. Fig. 26, population samples C, F), this variation is considered infraspecific.

Female reproductive tract (n = 4). Bursa copulatrix length 1.1–1.4× circumference, its surface thin, translucent, slightly to not wrinkled (Fig. 23D–E); spermathecal duct entering at apex of bursa separate from bursa-common oviduct juncture; rounded helminthoid sclerite on bursal wall between, and separate from both, bursal-common oviduct juncture and spermatheca; spermatheca of

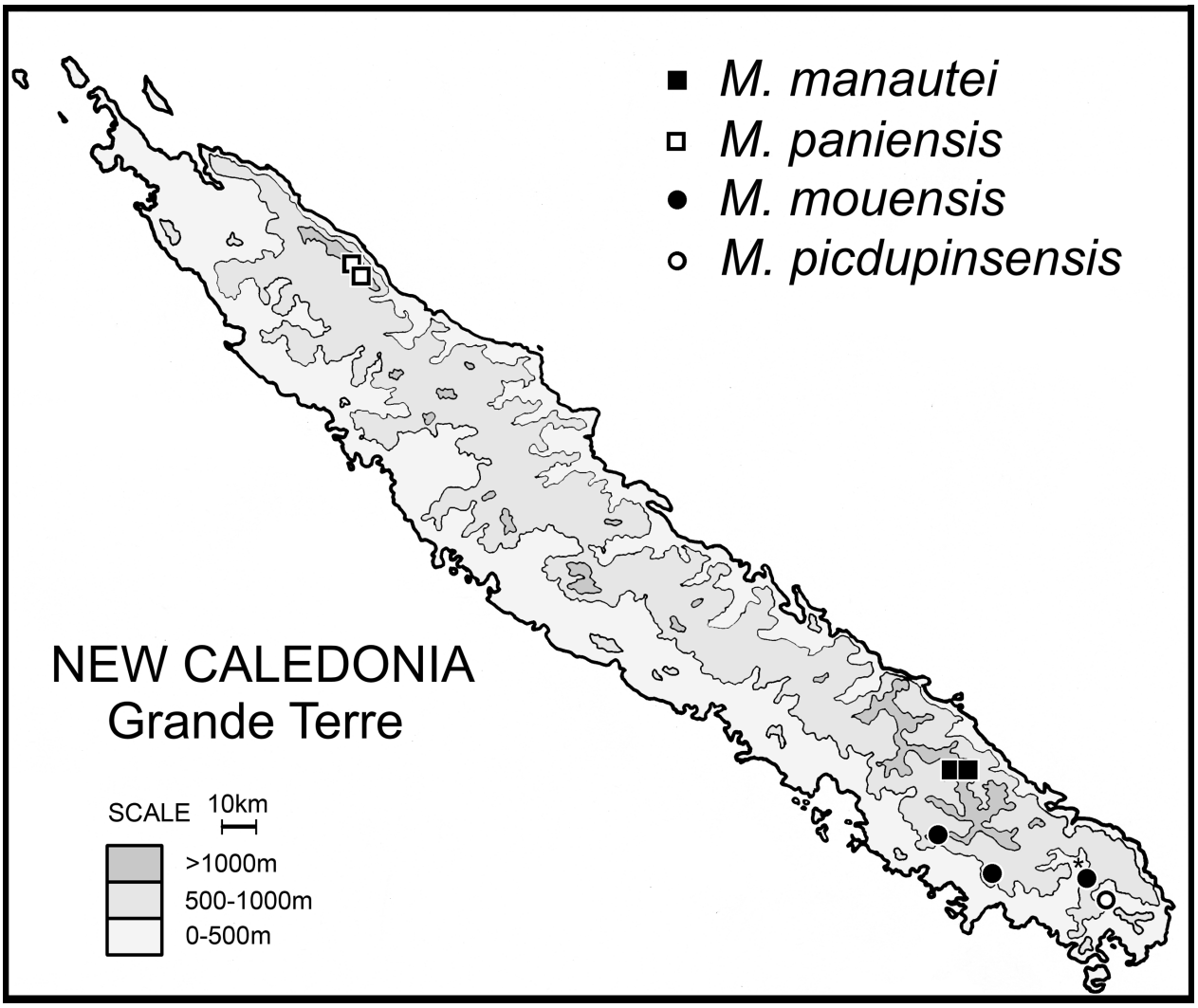

Figure 25. Geographical distributions of *Mecyclothorax* (*Phacothorax*) spp. (asterisked locality attributed to *M. mouensis* based on non-type female specimen).

only slightly greater circumference than spermathecal duct, reservoir about 1/2 length of spermathecal duct, spermathecal gland duct entering at base of spermathecal reservoir (Fig. 23E); ligular apophysis present on common oviduct; basal gonocoxite 1 with apical fringe of two to unilaterally three setae laterally, a very small setae may be present immediately mesad, and several smaller setae occur along apex of medial margin (Fig. 24D); medial margin bearing a dense field of spiculate microtrichia basally, this field about 3–4 microtrichia broad and appearing like the hooklike surface of a Velcro® closure; gonocoxite 2 moderately broad basally, basal width 1/2 medial length; two gracile lateral ensiform setae of moderate length present.

Types – Holotype male (MNHN): NEW CALEDONIA / Mt Dzumac / 28 May 1987 / R.Raven // Q.M. Berlesate No. 800 / 22.03'S. 166.28'E. / Rainforest 900m / Litter // QUEENSLAND / MUSEUM LOAN / DATE: Nov. 2003 / No. LEN-1686 (green label) // HOLOTYPE / Mecyclothorax / kanak / B.P. Moore & J.K. / Liebherr 2017 (black-bordered red label).

Paratypes (181 specimens; CUIC, EMEC, MBC, MHNG, MNHW, NHMW, PMGC, QMB): see Suppl. material 2.

Etymology. This species is named to honor the Kanak people of New Caledonia. As the species epithet kanak is not derived from Latin, it is to be treated as indeclinable (I.C.Z.N. 1999, Article 31.2.3). Dr. B. P. Moore diagnosed this species from the preceding sibling species *M. mouensis*, and as such it is appropriate that he receive senior authorship for the species.

Distribution and habitat. This species is densely and abundantly distributed across the southern reaches of Grande Terre, with records from Mt. Humboldt south to Forêt Nord (Fig. 26). Collecting localities range from 70 m elevation along the Tontouta River, to 1500 m on the slopes of Mt. Humboldt. Professor Alexander von Humboldt (Wulf 2015) would no doubt be very interested to learn that this species occurs from 580–1500 m elevation on his namesake mountain, inhabiting lowland rain forest, montane rain forest, and high-altitude maquis (Mueller-Dombois and Fosberg 1998), where this species was

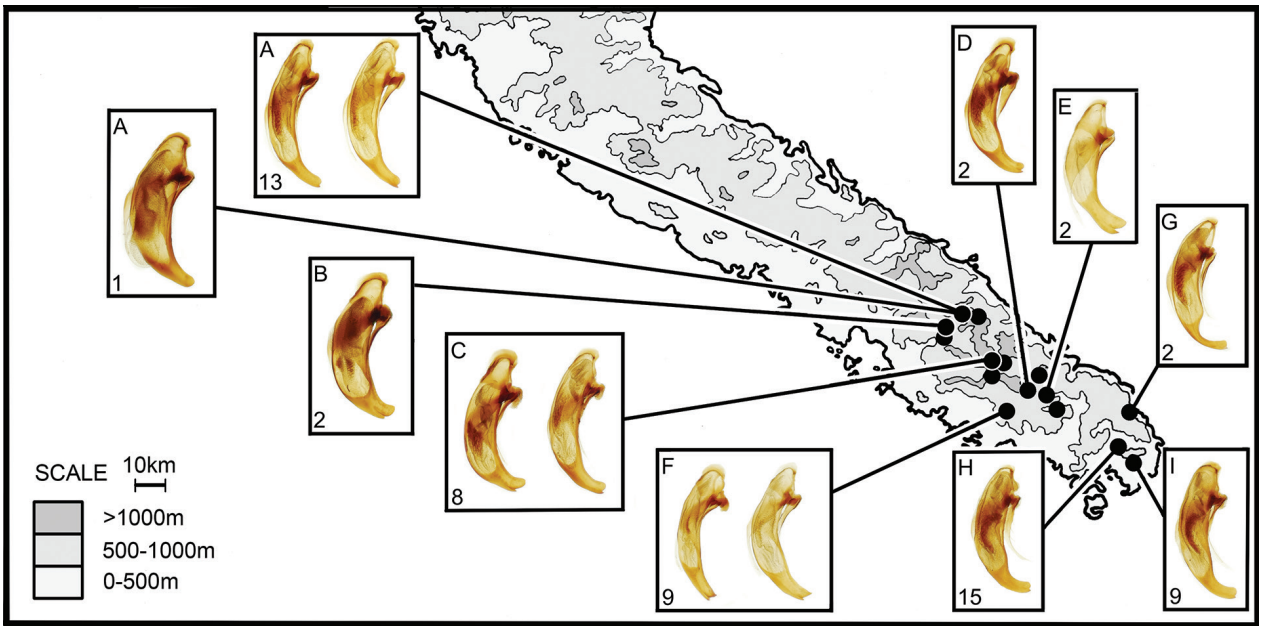

Figure 26. Recorded geographical distribution of *M. kanak* (including population samples A–I for which representative male aedeagi are figured): numbers of males sampled for each locality indicated in lower left of boxes. Sampled population localities include: **A**, Mt. Humboldt, 1300–1400 m; **B**, Mt. Humboldt, 600 m; **C**, Mt. Dzumac; **D**, Rivière Bleue, 800 m; **E**, Rivière Bleue, 400 m; **F**, Mts. Koghis; **G**, Col de Yaté; **H**, Pic du Grand Kaori; **I**, Forêt Nord.

collected from sifted litter under *Callitris neocaledonica* Dümmer (1, Wanat, MNHW). Of the 177 specimens examined, 133 were labeled as collected in sieved litter or by Berlese extraction. A further 34 specimens (Löbl, MHNG) can also be assigned as the products of these methods. This leaves the remaining 6% of specimens to be divided between such collecting methods as headlamp search at night, "at light", flight intercept trap, and no data. Thus this species can be characterized as a fastidious denizen of the ground-level litter layer.

15. *Mecyclothorax picdupinsensis* Liebherr, sp. n.

http://zoobank.org/469A110B-37CD-48A9-B118-E78BED4D6367
Figures 20H, 21L–N, 22B, 23F, 24E, 25

Diagnosis. This final member of the species triplet also including *M. mouensis* and M. *kanak* can be diagnosed from the former by characters listed in the *M. kanak* species diagnosis. As stated above, this species cannot be diagnosed from *M. kanak* based on external characters. The basis for species recognition lies both in the form of the male aedeagal median lobe apex–i.e., broadly rounded with a minute hitch present (Fig. 21L)–and female gonocoxae with a broad mediobasal patch covered with quadrate cuticular scales (Fig. 24E). Also, based on specimens at hand, the female bursa copulatrix is shorter and broader in this species, and the helminthoid sclerite is more narrowly extended as a laminar structure that is heavily melanized (Fig. 23F). Standardized body length 3.0-3.4 mm. Chaetotaxy +/+//+/–//+/2/+/+.

Description (n = 5). The description of *M. kanak* can serve to describe this species, with substitution of the following ranges of ratios of the measured specimens: ocular ratio 1.44–1.52; ocular lobe ratio 0.71–0.80; EyL/EyD = 2.08–2.38; MPW/BPW = 2.30–2.44; MPW/PL = 1.33–1.38; APW/BPW = 1.32–1.36; MEW/EL = 0.85–0.89.

Male genitalia (n = 2). Antecostal margin of abdominal mediotergite IX angulate, not extended (Fig. 21M); right paramere narrow, evenly narrowed from narrow base to whiplike apex, with one seta near midlength on ventral margin complementing two long apical setae (Fig. 22B); left paramere narrow basally, evenly narrowed to whiplike apex, two longer apical setae present; aedeagal median lobe robust, broad dorsoventrally, evenly curved dorsally and ventrally to a broadly downturned apex which bears a variously developed apical invagination, present as a small tubercle or change of angle of the apical margin (Fig. 21L); aedeagal median lobe internal sac with sclerotized region in position of dorsal plate, internal sac folded longitudinally toward apex (Fig. 21L, N).

Female reproductive tract (n = 1). Bursa copulatrix length subequal to circumference, its surface thin, translucent (Fig. 23F); spermathecal duct entering at apex of bursa separate from bursa-common oviduct juncture; rounded laminar helminthoid sclerite extended from bursal wall between, and separate from both, bursal-common oviduct juncture and spermatheca; spermatheca of only slightly greater circumference than spermathecal duct, reservoir about 1/2 length of spermathecal duct, spermathecal gland duct entering at base of spermathecal reservoir (Fig. 23F); ligular apophysis present on common oviduct; basal gonocoxite 1 with apical fringe of two setae laterally, a very small setae may be present immediately mesad, and several smaller setae occur near apex of medial margin (Fig. 24E); medial margin bearing a dense field of mi-

crotrichia basally, this field about 8 microtrichia maximal breadth, with the macrotrichia appearing like flattened scales; gonocoxite 2 moderately narrow basally, basal width 0.4× medial length; two gracile lateral ensiform setae of moderate length present, the apical seta broader.

Types – Holotype male (MNHN): NEW CALEDONIA 11787 / 22°15'Sx166°49'E, 280m / Pic du Pin, site 1,rainfor. / 26Nov2004, berlesate / G.Monteith,P.Grimbacher // QUEENSLAND / MUSEUM LOAN / DATE: July 2005 / No. LE 05.24 // *New Caledonia Mecyclothorax* revision / measured specimen 1 // HOLOTYPE / Mecyclothorax / picdupinsensis / J.K.Liebherr 2017 (black-bordered red label) /

Paratypes (11 specimens). NEW CALEDONIA: Pic du Pin[code PA 48], 22°15'S 166°49'E, 28-vi-1970, Franz (NHMW, 3), base, 280 m el., 22°14.9'S 166°49.7'E, sifted rainforest, litter, 26-xii-2006, Wanat & Dobosz (MNHW, 1), 22°15'S 166°49'E, sifted litter, 22-x-2008, Wanat (MNHW, 1), site 1, rainforest, 280 m el., 22°15'S 166°49'E, berlesate, 26-xi-2004, lot 11787, Monteith & Grimbacher (QMB, 5), 21-xii-2004, lot 12045, Monteith (QMB, 1).

Etymology. This species name represents the genitive adjectival form of the type locality, Pic du Pin; picdupinsensis. This final species name includes reference to the New Caledonian Pine, *Araucaria columnaris* J. R. Forster and W. J. Hooker, and partially recapitulates the final species named in Liebherr (2016); *Cyphocoleus iledespinsensis* Liebherr.

Distribution and habitat. This species is restricted to the vicinity of Pic du Pin, southern Grande Terre (Fig. 25), with all collecting localities recorded at 280 m elevation. Nine of the 12 specimens were collected from sieved litter, whereas three specimens (NHMW) are associated with the collecting note: "Total stehendes Stammen von *Aruacaria biramulata* (Herbert Franz field notebook: Jäch, pers. comm.)": Thus this species may climb the lower reaches and boles of larger trees in addition to occupying the ground-level litter layer.

Discussion

Phacothorax historical biogeography and ecology

The question regarding time of origin of the New Caledonian *Phacothorax* radiation is answered by the results of the cladistic analysis. As sister taxa (Fig. 7), subgenera *Phacothorax* and *Mecyclothorax* are of the same age. The earliest divergent lineage within subgenus *Mecyclothorax* comprises the two species precinctive to Lord Howe Island–*M. goweri* and *M. howei*–and the single species, *M. monteithi*, precinctive to Norfolk Island. Of these two islands, Lord Howe is the older, having been formed and become subaerial 5–6 Ma (Woodroffe et al. 2006, Kennedy et al. 2011), whereas the younger Norfolk Island developed 2.3–3.0 Ma (Jones and McDougall 1973). Thus the cladistic relationships at the base of subgenus *Mecyclothorax* (Fig. 7) support initial colonization of Lord Howe Island from New Guinea + Australia by the common ancestor of *M. goweri* + *M. howei* + *M. monteithi*, with subsequent colonization of Norfolk Island by the ancestor of *M. monteithi* after 3 Ma. Speciation of *M. goweri* and *M. howei* followed colonization of Norfolk Island by the propagule resulting in the present-day *M. monteithi*.

Given an age of origin for New Caledonian *Phacothorax* of 5–6 Ma, this lineage colonized New Caledonia over water. Subgenus *Phacothorax* is bracketed on the cladogram by subgenus *Mecyclothorax* with early divergent taxa in New Guinea, and subgenus *Meonochilus* of New Zealand. Any biogeographic relationship of *Phacothorax* and *Meonochilus* is likely based on overwater dispersal. Zealandic relationships tying together New Caledonia and New Zealand have been demonstrated for stick insects (Buckley et al. 2010), but the connections between the two areas are dated 24–46 Ma, and thus represent an earlier time when the Norfolk and Reinga Ridges were subaerial and could provide means for terrestrial dispersal (Herzer et al. 1997). Any post-Zealandic biogeographic hypothesis connecting these areas must implicate dispersalist expansion of distributions over water. Given the earliest divergence in Australia of the sister group to *Mecyclothorax* sensu lato (consisting of *Amblytelus* and associated genera, Fig. 7), plus Australian distributions of the subgenera *Eucyclothorax* and *Qecyclothorax*, independent colonization of New Zealand and New Caledonia from Australia by the ancestors of *Meonochilus* and *Phacothorax* represents the most parsimonious biogeographic hypothesis with regard to minimizing overwater dispersal events. Thus an Australian origin for the New Caledonian *Phacothorax* is proposed here.

The distributional ranges of the 15 New Caledonian *Mecyclothorax* spp. include a significant proportion of narrowly endemic species. Species richness is concentrated in relatively few localities for this taxonomic data set (Fig. 27A): **1**, Mt. Panié; **2**, Aoupinié; **3**, Me Maoya; **4**, Mt. Humboldt; **5**, Mts. Koghis. Of these localities, Mt. Panié and Me Maoya are each known to house three species, with that diversity represented in only 18 and 19 specimens respectively. Aoupinié is documented as the most diverse site with four species, based on collections totaling 58 specimens. Samples at all three of these sites differ in elevation by 300–700 m, indicating the great effort by collectors to sample different life zones on these mountains. Yet the more common species in each instance span these elevational transects, and the rarest–being known from only one specimen or a single collecting series–are restricted to a single elevation, meaning that we have a long way to go to determine how diversity is distributed elevationally at the richer sites in New Caledonia. Four of the most diverse sites–all except Me Maoya–are known to be hotspots housing many narrowly endemic plant species (Wulff et al. 2013), supporting the integration of invertebrate data into the comparatively more advanced conservation priority schemes based on New Caledonian plant species. Of the four sites held in common with Wulff et al.'s (2013) plant conservation prioritization protocol,

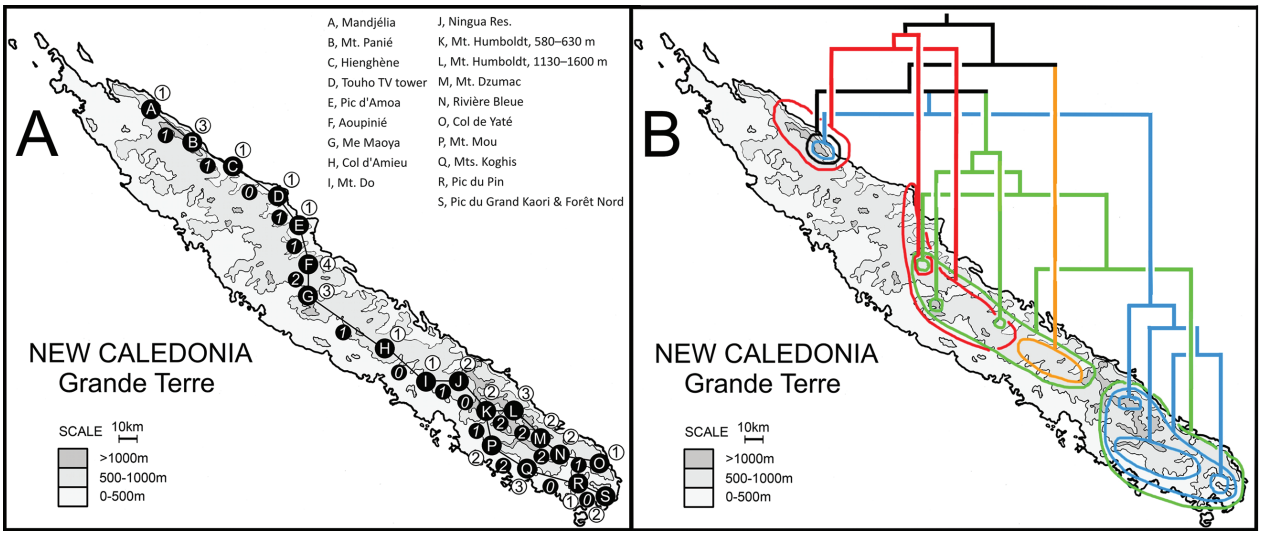

Figure 27. Distributional attributes of New Caledonian subgenus *Phacothorax* spp.: **A**, recorded species richness (open circles) at principal collecting localities represented in this revision (A–S), and species shared between adjacent localities (filled circles and italicized numerals) – see text regarding parallel networks of collection localities in southern end of Grand Terre; **B**, chorologically oriented cladogram of subgenus *Phacothorax* spp. (Fig. 7) with species terminals corresponding to areas of distribution, and the five monophyletic or monobasic constituent lineages spectrally colored red, orange, green, blue, and black (after Sharma & Giribet 2009).

Mt. Panié and Aoupinié each house two narrowly endemic *Mecyclothorax* spp.: *M. paniensis* and *M. megalovatulus* for the former, and *M. laterovatulus* and *M. plurisetosus* for the latter. These two sites are also among the most unique in the Northern Province based on endemic plant species composition (Ibanez et al. 2017).

The pattern of speciational diversification for New Caledonian *Mecyclothorax* indicates earlier diversification on the older, continental northern portion of Grand Terre, outside the areas of recently deposited ultramafic rocks. The most morphologically similar and therefore difficult to diagnose cryptic species comprise the clade of four species subtended by *M. manautei*; also including *M. kanak*, *M. mouensis*, and *M. picdupinsensis* (Figs 7; 27B, southerly blue-outlined distributions). These occur in the mountains from Mt. Humboldt south, an area exclusively dominated by ultramafic soils (Grandcolas et al. 2008, fig. 1). The adelphotaxon to this four-species clade is *M. paniensis* (Fig. 7), distributed only on Mt. Panié (Fig. 27B) far to the north in an area of older non-ultramafic continental rocks. The pattern of initial diversification in the north with more recent diversification in the ultramafic south is concordant with the taxon-area relationships exhibited both by *Augustonicus* cockroaches (Murienne et al. 2005) and by harvestman of the family Troglosironidae (Sharma and Giribet 2009). However, the timing of diversification of New Caledonian *Mecyclothorax* spp. is contemporaneous only with that of *Augustonicus*, as both cockroaches and *Mecyclothorax* beetles have radiated during the Pliocene. Conversely, divergence dating estimates for the *Trogolosiro* harvestman place the origin of that radiation in the Eocene, 49 Ma, with diversification on the ultramafic substrates dated to 6.7 Ma (the "Apex" clade of *T. longifossa* and *T. urbanus*, Sharma & Giribet 2009, fig. 6), a time contemporaneous with the origin of the entire New Caledonian *Mecyclothorax* radiation.

New Caledonian species of subgenus *Phacothorax* appear phylogenetically fickle with regard to occupation of ultramafic soils. In addition to the juxtaposition of *M. paniensis* on continental rocks versus its four-species adelphotaxon on ultramafic soils, the sister species *M. jeanneli* and *M. fleutiauxi*, though as closely related as possible phylogenetically, exhibit a stark dichotomy with regard to occupation of ultramafic soils; the former distributed strictly on such soils, the latter mostly not (Fig. 27B, Grandcolas et al. 2008, fig. 1). Thus soil type does not appear to correlate significantly among closely related species, with the single exception of the four species clade, *M. manautei*, *M. kanak*, *M. mouensis*, and *M. picdupinsensis*.

The ecological situations within which species of subgenus *Phacothorax* have been collected include both semi-arboreal and ground-level microhabitats. The former situations are represented by specimens collecting through the application of pyrethrin insecticide to the mossy surfaces of tree trunks and downed logs (G. Monteith pers. comm.). The area of application spanned the lower trunk or log upwards to where the insecticide fog stopped being effective: less than 4 m or so. Occupation of ground-level situations are guaranteed for specimens collecting by sieving leaf litter with or without subsequent Berlese extraction. Using these criteria, 8 of the 14 species for which data are available have been collected only in sieved litter: *M. laterobustus*, *M. laterorectus*, *M. laterosinuatus*, *M. megalovatulus*, *M. mouensis*, *M. octavius*, *M. paniensis*, and *M. picdupinsensis*. Four species have been collected only through pyrethrin fogging: *M. fleutiauxi*, *M. jeanneli*, *M. manautei*, and *M. plurisetosus*. Two species have been collected using both methods:

the very abundantly collected *M. kanak*, and *M. megalovatulus*. Occupation of ground-level microhabitats is the groundplan ecological condition for this radiation, with this behavior symplesiomorphically shared with the other basal lineages of *Mecyclothorax*: subgenera *Eucyclothorax*, *Qecyclothorax*, and *Meonochilus* (see below). The strict utilization of semiarboreal microhabitats by *M. plurisetosus*, *M. fleutiauxi*, and *M. jeanneli* is ecologically synapomorphous, as these three species constitute a triplet of species terminating one of the clades of the radiation (Fig. 7).

Mecyclothorax historical biogeography

The sister-group relationship between *Amblytelus* and allied genera (Baehr 2004) and *Mecyclothorax* (Liebherr 2011) establishes the basis for estimating the time of origin of the *Mecyclothorax* radiation. The earliest diverging lineage among the *Mecyclothorax* adelphotaxon (Fig. 7) comprises *Paratrichothorax brevistylus*, a species restricted to the southern coast of Western Australia. A second hypothesized early offshoot of the *Amblytelus* line not included in this analysis, *Trichamblytelus ovalipennis* Baehr, is also restricted to the coastal forests of southwestern Australia (Baehr 2004). This area was isolated during the Late Eocene to Early Oligocene by climatic cooling and marine incursions across southern Australia (Ladiges et al. 2011). Thus the time of origin of the sister group to *Mecyclothorax*, and therefore to *Mecyclothorax*, is hypothesized to be Late Eocene to Early Oligocene.

The initial divergence event within *Mecyclothorax* involved separation of the taxa newly proposed as subgenus *Eucyclothorax* (Fig. 7) from the remainder of the *Mecyclothorax* radiation. These taxa retain plesiomorphies including presence of a flagellar structure in the male aedeagal internal sac (Fig. 4A–C), and a female reproductive tract with the spermathecal duct entering the bursa ventrally in association with a sclerotized helminthoid sclerite (Fig. 6C). Individuals of these species autapomorphically present increased punctation on the body surface (Fig. 2D–F, L). The species are predominantly distributed in the east, although *M. blackburni* (Fig. 8A) is distributed across much of the more arid south and west and *M. punctatus peckorum* Baehr is restricted to southwestern Australia. Individuals of all of these species inhabit ground-level microhabitats, a plesiomorphic ecological association that differs from the derived occupation of semiarboreal, subcorticular habitats frequented by taxa in the sister group, including *Paratrichothorax brevistylus* and species of *Amblytelus* and *Districhothorax* (Baehr 2004).

Species now classified in subgenus *Qecyclothorax* constitute evolutionary products of the next divergence event along the *Mecyclothorax* line (Fig. 7). These species are all restricted to high-elevation mountain tops in Queensland, where, like *Eucyclothorax* spp., the individuals also inhabit ground-level microhabitats (Baehr 2003). Like those of subgenus *Eucyclothorax*, these species also retain the plesiomorphic presence of a male aedeagal flagellum (Fig. 4D–E) and a female reproductive tract with ventral entry of the spermathecal duct (Fig. 6D). Their external anatomy is remarkably canalized: a broad body and convex elytra with reduced striation being the norm for the clade (Fig. 8B). Populations on different, neighboring mountaintops are principally characterized by male aedeagal differences, leading Baehr (2003) to recognize such variation as infraspecific.

The third lineage to diverge from the main *Mecyclothorax* stem, those species in subgenus *Meonochilus* (Fig. 7), is distributed on North Island, New Zealand (Liebherr 2011). As in the subgenera *Eucyclothorax* and *Qecyclothorax*, the groundplan for this subgenus includes a male aedeagal flagellum and a female reproductive tract with a ventrally entering spermathecal duct, however this state synapomorphously transforms among species of this radiation. The groundplan female tract observed in females of *M. bellorum* has transformed in the other five species, four included in this analysis (Fig. 7), to a tract with the spermathecal duct entering the dorsal surface of the bursa near its distal end. All species exhibit vestigial flight wings, with the bodies characterized by the presence of heavy cuticle (least so in the most generalized *M. bellorum*). The elytra are broad, foreshortened and convexly domed, though the elytral striae are deeply impressed and distinctly punctate (Liebherr 2011, figs 9, 10). The North Island distributions of the constituent species are highly skewed to endemism in the northern peninsular extension of the Reinga Ridge–Northland–with three of the six species restricted to this administrative division. Only *M. amplipennis* (Fig. 8C) is distributed in the southern half of North Island. As in the first two subgenera–*Eucyclothorax* and *Qecyclothorax*–individuals of all species are restricted to ground-level microhabitats.

The nominate subgenus *Mecyclothorax* is by far the most diverse subgeneric taxon recognized here. Males for all species of this clade for which males are known, exhibit a modification of the male aedeagal internal sac whereby the apex of the sac bears either a roll of thickened cuticle, or a hardened, scooplike sclerite that is associated with the gonopore (Fig. 4F–G). Besides the earliest-divergent lineage that colonized the Lord Howe and Norfolk Islands, this clade exhibits its earliest diversification in New Guinea (Fig. 7). Comprehensive character analysis was possible only for species from Papua New Guinea (Liebherr 2017b), though this sampling viewed in light of the descriptions by Baehr (1992, 1995, 1998, 2002, 2008) supports an interpretation that the entire New Guinean *Mecyclothorax* fauna is assignable to this subgenus. The core of the subgenus *Mecyclothorax* radiation has produced propagules that have colonized the Greater Sunda Islands of Borneo and Java. The Australian *Mecyclothorax* fauna has diverse roots, even after taking into account the Australian *Eucyclothorax* and *Qecyclothorax* spp. removed to those subgenera. The Australian sister-species pair *M. minutus* + *M. lateralis* comprise the adelphotaxon to New Guinea's *M. sedlaceki* + *M. kavanaughi* among species sampled for the cladistic analysis. Given that *M. kavanaughi* is hypothesized to have evolved after the geo-

logical suturing of its home Finisterre Range to mainland New Guinea 3.0–3.7 Ma (Liebherr 2008a), the ancestor of these Australian taxa has been in residence since at least that time. Two other Australian *Mecyclothorax* species are highly interdigitated biogeographically with taxa that have colonized other areas over water. *Mecyclothorax ambiguus* and *M. punctipennis*, abundant species of Australian carabid beetles within their ranges (Moore 1984), are related respectively to *M. rotundicollis* of New Zealand, and *M. punctipennis* of Hawaii. *Mecyclothorax punctipennis* was also the source taxon for the propagule that colonized St. Paul and Amsterdam Islands, resulting in the very similar but distinct species *M. sculptopunctatus*. Liebherr (2013) proposed that *M. punctipennis* is also the species that produced a propagule that colonized Tahiti in the Society Islands, with *M. striatopunctatus* Perrault as the most generalized taxon in that radiation. Individuals of *M. striatopunctatus* were not available for this analysis, being returned to the Paris Museum when all types were deposited (Liebherr 2013), and so the less generalized *M. marau* was used as a surrogate. This substitution results in the French Polynesian representative species being placed as adelphotaxon to the five species associated with *M. ambiguus* and *M. punctipennis*. However, given the subaerial geological history of Tahiti and the Hawaiian Island of Maui where *M. punctipennis* resides as the most generalized Hawaiian species (Britton 1948, Liebherr 2015), all evolution in this nexus of the cladogram (Fig. 7) has taken place within the last 1–2 Myr, the time of subaerial appearance of Tahiti Nui and Maui (1.4 and 1.8 Ma respectively; Hildenbrand et al. 2004, Sherrod et al. 2007).

Mecyclothorax and flight wing loss

The species included to represent diversity of subgenus *Mecyclothorax* are a small subset of all known species. Only one of the 108 French Polynesian *Mecyclothorax* (Liebherr 2012, 2013) and one of the 239 Hawaiian *Mecyclothorax* (Liebherr 2015) are included. For New Guinea, 8 of the 22 species are represented. All 369 *Mecyclothorax* species known to date from these geographical areas lack functional flight wings, and nearly all have the wings reduced to vestigial flaps shorter than the apical margin of the metanotum. Based on taxa in this analysis, only three species within subgenus *Mecyclothorax* exhibit fully functional flight wings; *M. ambiguus*, *M. punctipennis*, and *M. rotundicollis* (Fig. 7; character 75, state 0). Two species, *M. lateralis* and *M. sculptopunctatus* include individuals studied for this revision that have brachypterous flight wings the alar surface reduced so that little of the wing extends beyond the wing fold (character 75, state 1). And two other species, *M. lissus* of Java and *M. montivagus* of Hawaii, exhibit flight wings reduced to stenopterous straps that extend beyond the apex of the metanotum, though the alar surface is very narrow and the medial and cubital wing veins are greatly reduced (character 75, state 2). In the initially diverging subgenus *Eucyclothorax*, two of the nine species are known from macropterous individuals–*M. blackburni* and *M. eyrensis*–and two exhibit dimorphic wing polymorphism with the flight wings either fully developed or completely vestigialized; *M. peryphoides* and *M. lophoides* (Fig. 7). The other four species of *Eucyclothorax* are all monomorphically vestigially winged. These four examples of wing presence in *Eucyclothorax* and three examples of wing presence in subgenus *Mecyclothorax* stand in stark contrast to the hundreds of species that exhibit flight wing loss, in many instances that loss associated with thickening of the cuticle, and remarkable changes in body shape (Figs 8B–C, 9, 16, 20). The metathoracic flight wing character was coded as an unordered four-state character so as not to unduly distort the cladistic analysis. This is especially important as the wing-dimorphic taxa polymorphically exhibit the end states 0 and 3 along the character transformation series. Although this cladistic analysis is based on the principal of parsimony–i.e. minimizing the number of character-state changes in either direction on the cladogram–this reduction character should be interpreted under Dollo Parsimony (Farris 1977); i.e., the evolutionary transformation, in this case the loss of flight wings, cannot be reversed in the cladistic hypothesis.

The interpretation of carabid beetle flight wing loss under Dollo Parsimony is consistent with flight wing polymorphism in carabid beetles and the observed transformation over ecological time from populations comprising predominantly macropterous individuals to those within which nearly all individuals lack wings. Such a change was documented over only two seasons in a population of *Trechus obtusus* colonizing a newly available polder in the Netherlands (den Boer 1970). This phenomenon was observed again in Hawaii, when samples of *T. obtusus* taken after colonization of Maui in 1998 by this European species contained only macropterous individuals (Liebherr and Takumi 2002), but samples subsequently taken four years later at the same site contained 33% brachypterous individuals (Liebherr and Krushelnycky 2007). Wing polymorphism is determined by few genes in those carabid beetles studied, with a single gene determining wing development in the European *Pterostichus anthracinus* (Illiger) (Lindroth 1946) and *P. melanarius* (Illiger) (Aukema et al. 1996). A somewhat more complex hereditary basis involving either two genes or three alleles of one gene is posited for *Bembidion lampros* (Herbst), where several different brachypterous forms complement the macropterous form (Langor and Larson 1983). In these three instances, the macropterous allele is recessive to the brachypterous, necessitating the presence of either a homozygous or heterozygous brachypterous individual within a propagule in order to introduce the short-winged allele to a new locale. If that new location offers ecological stability, selection will favor brachypterous individuals due to physiological advantage (Darlington 1936, Southwood 1977), or disfavor flighted individuals due to increased mortality (Darwin 1859, Short and Liebherr 2007), or both (Kavanaugh 1985). The end point

of these strong selective forces, assuming the habitat is stable enough to preclude extinction of the populations or species, is functional elimination of the recessive macropterous allele from the population, and the cascade of evolutionary changes to the metathoracic flight apparatus–foreshortening of the segment, sclerite fusion–and modification of the elytra, now converted to dorsal protective shells without the need to open during flight.

Given the preponderance of brachypterous lineages branching off the *Mecyclothorax* radiation, with isolated radiations occupying New Zealand, New Caledonia, New Guinea, and Polynesia, it is tempting to suggest that the many independent origins of island lineages during the evolution of *Mecyclothorax* may have been accomplished by 100% brachypterous propagules. Such a conclusion is contrary to the evidence for at least some of the radiations. The Hawaiian *Mecyclothorax* include the most generalized species, *M. montivagus*, individuals of which retain stenopterous wing stubs 3.3× long as broad with rudimentary Sc, R, M, and Cu veins present, indicating this species' recently evolved brachypterous condition. Similarly, species of the generalized *M. striatopunctatus* group in Tahiti–e.g. *M. curtisi* Liebherr (2013)–exhibit stenopterous wing rudiments 4× long as wide, with the alar surface including rudimentary Sc, R, and M veins. The cladistic relationships among the four macropterous or wing-polymorphic species in subgenus *Eucyclothorax* ambiguously optimize the base of that clade as either macropterous or brachypterous. It is among the subgenera *Qecyclothorax*, *Meonochilus*, and *Phacothorax*, that all evidence of macroptery has been evolutionarily erased. One could argue that flight wings have re-evolved with a small subset of species in subgenus *Mecyclothorax* à la Whiting et al. (2003). However that would require reversals in a suite of characters associated with metathoracic reduction, and elytral configuration including fusion along the sutural margin. An interpretation of independent, repetitive wing loss, as repeatedly observed within wing-polymorphic populations during ecological time (den Boer 1970), is preferred as an explanation for the observed pattern of brachyptery (Trueman et al. 2004).

Mecyclothorax genitalic evolution

Isolation of closely related carabid beetle species is mediated by physical incompatibility between the male aedeagal intromittent organ and the female bursa copulatrix (Nagata et al. 2009, Kubota et al. 2013). Specific structures of the male aedeagal internal sac may interact with specific structures or lobes in the bursa to emplace or remove male spermatophores (Jeannel 1941, fig. 30), positioning the mating male's spermatophore near the spermathecal duct (Okuzaki and Sota 2014). Correlation of male and female reproductive parts is documented here for the adelphotaxa *M. fleutiauxi* and *M. jeanneli*. Females of both species exhibit a bilobed bursa copulatrix, with a dorsal lobe complementing the plesiomorphically present ventral lobe. In females of *M. fleutiauxi*, the dorsal lobe is much shorter than the ventral lobe (Fig. 12D), and the spermathecal duct enters at its apex. In *M. jeanneli* females the spermathecal duct also enters the apex of the bursal dorsal lobe, but the lobe itself is as long as the ventral lobe (Fig. 12E). The aedeagal internal sac is also bilobed in these two species, with an apical lobe that bears the reduced flagellar sheath at its apex and a dorsal lobe that extends from the sac near the base of the ostial opening (Fig. 10L versus Q). The dorsal lobe is of similar length for the two species, however the apical lobe is much shorter in males of *M. fleutiauxi* (Fig. 10L), being about half the length of the dorsal lobe. In contrast, the apical and dorsal lobes are of approximately equal length in *M. jeanneli* males. Given the male above, head to head mating posture of carabid beetles that necessitates inversion of the male's aedeagus from its anatomical position (Deuve 1993), the male's apical lobe would enter the female's bursal dorsal lobe –the lobe joining the spermathecal duct–during intromission, and the male's dorsal lobe would inflate to fill at least part of the female's ventral lobe; the lobe joining the common oviduct. The male gonopore is associated with the flagellum, in these instances represented by the reduced flagellar sheath, and so in both species, the apex of the male apical lobe would be proximate to the base of the spermathecal duct at the apex of the female dorsal lobe. Given the lack of any known zone of parapatry between these two species (Fig. 15), it is not known how these two species may interact when individuals are present at the same site. The frontier between these two species is correlated with a faunal break isolating the southern five species restricted to ultramafic substrates (Fig. 27B). Thus given present knowledge, an initial hypothesis is proposed wherein these correlated structures of *M. fleutiauxi* and *M. jeanneli* evolved in allopatry.

Occurrence of either bilobed male aedeagal internal sacs or bilobed female bursae has been documented repeatedly for species in subgenus *Mecyclothorax*. Males of *M. bilobatus* Liebherr from Haleakalā, Maui have bilobed internals sacs, with the large scoop-like flagellar plate characteristic of the subgenus located at the apex of the apical lobe (Liebherr 2015, figs 150E–F), however this species is characterized by a single-lobed female bursa (Liebherr 2015, fig. 145D). The converse presence of bilobed female bursae and single-lobed male aedeagal sacs has evolved independently four times among various species in Hawaii and New Zealand: **1**, *M. oculatus* Sharp of Molokai (Liebherr 2007, fig. 125); **2**, *M. flavipes* Liebherr of Lanai (Liebherr 2009a, fig. 4A); **3**, *M. simiolus* (Blackburn) of Oahu (Liebherr 2009b, fig. 14C); and **4**, *M. oopteroides* Liebherr & Marris from New Zealand (Liebherr and Marris 2009, fig. 18). Details among these instances of bilobed bursae vary, including differential lengths of dorsal versus ventral lobes, and possible presence of sclerotization on the dorsal lobe. These details strongly support an underlying developmental pathway that triggers a bilobed bursa, though other genes are differentially associated with that genetic program resulting in different configurations of the bilobed condition.

However, the association of male and female "bilobism" observed for the New Caledonian *M. fleutiauxi* and *M. jeanneli* is unique among *Mecyclothorax* species studied to date.

Infraspecific variation of the male genitalia can be documented for several species of New Caledonian *Phacothorax* recognized in this revision. Males of *M. laterosinuatus* exhibit uniform flagellar structures associated with the internal sac (Fig. 10C, D), however the aedeagal median lobe differs about 10% in length for males of nearly the same external body dimensions. As no other external characters diagnose these males, they were considered conspecific, though of course more specimens or molecular sequence data could provide the means to assign these populations to more than one species. The aedeagal tip in males of *M. fleutiauxi* varies in length and dorsoventral breadth among individuals available for study (Fig. 15A–E), though individuals within population samples exhibit relatively consistent aedeagal conformations. Much more dramatic aedeagal variation is presented by members of *M. kanak*, a comparatively widespread species across southern Grand Terre (Fig. 26A–I). No external anatomical characters allowed differential diagnosis of the individuals studied from these population samples. Moreover, while all but one of the males exhibited the diagnostic invaginated "hitch" at the apex of the median lobe, other attributes of the aedeagal apex–e.g., dorsoventral breadth, apical curvature, length of the dorsal projection relative to the ventral tip, and whether the ventral tip was rounded or acuminate–varied somewhat within some of the population samples (e.g., Mt. Dzumac, Mts. Koghis, Fig. 26C, F). In several instances, aedeagal configuration differs dramatically among samples separated by 10–20 kilometres; e.g. Mt. Humboldt low elevation versus high elevation sites (Fig. 26A–B), and Col de Yaté versus Pic du Grand Kaori (Fig. 26G–H). The general pattern of geographic variation that can be advanced involves the occurrence of longer and more curved apical portions of the median lobe toward the southern limits of Grand Terre. The endpoint for this trend would be the two males known from Col de Yaté, where the apical portion of the lobe beyond the ostial opening is extremely narrow and distinctly curved. What the relatively smaller, though non-diagnostic body size exhibited by the three known specimens from Col de Yaté signifies must await more data. Among all the examined *M. kanak* males, one stands out due to its lack of the "hitch" in the median lobe apical margin (Fig. 26, sample A, Mt. Humboldt 1300–1400 m elevation). This male is one of nine other syntopic males, with the complementary eight exhibiting the diagnostic apical invagination (Fig. 26). That this specimen represents a hybrid between *M. kanak* and *M. manautei* (the only other sympatric, small bodied species) can be discounted because the aedeagus of *M. manautei* males exhibits extensive internal sac spination and a broad, asymmetrical apex (Fig. 17I), traits not present in this non-conforming male. At present this male's aedeagal configuration can only be interpreted to represent an extreme in aedeagal morphology observed within this species.

The amount and manner of variation in the *M. kanak* male aedeagus is much greater than that observed within species of the very speciose *Mecyclothorax* radiation from Haleakalā, Maui (Liebherr 2015). Among the more widespread species of that 116-species radiation–e.g. species with distributions spanning either the 20–30 km breadth of Haleakalā's windward forest, or elevations ranging 1200–2800 m–aedeagal conformation is remarkably stable and thus extremely useful for species diagnosis; e.g. *M. consanguineus* Liebherr (Liebherr 2015, figs 34–35), *M. cordithorax* Liebherr (ibid, figs 88–89), and *M. montivagus* (Blackburn) (ibid, figs 131–132). These widespread, morphologically consistent species occur within a diverse species swarm where up to 39 *Mecyclothorax* spp. have been recorded from a 1′ × 1′ quadrat (Fig. 28A). The 63 such latitude × longitude quadrats occupied by *Mecyclothorax* on Haleakalā house an average of nine species. With such extensive species packing, even given the diversity of microhabitats from which these beetles have been recorded, and the extensive variation in body size represented among the various species, more uniform genitalia within species would allow more precise species recognition during male-female encounters (Nagata et al. 2009, Okuzaki and Sota 2014). The very low levels of sympatry in New Caledonia, where maximally four *Mecyclothorax* species occur at any locality (average of 1.9 species per locality; Fig. 27A), are associated with more extensive infraspecific male genitalic variation. A useful intermediate comparison may be made using the *Mecyclothorax* fauna of Hawaii Island (Liebherr 2008b), an island housing 30 species of *Mecyclothorax*. Taking the larger area of that island into consideration (10,432 km^2 versus 1450 km^2 for Haleakalā), a calculation of sympatry level using 5′ × 5′ latitude × longitude quadrats results in an average of 4.2 species per occupied quadrat, with a maximal quadrat diversity of 12 species (Fig. 28B). In this fauna, based on multiple dissections of specimens, two species have been shown to exhibit extensively variable male genitalia. *Mecyclothorax deverilli* (Blackburn) (Liebherr 2008b, figs 67–78) and *M. konanus* Sharp (ibid, figs 153–165). Patterns of variation in both species represent a mosaic of forms not associated strongly with geographic distance. In fact, variation among males of *M. konanus* is rampant as much within collecting series as it is among samples separated by up to 70 km straight-line distance, as demonstrated by a parsimony network based on 12 aedeagal attributes joining 84 specimens (Liebherr 2008b, fig. 181). Although data are preliminary, male aedeagal morphology is also infraspecifically variable among New Guinea *Mecyclothorax* (Liebherr 2017b), with *M. andersoni* exhibiting variation in the median lobe apex similar to that observed in *M. kanak*. The New Guinean fauna is very poorly known, however based on current knowledge sympatry levels are very low with a maximum of two species known from any locality. As male genitalic morphology in carabid beetles has been shown

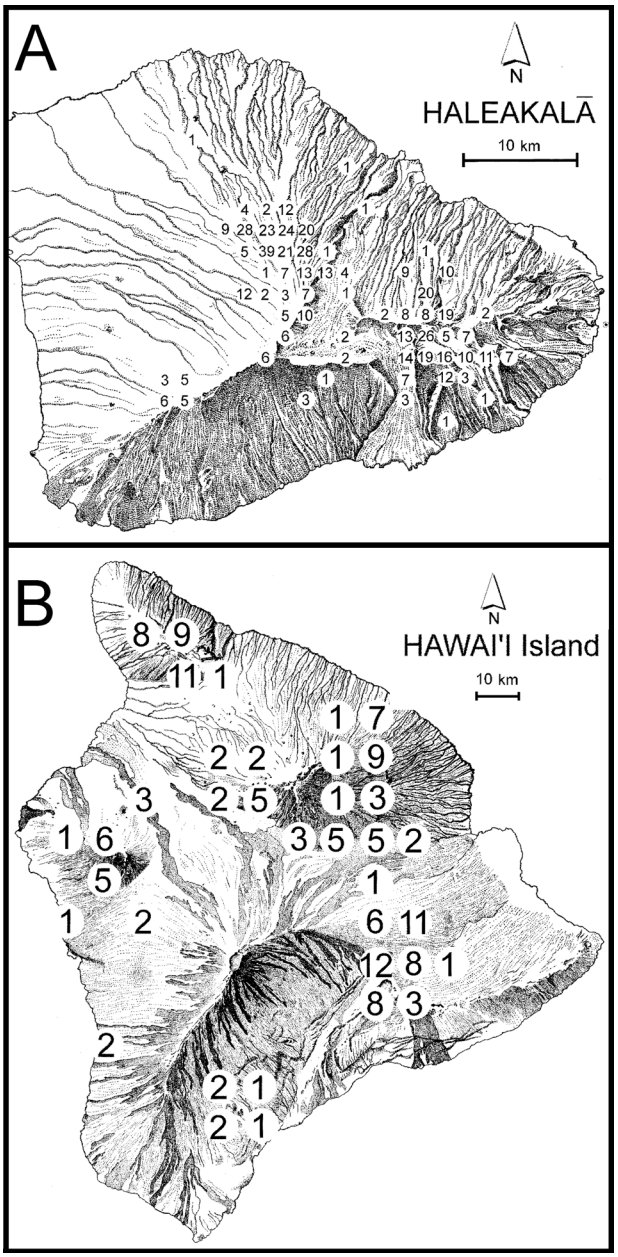

Figure 28. Number of *Mecyclothorax* spp. present in latitude × longitude quadrats for two Hawaiian Islands: **A**, Haleakalā volcano, Maui (area 1450 km^2) with species recorded within 1′ × 1′ cells; **B**, Hawai`i Island (10,432 km$^2$) with species recorded within 5′ × 5′ cells. A total of 116 species of *Mecyclothorax* are known to occur on Haleakalā (Liebherr 2015), and 30 species are known from Hawai`i Island (Liebherr 2008b).

to be controlled by relatively few genes (Sasabe et al. 2007), large amounts of infraspecific genitalic variation in depauperate *Mecyclothorax* faunas support the presence of abundant genetic variability in and among populations of these flightless species (Liebherr 1988, Ikeda et al. 2012). Thus the patterns of variation observed among these anatomically variable species supports the existence of genetic variation sufficient for subsequent diversification and adaptation as observed in the hyperdiverse island radiations.

Acknowledgements

This study was made possible through the kind loan offer of significant numbers of New Caledonian *Mecyclothorax* specimens made by Dr. Geoff Monteith, Queensland Museum. Receipt of additional specimens from other curators resulted in access to specimens from nine institutional and two personal collections. I thank the following curators and collection managers (institutional coden presented in Material and Methods follows parenthetically): James Boone (BPBM); Yves Bousquet (CNC); Jason Dombroskie, Cornell University Insect Collection (CUIC); Peter Oboyski and Kipling W. Will (EMEC); Győző Szél, Hungarian Natural History Museum, Budapest (HNHM); Giuluo Cuccodoro, Muséum d'Histoire naturelle, Genève (MHNG); Thierry Deuve and Azadeh Taghavian (MNHN); Pawel Jałoszyński (MNHW); Manfred Jäch (NHMW); Susan Wright (QMB); Martin Baehr personal collection (MBC); Pier M. Giachino personal collection (PMGC). Additional specimens were used for the cladistic analysis of *Mecyclothorax* and allied genera, with the following curators and collection managers thanked for access to that material: Robert L. Davidson, Carnegie Museum of Natural History, Pittsburgh; Borislav Guéorguiev, National Museum of Natural History, Sofia; Peter Hudson, South Australian Museum, Adelaide; Beulah Garner, The Natural History Museum, London; Kate Lemann, Australian National Insect Collection, Canberra; John Marris, Lincoln University Entomological Research Collection, Canterbury, New Zealand; Catriona McPhee, Museums Victoria, Melbourne; Philip D. Perkins, Museum of Comparative Zoology, Harvard University, Cambridge; Roberto Poggi, Museo Civico di Storia Naturale "G. Doria", Genova; Chris Reid, Australian Museum, Sydney; Danny Shpeley, Strickland Entomological Museum, University of Alberta, Edmonton. I thank Manfred Jäch for providing a copy the pertinent pages of Herbert Franz's field notebook that detail the itinerary and stops during his 1970 New Caledonian expedition. Photographic equipment essential to this research project was underwritten by National Science Foundation award DEB-0315504. I thank Borislav Guéorguiev and Kipling W. Will for their comprehensive critical editorial reviews, which substantially improved the manuscript.

References

Allen RT, Ball GE (1980) Synopsis of Mexican taxa of the *Loxandrus* series (Coleoptera: Carabidae: Pterostichini). Transactions of the American Entomological Society 105: 481–576.

Andrewes HE (1933) On some new species of Carabidae, chiefly from Java. Treubia 14: 273–286.

Andrewes HE (1939) Papers on Oriental Carabidae.–XXXV. On the types of some Indian genera. Annals and Magazine of Natural History 3(series 11): 128–139.

Aukema B, Spee AJ, van Dijk TS (1996) Wing dimorphism and development in Pterostichus melanarius (Coleoptera: Carabidae). Entomologische berichten (Amsterdam) 56: 93–100.

Baehr M (1992) A new *Mecyclothorax* Sharp from New Guinea (Insecta, Coleoptera, Carabidae, Psydrinae). Spixiana 15: 249–252.

Baehr M (1995) The genus *Mecyclothorax* Sharp, 1903 in New Guinea (Coleoptera, Carabidae, Psydrinae). Mitteilungen der Münchner Entomologische Gesellschaft 85: 3–19.

Baehr M (1998) A further new species of the genus *Mecyclothorax* Sharp from western New Guinea. Spixiana 21: 21–24.

Baehr M (2002) Two new species of the genus *Mecyclothorax* Sharp from Papua New Guinea (Insecta, Coleoptera, Carabidae, Psydrinae). Revue Suisse de Zoologie 109: 695–704. https://doi.org/10.5962/bhl.part.79563

Baehr M (2003) Psydrine ground beetles (Coleoptera: Carabidae: Psydrinae), excluding Amblytelini, of eastern Queensland rainforests. Memoirs of the Queensland Museum 49: 65–109.

Baehr M (2004) The Amblytelini. A tribe of corticolous ground beetles from Australia. Taxonomy, phylogeny, biogeography. (Coleotera: Carabidae: Psydrinae). Coleoptera 8: 286 pp.

Baehr M (2008) Two new species of the genus *Mecyclothorax* Sharp from New Guinea (Coleoptera: Carabidae: Psydrinae). Tijdschrift voor Entomologie 151: 133–140. https://doi.org/10.1163/22119434-900000258

Baehr M (2009) A new species of the genus *Mecyclothorax* Sharp from New South Wales (Insecta: Carabidae: Psydrinae). Records of the Australian Museum 61: 89–92. https://doi.org/10.3853/j.0067-1975.61.2009.1519

Baehr M (2014) A new species of the genus *Mecyclothorax* Sharp from New Guinea (Coleoptera, Carabidae, Psydrini, Mecyclothoracina). Spixiana 37: 123–129.

Baehr M (2016) A new subspecies of *Mecyclothorax punctatus* (Sloane) from south-western Australia. Spixiana 39: 93–97.

Baehr M, Lorenz W (1999) A reevaluation of *Loeffleria globicollis* Mandl from Borneo (Insecta, Coleoptera, Carabidae, Psydrinae). Spixiana 22: 263–267.

Baehr M, Reid CAM (2017) On a collection of Carabidae from Timor Leste, with descriptions of nine new species (Insecta: Coleoptera: Carabidae). Records of the Australian Museum 69: 421–450. https://doi.org/10.3853/j.2201-4349.69.2017.1660

Britton EB (1948) A revision of the Hawaiian species of *Mecyclothorax* (Coleoptera: Carabidae). Occasional Papers of the Bernice P. Bishop Museum 19: 107–166.

Buckley TR, Attanayake D, Nylander JAA, Bradler S (2010) The phylogenetic placement and biogeographical origins of the New Zealand stick insects (Phasmatodea). Systematic Entomology 35: 207–225. https://doi.org/10.1111/j.1365-3113.2009.00505.x

Csiki E (1931) Carabidae: Harpalinae V., Coleopterorum Catalogus. In Junk W, Schenkling S (Eds) Dr W Junk Publishers, Berlin 115: 739–1022.

Darlington PJ Jr (1936) Variation and atrophy of flying wings of some carabid beetles. Annals of the Entomological Society of America 24: 136–179. https://doi.org/10.1093/aesa/29.1.136

Darlington PJ Jr (1952) The carabid beetles of New Guinea part 2. the Agonini. Bulletin of the Museum of Comparative Zoology 107: 89–252 + 4 pls.

Darwin C (1859) On the Origin of Species. John Murray, London.

den Boer PJ (1970) On the significance of dispersal power for populations of carabid-beetles (Coleoptera: Carabidae). Oecologia 4: 1–28. https://doi.org/10.1007/BF00390612

Deuve T (1987) Descriptions de deux carabiques nouveaux de Nouvelle-Caledonie et de Thaïlande (Coleoptera, Caraboidea, Psydridae, Trechidae). Revue française d'Entomologie (NS) 9: 143–146.

Deuve T (1993) L'abdomen et les genitalia des femelles de Coléoptères Adephaga. Mémoires du Muséum national d'Histoire naturelle Serie A Zoologie 155: 1–184.

Enderlein G (1909) 9. Des Insektenfauna der Insel Neu-Amsterdam. In Enderlein G (ed). Die Insekten des Antarktischen Gebietes, 10. Druck und Verlag von Georg Reimer, Berlin: pp. 486–492.

Farris JS (1977) Phylogenetic Analysis Under Dollo's Law. Systematic Zoology 26: 77–88. https://doi.org/10.2307/2412867

Frauenfeld GR von (1868) Zoologische Miscellen, XV. Verhandlungen der kaiserlich-königlichen zoologisch-botanischen Gesellschaft in Wien 18(6 Mai): 885–899.

Goloboff PA (1999) NONA (NO NAME). Tucumán, Argentina, Published by the author. http://www.softpedia.com/get/Science-CAD/NONA.shtml [accessed 6-ix-2016]

Google Earth Pro (2017) Earth version 7.1.8.3036, https://earth.google.com/ [Accessed 2-ix-2017]

Grandcolas P, Murienne J, Robillard T, Desutter-Grandcolas L, Jourdan H, Guilbert E, Deharveng L (2008) New Caledonia: a very old Darwinian island? Philosophical Transactions of the Royal Society B 363: 3309–3317. https://doi.org/10.1098/rstb.2008.0122

Guéorguiev B (2013) Taxonomic, nomenclatural, and faunistic records for species in tribes Melaenini, Moriomorphini, Pterostichini, Licinini, and Sphodrini (Coleoptera: Carabidae). Zootaxa 3709: 52–70. https://doi.org/10.11646/zootaxa.3709.1.2

Hennig W (1966) *Phylogenetic Systematics*. University of Illinois Press, Champaign-Urbana.

Herzer RH, Charponiere GCH, Edwards AR, Hollis CJ, Pelletier B, Raine JI, Scott GH, Stagpoole V, Strong CP, Symonds P, Wilson GJ, Zhu H (1997) Seismic stratigraphy and structural history of the Reinga Basin and its margins, southern Norfolk Ridge system. New Zealand Journal of Geology and Geophysics 40: 425–451. https://doi.org/10.1080/00288306.1997.9514774

Hildenbrand A, Gillot P-Y, Le Roy I (2004) Volcano-tectonic and geochemical evolution of an oceanic intra-plate volcano: Tahiti-Nui (French Polynesia). Earth and Plaetary Science Letters 217: 349–365. https://doi.org/10.1016/S0012-821X(03)00599-5

Ibanez T, Blanchard E, Hequet V, Keppel G, Laidlaw M, Pouteau R, Vandrot H, Birnbaum P (2017) High endemism and stem density distinguish New Caledonian from other high-diversity rainforests in the Southwest Pacific. Annals of Botany, mcx107. https://doi.org/10.1093/aob/mcx107

Ikeda H, Nishikawa M, Sota T (2012) Loss of flight promotes beetle diversification. Nature Communications 3: 648. https://doi.org/10.1038/ncomms1659

International Commission on Zoological Nomenclature (1999) *International Code of Zoological Nomenclature*. London, England, The International Trust for Zoological Nomenclature. http://iczn.org/iczn/index.jsp [accessed 12 September 2017]

Jeannel R (1940) Coléoptères. In Jeannel R (ed). Croisière de Bougainville aux Iles Australes Françaises. Mémoires de Muséum National d'Histoire Naturelle, Paris 14(N.S.): 63–201.

Jeannel R (1941) Coléoptères Carabiques, première partie. Faune de France 39: 1–571.

Jeannel R (1942) La Genèse des Faunes Terrestres: Éléments de Biogéographie. Presses Universitaires de France, Paris.

Jeannel R (1944) Un carabique nouveau de la Nouvelle-Calédonie. Revue Française d'Entomologie 10: 84–86.

Jeannel R (1955) L'Édéage, initiation aux recherches sur la systématique des Coléoptères. Publications du Muséum national d'Histoire naturelle No. 16: 155 pp.

Jones JG, McDougall I (1973) Geological history of Norfolk and Philip Islands, southwest Pacific Ocean. Journal of the Geological Society of Australia 20: 239–254. https://doi.org/10.1080/14400957308527916

Kavanaugh DH (1985) On wing atrophy in carabid beetles (Coleoptera: Carabidae) with special reference to *Nebria*. In Ball GE (ed). Taxonomy, Phylogeny and Zoogeography of Beetles and Ants, Dr W Junk Publishers, Dordrecht: 408–431.

Kennedy DM, Brooke BP, Woodroffe CD, Jones BG, Waikari C, Nichol S (2011) The geomorphology of the flanks of Lord Howe Island volcano, Tasman Sea, Australia. Deep-Sea Research II 58: 899–908. https://doi.org/10.1016/j.dsr2.2010.10.046

Kubota K, Miyazaki K, Ebihara S, Takami Y (2013) Mechanical reproductive isolation via divergent genital morphology between *Carabus insulicola* and *C. esakii* with implications in species coexistence. Population Ecology 55: 35–42. https://doi.org/10.1007/s10144-012-0335-4

Ladiges PY, Cantrill D (2007) New Caledonia–Australian connections: biogeographic patterns and geology. Australian Systematic Botany 20: 383–389. https://doi.org/10.1071/SB07018

Ladiges P, Parra-O C, Gibbs A, Udovicic F, Nelson G, Bayly M (2011) Historical biogeographical patterns in continental Australia: congruence among areas of endemism of two major clades of eucalypts. Cladistics 27: 29–41. https://doi.org/10.1111/j.1096-0031.2010.00315.x

Langor DW, Larson DJ (1983) Alary polymorphism and life history of a colonizing ground beetle, *Bembidion lampros* Herbst (Coleoptera: Carabidae The Coleopterists Bulletin 37: 365–377.

Liebherr JK (1988) Geme flow in ground beetles (Coleoptera: Carabidae) of different habitat preference and flight-wing development. Evolution 42: 129–137. https://doi.org/10.1111/j.1558-5646.1988.tb04113.x

Liebherr JK (2007["2006"]) Taxonomic revision of the *Mecyclothorax* beetles (Coleoptera: Carabidae, Psydrini) of Molokai, Hawaii and recognition of areas of endemism on Kamakou volcano. Journal of the New York Entomological Society 114: 179–281. https://doi.org/10.1664/0028-7199(2007)114[179:TROTMB]2.0.CO;2

Liebherr JK (2008a) *Mecyclothorax kavanaughi* sp. n. (Coleoptera: Carabidae) from the Finisterre Range, Papua New Guinea. Tijdschrift voor Entomologie 151: 147–154. https://doi.org/10.1163/22119434-900000260

Liebherr JK (2008b) Taxonomic revision of *Mecyclothorax* Sharp (Coleoptera, Carabidae) of Hawaii Island: abundant genitalic variation in a nascent island radiation. Deutsche Entomologische Zeitshrift 55: 19–78. https://doi.org/10.1002/mmnd.200800004

Liebherr JK (2009a) Native and alien Carabidae (Coleoptera) share Lanai, an ecologically devastated island. The Coleopterists Bulletin 63: 383–411. https://doi.org/10.1649/1176.1

Liebherr JK (2009b) Taxonomic revision of the *Mecyclothorax* beetles (Coleoptera: Carabidae) of Oahu: epithets as epitaphs for an endangered fauna? Systematic Entomology 34: 649–687. https://doi.org/10.1111/j.1365-3113.2009.00477.x

Liebherr JK (2011) Cladistic assessment of subtribal affinities within the tribe Moriomorphini with description of *Rossjoycea glacialis*, gen. n. and sp. n. from the South Island, and revision of *Meonochilus* Liebherr and Marris from the North Island, New Zealand (Coleoptera, Carabidae ZooKeys 147: 277–335. https://doi.org/10.3897/zookeys.147.1898

Liebherr JK (2012) The first precinctive Carabidae from Moorea, Society Islands: new *Mecyclothorax* spp. (Coleoptera) from the summit of Mont Tohiea. ZooKeys 224: 37–80. https://doi.org/10.3897/zookeys.224.3675

Liebherr JK (2013) The *Mecyclothorax* beetles (Coleoptera, Carabidae, Moriomorphini) of Tahiti, Society Islands. ZooKeys 322: 1–170. https://doi.org/10.3897/zookeys.322.5492

Liebherr JK (2015) The *Mecyclothorax* beetles (Coleoptera, Carabidae, Moriomorphini) of Haleakalā, Maui: Keystone of a hyperdiverse Hawaiian radiation. ZooKeys 544: 1–407. https://doi.org/10.3897/zookeys.544.6074

Liebherr JK (2016) *Cyphocoleus* Chaudoir (Coleoptera, Carabidae, Odacanthini): descriptive taxonomy, phylogenetic relationships, and the Cenozoic history of New Caledonia. Deutsche Entomologische Zeitschrift 63: 211–270. https://doi.org/10.3897/dez.63.10241

Liebherr JK (2017a) *Bryanites graeffi* sp. n. (Coleoptera, Carabidae): museum rediscovery of a relict species from Samoa. Zoosystematics and Evolution 93: 1–11. https://doi.org/10.3897/zse.93.10802

Liebherr JK (2017b) Review of *Mecyclothorax* Sharp (Coleoptera: Carabidae: Moriomorphini) from Papua New Guinea with descriptions of five new species. The Coleopterists Bulletin 71: 679–703.

Liebherr JK, Krushelnycky PD (2007) Unfortunate encounters? Novel interactions of native *Mecyclothorax*, alien *Trechus obtusus* (Coleoptera: Carabidae), and Argentine ant (*Linepithema humile*, Hymenoptera: Formicidae) across a Hawaiian landscape. Journal of Insect Conservation 11: 61–73. https://doi.org/10.1007/s10841-006-9019-8

Liebherr JK, Marris JWM (2009) Revision of the New Zealand species of *Mecyclothorax* Sharp (Coleoptera: Carabidae: Psydrinae, Mecyclothoracini) and the consequent removal of several species to *Meonochilus* gen. n. (Psydrinae: Meonini New Zealand Entomologist 32: 5–22.

Liebherr JK, Takumi R (2002) Introduction and distributional expansion of *Trechus obtusus* (Coleoptera: Carabidae) in Maui, Hawaii. Pacific Science 56: 365–375.v https://doi.org/10.1353/psc.2002.0035

Liebherr JK, Will KW (1998) Inferring phylogenetic relationships within Carabidae (Insecta, Coleoptera) from characters of the female reproductive tract. In Ball GE, Casale A, Vigna Taglianti V (eds Atti Museo Regionale di Scienze Naturali, Museo Regionale di Scienze Naturali, Torino: 107–170.

Lindroth CH (1946) Inheritance of wing dimorphism in *Pterostichus anthracinus* Ill. Hereditas 32: 37–40. https://doi.org/10.1111/j.1601-5223.1946.tb02769.x

Lindroth CH (1974) On the elytral microsculpture of carabid beetles (Col.). Carabidae Entomologica Scandanavica 5: 251–264. https://doi.org/10.1163/187631274X00290

Lorenz W (1998) Nomina Carabidarum, A Directory of the Scientific Names of Ground Beetles. Published by the author, Tutzing.

Lorenz W (2005) Systematic List of Extant Ground Beetles of the World (Insecta Coleoptera "Geadephaga": Trachypachidae and Carabidae incl. Paussinae, Cicindelinae, Rhysodinae), 2nd Ed. Published by the author, Tutzing.

Louwerens CJ (1949) Some notes on the Carabidae, collected by Mr. P. H. van Doesburg in the Malay Archipelago with descriptions of new species. Tijdschrift voor Entomologie 90: 45–53.

Louwerens CJ (1953) Carabidae (Col.) from the Sunda Islands. Verhandlungen der Naturforschenden Gesellschaft in Basel 64: 303–327.

MacLeay W (1871) Notes on a collection of insects from Gayndah. Transactions of the Entomological Society of New South Wales 2(2): 79–205.

Mandl K (1969) Zwei neue *Heptodonta*-Arten und eine neue Carabidae-Gattung (Col.) aus Nord-Borneo. Zeitschrift der Arbeitsgemeinschaft Österreiches Entomologen 21: 51–54.

Moore BP (1963) Studies on Australian Carabidae (Coleoptera)–3. the Psydrinae. Transactions of the Royal Entomological Society, London 115: 277–290. https://doi.org/10.1111/j.1365-2311.1963.tb00810.x

Moore BP (1984) Taxonomic notes on some Australasian *Mecyclothorax* Sharp (Coleoptera: Carabidae: Psydrinae) and descriptions of new species. Journal of the Australian Entomological Society 23: 161–166. https://doi.org/10.1111/j.1440-6055.1984.tb01935.x

Moore BP (1985) The Carabidae of Norfolk Island. In Ball GE (ed Taxonomy, Phylogeny and Zoogeography of Beetles and Ants, Dr W Junk Publishers, Dordrecht: 237–256.

Moore BP (1992) The Carabidae of Lord Howe Island. In Noonan GR, Ball GE, Stork NE (Eds) The Biogeography of Ground Beetles of Mountains and Islands, Intercept Ltd., Andover, Hampshire, UK.

Moore BP, Weir TA, Pyke JE (1987) Coleoptera: Adephaga: Rhysodidae and Carabidae. In: Walton DW (Ed.) Zoological Catalogue of Australia Vol 4, Australian Government Printing Service, Canberra: 17–320.

Mueller-Dombois D, Fosberg FR (1998) Vegetation of the Tropical Pacific Islands. Springer Verlag, New York, Inc. https://doi.org/10.1007/978-1-4419-8686-3

Murienne J, Grandcolas P, Piulachs MD, Bellés X, D'Haese C, Legendre F, Pellens R, Guilbert E (2005) Evolution on a shaky piece of Gondwana: is local endemism recent in New Caledonia? Cladistics 21: 2–7. https://doi.org/10.1111/j.1096-0031.2004.00042.x

Nagata N, Kubota K, Takami Y, Sota T (2009) Historical divergence of mechanical isolation agents in the ground beetle *Carabus arrowianus* as revealed by phylogeographical analyses. Molecular Ecology 18: 1408–1421. https://doi.org/10.1111/j.1365-294X.2009.04117.x

Nattier R, Pellens R, Robillard T, Jourdan H, Legendre F, Caesar M, Nel A, Grandcolas P (2017) Updating the phylogenetic dating of New Caledonian biodiversity with a meta-analysis of the available evidence. Scientific Reports 7(3705). https://doi.org/10.1038/s41598-017-02964-x

Nelson G, Platnick N (1981) Systematics and Biogeography, Cladistics and Vicariance. Columbia University Press, New York.

Nixon KC (1999) The parsimony ratchet, a new method for rapid parsimony analysis. Cladistics 15: 407–414. https://doi.org/10.1111/j.1096-0031.1999.tb00277.x

Nixon KC (2002) WinClada. Ithaca, NY, Published by the author. http://www.softpedia.com/get/Science-CAD/WinClada.shtml [accessed 16-ix-2016]

Okuzaki Y, Sota T (2014) How the length of genital parts affects copulation performance in a carabid beetle: implications for correlated evolution between the sexes. Journal of Evolutionary Biology 27: 565–574. https://doi.org/10.1111/jeb.12323

Perrault GG (1984) La faune des Carabidae de Tahiti VI. révision du genre *Mecyclothorax* (Sharp) (Psydrini 1. le groupe de *M. muriauxi* Perrault (Coleoptera Nouvelle Revue d'Entomologie (NS) 1: 19–31.

Reid CAM, Smith KI (2004) A new genus and first record of Chrysomelinae from New Caledonia (Coleoptera: Chrysomelidae Memoirs of the Queensland Museum 49: 705–711.

Sasabe M, Takami Y, Sota T (2007) The genetic basis of interspecific differences in genital morphology of closely related carabid beetles. Heredity 98: 385–391 https://doi.org/10.1038/sj.hdy.6800952

Sharma P, Giribet G (2009) A relict in New Caledonia: phylogenetic relationships of the family Troglosironidae (Opiliones: Cyphophthalmi Cladistics 25: 279–294. https://doi.org/10.1111/j.1096-0031.2009.00252.x

Sharp D (1903) Coleoptera II. Caraboidea. In Sharp D (ed Fauna Hawaiiensis 3. The University Press, Cambridge: pp. 175–292 + pls. VI–VII.

Sherrod DR, Sinton JM, Watkins SE, Brunt KM (2007) Geological Map of the State of Hawai`i. US Geological Survey Open-File Report 2007-1089, Version 1.0 (22 May 2007). http://pubs.usgs.gov/of/2007/1089/ [accessed 5 July 2013]

Short AEZ, Liebherr JK (2007) Systematics and biology of the endemci water scavenger beetles of Hawaii (Coleoptera: Hydrophilidae, Hydrophilini Systematic Entomology 32: 601–624. https://doi.org/10.1111/j.1365-3113.2007.00403.x

Sloane TG (1903) Studies in Australian Entomology No. XII. New Carabidae (Panagaeini, Bembidiini, Pogonini, Platysmatini, Platynini, Lebiini, with revisional lists of genera and species, some notes on synonymy, &c. Proceedings of the Linnean Society of New South Wales 28: 566–642.

Southwood TRE (1977) Habitat, the templet for ecological strategies? Journal of Animal Ecology 46: 337–365. https://doi.org/10.2307/3817

Trueman JWH, Pfeil BE, Kelchner SA, Yeates DK (2004) Did stick insects *really* regain their wings? Systematic Entomology 29: 138–139. https://doi.org/10.1111/j.0307-6970.2004.00251.x

Whiting MF, Bradler S, Maxwell T (2003) Loss and recovery of wings in stick insects. Nature 412: 264–267. https://doi.org/10.1038/nature01313

Will KW (2011) Taxonomic review of the Pterostichini and Loxandrini fauna of New Caledonia (Coleoptera, Carabidae) ZooKeys 147: 337–397. https://doi.org/10.3897/zookeys.147.1943

Woodroffe CD, Kennedy DM, Brooke BP, Dickson ME (2006) Geomorphological evolution of Lord Howe Island and carbonate production at the latitudinal limit to reef growth. Journal of Coastal Research 22: 188–201. https://doi.org/10.2112/05A-0014.1

Wulf A (2015) The Invention of Nature, Alexander von Humboldt's New World. Alfred A. Knopf, New York.

Wulff AS, Hollingsworth PM, Ahrends A, Jaffré T, Veillon J-M, L'Huillier L, Fogliani B (2013) Conservation priorities in a biodiversity hotspot: analysis of narrow endemic plant species in New Caledonia. PLOS One 8: E73371. https://doi.org/10.1371/journal.pone.0073371

Supplementary material 1
Data file for cladistic analysis of Mecyclothorax Sharp.
Author: James K. Liebherr
Data type: NONA format data file

Link: https://doi.org/10.3897/dez.65.21000.suppl1

Supplementary material 2
Date-locality data for Mecyclothorax (Phacothorax) species represented by more than 50 specimens.
Author: James K. Liebherr
Data type: specimen records

Link: https://doi.org/10.3897/dez.65.21000.suppl2